Table 1 Structural and magnetic data for triply-bridged dinuclear copper(II) complexes

Compound[a]	Coordination geometry[b]	τ	Chromophore	μ-OH position[c]	Cu-OH-Cu (°)	J (cm^{-1})	Ref.
$[Cu_2(dpyam)_2(\mu\text{-}O_2CH)(\mu\text{-}OH)(\mu\text{-}OCH_3)](ClO_4)$ **(I)**	Dist. TBP.	0.61	CuN_2O_3	Axial/Axial	104.0	62.5	This work
$[Cu_2(dpyam)_2(\mu\text{-}O_2CH)_2(\mu\text{-}OH)](PF_6)$ **(III)**	Dist. TBP.	0.59	CuN_2O_3	Axial/Axial	107.2	30.8	This work
$[Cu_2(dpyam)_2(\mu\text{-}O_2CH)(\mu\text{-}OH)(\mu\text{-}Cl)](ClO_4)\cdot 0.5H_2O$ **(IV)**	Dist. TBP.	0.60	CuN_2O_2Cl	Axial/Axial	104.7	79.1	This work
$[Cu_2(dpyam)_2(\mu\text{-}O_2CH)(\mu\text{-}OH)(\mu\text{-}Cl)](PF_6)$ **(V)**	Dist. TBP.	0.72	CuN_2O_2Cl	Axial/Axial	105.9	36.7	This work
$[Cu_2(bpy)_2(\mu\text{-}OH)(\mu\text{-}H_2O)(\mu\text{-}O_2CCH_3)](ClO_4)_2$	Dist. Spy.	0.14, 0.25[f]	CuN_2O_3	Eq./Eq	103.8	19.3	3
$[Cu_2(\mu\text{-EtBITP})(\mu\text{-}OH)(\mu\text{-}Cl)Cl_2]\cdot DMF$	intermediate[d]	0.58, 0.55[f]	CuN_2Cl_2O	Axial/Axial	104.7	-260	11
$[Cu_2(\mu\text{-PTP})(\mu\text{-}OH)(\mu\text{-}Cl)Cl_2]\cdot 2CH_3CN$	intermediate[d]	0.51	CuN_2Cl_2O	Axial/Axial	106.2	-296	12
$[Cu_2(\mu\text{-PAP})(\mu\text{-}OH)(\mu\text{-}IO_3)(IO_3)_2]\cdot 4H_2O$	Dist. Spy.[e]	0.40	CuN_2O_3	Eq/Eq	113.8	-283	12, 13
$[Cu_2(\mu\text{-PAP})(\mu\text{-}OH)(\mu\text{-}SO_4)Cl]\cdot 2H_2O$	Dist. Spy.	0.35, 0.37[f]	CuN_2O_3	Eq./Eq	115.5	-532	14

[a] Abbreviations: dpyam = di-2-pyridylamine; bpy = 2,2'-bipyridine; EtBITP = 3,6-bis(2-benzimidazolylthio)pyridazine; PTP = 3,6-bis(2-pyridylthio)phthalazine; PAP = 1,4-bis-(2-pyrodyl amino)phthalazine), [b] Dist. TBP = distorted trigonal bipyramidal, Dist. Spy. = distorted square pyramidal, [c] Eq. = Equatorial, [d] Trigonality (τ). According to the τ value of 0.58 and 0.55, the preferred geometry should be intermediate towards distorted trigonal bipyramidal.,

[e] Average trigonality (τ_{av}). According to the τ value of 0.40, the preferred geometry should be intermediate towards distorted square pyramidal.

[f] Calculated from the known structural parameters.

3.4.6 The proposed stereochemistry of $[Cu_2(dpyam)_2(\mu\text{-}O_2CH)(\mu\text{-}OH)(\mu\text{-}Cl)](BF_4)$ (VI)

3.4.6.1 The stoichiometry and IR spectrum

The stoichiometry of the complex $[Cu_2(dpyam)_2(\mu\text{-}O_2CH)(\mu\text{-}OH)(\mu\text{-}Cl)](BF_4)$ **(VI)** has been characterized by microanalyses. The infrared spectrum of **VI** (Appendix IIIC) exhibits a broad band at 3455 cm^{-1}, which can be assigned to the bridging OH vibrations of the hydroxo group. A broad and intense band at 1562 cm^{-1} corresponds to the $\nu_{as}(COO^-)$ vibration and a medium broad band at 1356 cm^{-1} corresponds to the $\nu_s(COO^-)$ vibration, the difference Δ [$\Delta = \nu_{as}(COO^-) - \nu_s(COO^-)$; 206 cm^{-1}] is close to that for NaO_2CH (201 cm^{-1}) as expected for the triatomic bridging coordination mode of the formate group. The spectrum also displays a broad and intense band at approximately 1090-1083 cm^{-1}, consistent with the characteristic peak of BF_4^- anion. This spectrum is comparable to those of **IV** and **V** suggesting the comparable functional groups in these complexes except that of the ClO_4^- and PF_6^- in **IV** and **V**, respectively.

3.4.6.2 The electronic diffuse reflectance spectrum

The electronic diffuse reflectance spectrum of **VI** (Fig. 15) displays a broad asymmetric band at ca. 11.56-12.76 kK, centered at 12.74 kK, corresponding to the distorted trigonal bipyramidal copper(II) stereochemistry. This feature is assigned to be the d_{x2-y2}, d_{xy}, d_{xz}, $d_{yz} \rightarrow d_{z2}$ transition.

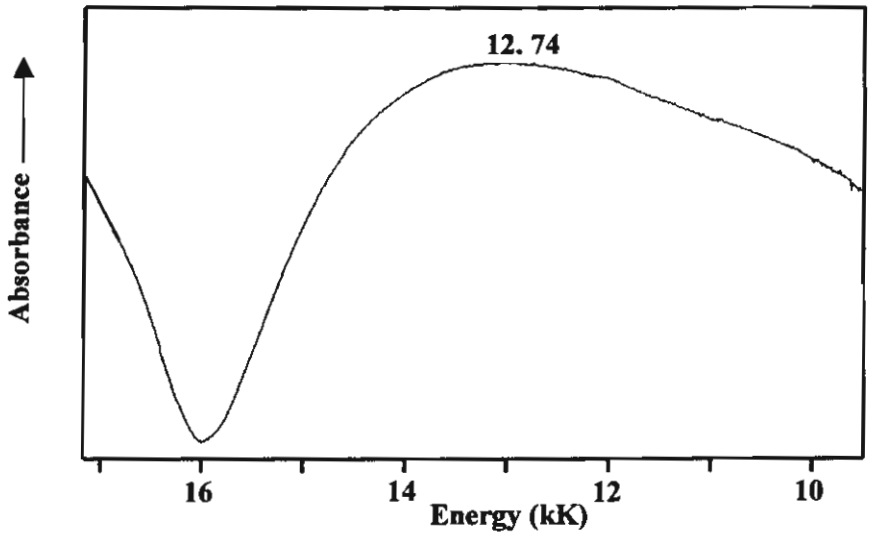

Figure 15 The electronic diffuse reflectance spectrum of $[Cu_2(dpyam)_2(\mu\text{-}O_2CH)(\mu\text{-}OH)(\mu\text{-}Cl)](BF_4)$ **(VI)**

3.4.6.3 The EPR spectrum

The X-band polycrystalline EPR spectra of **VI** (Appendix IIID) at room temperature and liquid nitrogen temperature (77 K) are either very weak and display an isotropic copper (II) signal at 2.09 and 2.10, respectively. These spectra give no information regarding to the ground state (Appendix IIID).

Taken together, microanalysis and infrared spectrum suggest the stoichiometry of $[Cu_2(dpyam)_2(\mu\text{-}O_2CH)(\mu\text{-}OH)(\mu\text{-}Cl)](BF_4)$ **(VI)** which is consistent with the formato complex. The electronic properties of **VI** are consistent with a distorted trigonal bipyramidal geometry. The isotropic-type EPR spectra give no information regarding to the electronic ground state. Consequently, the possible stereochemistry for **VI** is suggested as shown in Fig. 16.

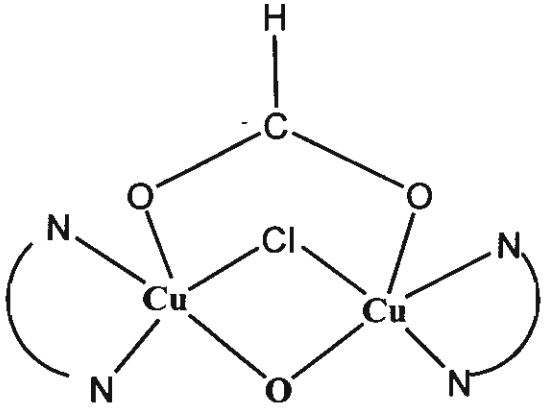

Figure 16 Suggested possible stereochemistry of $[Cu_2(dpyam)_2(\mu\text{-}O_2CH)(\mu\text{-}OH)(\mu\text{-}Cl)](BF_4)$ **(VI)**

3.4.6.4 Magnetic properties and superexchange mechanism

The effective magnetic moment (μ_{eff}) of **VI** measuring by the Faraday method at room temperature is 2.43 μ_B, which is close to the normal value (2.45 μ_B) of the uncoupled d^9 copper(II) ions suggesting noninteraction between the copper(II) centers in a dimeric unit at room temperature. However, the ferromagnetic behavior is expected for this complex at low temperature which occurs via the Cu-O-Cu pathway similar to those of the closely related complexes, $[Cu_2(dpyam)_2(\mu\text{-}O_2CH)(\mu\text{-}OH)(\mu\text{-}OCH_3)](ClO_4)$ **(I)**, $[Cu_2(dpyam)_2(\mu\text{-}O_2CH)(\mu\text{-}OOCH)(\mu\text{-}OH)](PF_6)$ **(III)**, $[Cu_2(dpyam)_2(\mu\text{-}O_2CH)(\mu\text{-}OH)(\mu\text{-}Cl)](ClO_4)\cdot 0.5H_2O$ **(IV)** and $[Cu_2(dpyam)_2(\mu\text{-}O_2CH)(\mu\text{-}OH)(\mu\text{-}Cl)](PF_6)$ **(V)**.

3.5 Conclusions

The triply-bridged dinuclear copper(II) carboxylato complexes $[Cu_2(dpyam)_2(\mu\text{-}O_2CH)(\mu\text{-}OH)(\mu\text{-}OCH_3)](ClO_4)$ **(I)**, $[Cu_2(dpyam)_2(\mu\text{-}O_2CH)_2(\mu\text{-}OH)](PF_6)$ **(III)**, $[Cu_2(dpyam)_2(\mu\text{-}O_2CH)(\mu\text{-}OH)(\mu\text{-}Cl)](ClO_4)\cdot 0.5H_2O$ **(IV)** and $[Cu_2(dpyam)_2(\mu\text{-}O_2CH)(\mu\text{-}OH)(\mu\text{-}Cl)](PF_6)$ **(V)** have been synthesized from their components by the mole ratio method. The crystal structures of all four complexes were determined by X-ray crystallography in this laboratory. All complexes involve the five coordinate distorted trigonal bipyramidal copper(II) ion stereochemistry. The copper(II) environment in **I** and **III** are similar with CuN_2O_3 chromophore, while **IV** and **V** display the CuN_2O_2Cl chromophore. The formato bridging ligands in **I, IV** and **V** are in a familiar didentate syn,syn η^1: η^1: μ_2-bridging mode. Whereas two formato ligands in **III** exhibit different coordination modes, which one formato ligand is in a familiar didentate syn,syn η^1: η^1: μ_2-bridging mode and the other is in the monoatomic bridging mode.

All complexes have the magnetic d_{z2} orbitals with lobe directed toward the bridging hydroxo group, which is positioned in the apical site of each trigonal bipyramidal copper(II) chromophore. This feature should cause the superexchange pathway that can occur through this bridging ligand contributing to a ferromagnetic interaction between two copper(II) ions.

Complex **VI** has been characterized by spectroscopy and microanalysis to be the triply-bridged dinuclear copper(II) formato complex, $[Cu_2(dpyam)_2(\mu\text{-}O_2CH)(\mu\text{-}OH)(\mu\text{-}Cl)](BF_4)$ **(VI)**. The suggested coordination environment around copper(II) ion involves a distorted trigonal bipyramidal geometry. The expected magnetic behavior is ferromagnetic interaction due to the Cu-OH-Cu superexchange pathway.

The magnetic properties of compounds **I** and **IV** mutually show a very similar behaviour with the singlet-triplet energy gaps (J) of +62.5 and +79.1 cm^{-1}, respectively and the very similar structure is also found **III** and **V** with J values of +30.8 and +36.7 cm^{-1}. The ferromagnetic interaction in the latter two compounds is smaller than that of the former two compounds, resulting in the conclusion that the bigger the bridging Cu-O(H)-Cu angle and the longer the Cu-Cu distance, the smaller the ferromagnetic interaction is found. It is noted that the τ values in the studied ranges do not affect the magnitude of exchange interaction. The coordination geometry around each copper(II) ion of **I, III, IV** and **V** is distorted trigonal bipyramidal, which the unpaired electron resides primarily in d_{z2} orbital with orientation along the apical hydroxo bridging ligand. In this case a major σ pathway via (Cu-OH-Cu) is possible for the electron delocalization via the d_{z2} magnetic orbitals, corresponding to the weak or strong ferromagnetic interaction. The unpair electron of first copper ion couples with

an electron in p-orbital of oxygen atom and the unpair electron of second copper ion couples with an electron in the other p-orbital of oxygen atom resulting in the existence of two parallel unpair electrons, each from different p-orbitals. A strong magnetic interaction requires both good σ orientation of the magnetic orbitals and good superexchange properties of the bridging atom(s). Therefore, these complexes contribute a moderate ferromagnetic exchange. It should be noted that when the copper(II) geometry is close to regular square pyramidal, an often strong antiferromagnetic interaction will be predominant, but a reduction of an antiferromagnetic contribution will be observed when the geometry becomes closer to trigonal bipyramidal. Compound **II** exhibits the distinct copper(II) environment, a distorted square pyramidal geometry, as compared to other complexes which the unpaired electron is located in a d_{x2-y2} type orbital. The d_{x2-y2} magnetic orbital in **II** is directed toward both hydroxo bridges, the Cu-O-Cu angles of 95.8 and 96.0°. For these bridging angles, a moderate antiferromagnetic coupling ($J = -122.54\ cm^{-1}$) should be expected following Hodgson and Hatfield's linear relationship which is usually applied successfully for the planar dihydroxo-bridged complexes.

References

1. Towle DK, Hoffmann SK, Hatfield WE, Singh P, Chaudhuri P. ***Inorg. Chem.*** 1988; 27: 394.
2. Wojtczak WA, Hampden-Smith MJ, Duesler EN. ***Inorg. Chem.*** 1998; 37: 1781.
3. Christou G, Perlepes SP, Libby E, Folting K, Huffman JC, Webb RJ, Hendrickson DN. ***Inorg. Chem.*** 1990; 29: 3657.
4. Perlepes SP, Huffman JC, Christou G. ***Polyhedron*** 1991; 10: 2301.
5. Perlepes SP, Huffman JC, Christou G. ***Polyhedron*** 1995; 14: 1073.
6. Neels A, Stoeckli-Evans H, Escuer A, Vicente R. ***Inorg. Chim. Acta*** 1997; 260: 189-198.
7. Graham B, Hearn MTW, Junk PC, Kepert CM, Mabbs FE, Moubaraki B, Murray KS, Spiccia L. ***Inorg. Chem.*** 2001; 40: 1536.
8. Rajendiran TM, Kannappan R, Venkatesan R, Rao PS, Kandaswamy M. ***Polyhedron*** 1999; 18: 3085.
9. Chadjistamatis I, Terzis A, Raptopoulou CP, Perlepes SP. ***Inorg. Chem. Com.*** 2003; 6: 1365.
10. Lubben M, Hage R, Meetsma A, Büma K, Feringa BL. ***Inorg. Chem.*** 1995; 34: 2217.
11. Thompson LK, Mandal SK, Rosenberg L. ***Inorg. Chim. Acta.*** 1987; 133: 81.
12. Chen L, Thompson LK, Bridson JN. ***Inorg. Chim. Acta.*** 1996; 244: 87.
13. Thompson LK, Lee FL, Gabe EJ. ***Inorg. Chem.*** 1988; 27: 39.
14. Thompson LK, Hanson AW, Ramaswamy BS. ***Inorg. Chem.*** 1984; 23: 2459.
15. Addison AW, Rao TN, Reedijk J, Van Rijn J, Verschoor GC ***J. Chem. Soc., Dalton Trans.*** 1984; 1349.
16. Kahn O. ***Molecular Magnetism.*** Cambridge: VCH Publishers; 1993.
17. Haddad MS, Wilson SR, Hodgson DJ, Hendrickson DN. ***J. Am. Chem. Soc.*** 1981; 103: 384.

OUTPUT OF THE RESEARCH

M.Sc. Students

1. Miss Pimprapun Gunnasoot: (1999-2002), "The Synthesis, Crystal Structure, Spectroscopic and Magnetic Properties of Dinuclear Oxalato-bridged Copper(II) Complexes Containing the 2,2′-Bipyridylamine Ligand" Master of Science Thesis in Chemistry, Graduate School, Khon Kaen University.
2. Mr. Pongthipun Phuengphai: (2001-2004), "Structural Diversity of Hydrogenphosphato-bridged Polynuclear Copper(II) Complexes Containing the di-2-pyridylamine: Synthesis Spectroscopic and Magnetic Properties" Master of Science Thesis in Chemistry, Graduate School, Khon Kaen University. Khon Kaen University Thesis Good Achievement Award in 2006.
3. Miss Chatkeaw chailuecha: (2001-2004), "The Synthesis, Crystal Structure, Spectroscopic and Magnetic Properties of Dinuclear Triply-bridged Copper(II) Compounds Containing the Di-2-pyridylamine Ligand with the Carboxylato Bridge" Master of Science Thesis in Chemistry, Graduate School, Khon Kaen University. Khon Kaen University Thesis Distinguished Achievement Award in 2006.

PUBLICATION PAPERS

1. S. Youngme, G.A. van Albada, N. Chaichit, P. Gunnasoot, P. Kongsaeree, I. Mutikainen, O. Roubeau, J. Reedijk, U. Turpeinen, "Synthesis, Spectroscopic Characterization, X-ray Crystal Structure and Magnetic Properties of Oxalato-bridged Copper(II) Dinuclear Complexes with Di-2-pyridylamine", ***Inorg. Chim. Acta***, 2003, **353**, 119-128.
2. S. Youngme, C. Chailuecha, N. Chaichit, "The novel dinuclear doubly and tripy-bridged copper(II) compound with monoatomic bridges", ***Polyhedron***, 2004, **23**, 1641-1647.
3. S. Youngme, C. Chailuecha, G.A. van Albada, C. Pakawatchai, N. Chaichit, J. Reedijk, "Synthesis, crystal structure, spectroscopic and magnetic properties of doubly and triply bridged dinuclear copper(II) compounds containing di-2-pyridylamine as a ligand", ***Inorg. Chim. Acta***, 2004, **357**, 2532-2542.
4. S. Youngme, P. Phuengphai, N. Chaichit, C. Pakawatchai, G.A. van Albada, O. Roubeau, J. Reedijk, "The coordination chemistry of mono(di-2-pyridylamine) copper(II) complexes with monovalent and divalent oxoanions: Crystal structure, spectroscopic and magnetic properties

of dinuclear $[Cu(L)(\mu\text{-}H_2PO_4)(H_2PO_4)]_2$ and polynuclear $[Cu(L)(\mu_3\text{-}HPO_4)]_n$", ***Inorg. Chim. Acta***, 2004, **357**, 3603-3612.

5. S. Youngme, P. Gunnasoot, N. Chaichit, C. Pakawatchai " New examples of dinuclear copper (II) complexes with ferromagnetic and antiferromagnetic interactions mediated by bridging oxalato group: structures and magnetic properties of $[Cu_2L_4(\mu\text{-}C_2O_4)](PF_6)_2(H_2O)_2$ and $[Cu_2L_2(\mu\text{-}C_2O_4)(NO_3)_2(CCH_3)_2N(OH)_2]$ (L = di-2-pyridylamine)" ***Trans. Metal Chem.***, 2004, **29**, 840-846.
6. S. Youngme, P. Phuengphai, N. Chaichit, G.A. van Albada, O. Roubeau, J. Reedijk "An unprecedented tetranuclear Cu(II) cluster, exclusively bridged by two μ_3,η^3-hydrogenphosphate anions. Synthesis, structure, and magnetic properties" ***Inorg. Chim. Acta***, 2005, **358**, 849-853.
7. S. Youngme, C. Chailuecha, G.A. van Albada, C. Pakawatchai, N. Chaichit, J. Reedijk "Dinuclear triply-bridged copper(II) compounds containing carboxylato bridges and di-2-pyridylamine as a ligand. Synthesis, crystal structure, spectroscopic and magnetic properties" ***Inorg. Chim. Acta***, 2005, **358**, 1068-1078.
8. S. Youngme, P. Phuengphai, N. Chaichit, G.A. van Albada, O. Roubeau, J. Reedijk "A novel tetranuclear hydrogenphosphate-bridged Cu(II) cluster. Synthesis, structure, spectroscopy and magnetism of $[Cu_4(dpyam)_4(\mu_4, \eta^3\text{-}HPO_4)_2(\mu\text{-}X)_2]X_2(H_2O)_6$ (X = Cl, Br)" ***Inorg. Chim. Acta***, 2005, **358**, 2262-2268.
9. S. Youngme, P. Phuengphai, C. Pakawatchai, G.A. van Albada, S. Tanase, I. Mutikainen, U. Turpeinen, Jan Reedijk "A copper(II) chain compound with hydrogenphosphate bridges organized in a double-chain structure. Synthesis, structure and magnetic properties of $[Cu(1,10\text{-phenanthroline})(\mu\text{-}HPO_4)(H_2O)_2]_n$" ***Inorg. Chem. Commun.***, 2005, **8**, 335-338.
10. S. Youngme, P. Phuengphai, C. Pakawatchai, G.A. van Albada, J. Reedijk "A novel polymeric trinuclear-based μ_3-phosphato-bridged Cu(II) complex containing two different types of monophosphate. Synthesis, structure and magnetism of $\{[Cu_3(di\text{-}2\text{-}pyridylamine)_3(\mu_3, \eta^3\text{-}HPO_4)(\mu_3, \eta^4\text{-}PO_4)(H_2O)](PF_6)(H_2O)_3\}_n$" ***Inorg. Chim. Acta***, 2005, **358**, 2125-2128.
11. S. Youngme, P. Phuengphai, N. Chaichit, G.A. van Albada, S. Tanase, J. Reedijk "Synthesis, crystal structure and magnetic properties of a polynuclear Cu(II) complex: *catena*-poly[aqua (di-2-pyridylamine)copper(II)(μ-formato-*O,O'*)nitrate]" ***Inorg. Chim. Acta***, 2005, **358**, 3267-3271.

12. P. Phuengphai, **S. Youngme**, C. Pakawatchai, G.A. van Albada, M. Quesada and J. Reedijk "Synthesis, crystal structure and magnetic properties of an unexpected new coordination Cu (II) compound, containing two different phosphato-bridged dinuclear units; $[Cu_2(phen)_2(\mu\text{-}H_2PO_4\text{-}O,O')_2(H_2PO_4)_2][Cu_2(phen)_2(\mu\text{-}H_2PO_4\text{-}O,O')(\mu\text{-}H_2PO_4\text{-}O)(\mu\text{-}HPO_4\text{-}O)]_2(H_2O)_9$(phen = 1,10-phenanthroline)", ***Inorg. Chem. Commun.***, 2006, **9**, 147-151.

Presentations

1. P. Gunnasoot, S. Youngme, N. Chaichit "The chemistry of dinatrato-di-2-pyridylamine copper(II). Crystal structures of *catena*-Poly[[(di-2-pyridylamine)(nitrato-0,0′)copper (II)]-μ-nitrato-0:0′] and Bis(nitrato-0,0′)(di-2-pyridylame)copper(II) Dihydrate" ***Oral presented at the 27th Congress on Science and Technology of Thailand***, Hatyai, Songkhla, Thailand. 16-18 October 2001.
2. P. Gunnasoot, S. Youngme, N. Chaichit, and J. Reedijk "Synthesis, Crystal Structure, Spectroscopic and Magnetic Properties of Oxalato Bridged Dinuclear Copper(II) Compound with Di-2-pyridylamine as a Ligand " ***Oral presented at the 28th Congress on Science and Technology of Thailand***, Bangkok, Thailand. 24-26 October 2002.
3. P. Gunnasoot, S. Youngme, N. Chaichit, "Synthesis, Crystal Structure, Spectroscopic and Magnetic Properties of Dinuclear Oxalato-Bridged Copper(II) Containing the 2,2'-Bipyridylamine as a Ligand " ***Oral*** *presented at the 5th Symposium on Graduate Research KKU,* Khon Kaen, Thailand. 20 January 2002. Oral presented distinguished achievement award.
4. P. Gunnasoot, S. Youngme, N. Chaichit "Synthesis, Crystal structure, Spectroscopy and Magnetic Properties of Oxalato-Bridged Copper(II) Complexes with Di-2-pyridylamine" ***Oral*** *presented at the 1st PERCH Annual Scientific Congress,* Chonburi, Thailand. 12-15 May 2002.
5. P. Phuengphai, S. Youngme, N. Chaichit "Synthesis, spectroscopic properties and crystal structure of polynuclear copper (II) complexes containing the di-2-pyridylamine and hydrogenphosphate ligands" ***Oral presented at the 29th Congress on Science and Technology of Thailand***, Khon Kaen, Thailand. 20-22 October 2003.
6. C. Chailuecha, S. Youngme, C. Pakawatchai "Synthesis, crystal structures, spectroscopic and magnetic properties of the doubly- and triply-bridged dinuclear copper(II) compounds containing the di-2-pyridylamine ligand" ***Poster*** *presented at the 29th*

Congress on Science and Technology of Thailand, Khon Kaen, Thailand. 20-22 October *2003.*

7. P. Phuengphai, S. Youngme, N. Chaichit "Synthesis, Spectroscopic Properties and Crystal stricture of Polynuclear Copper(II) Containing the Di-2-pyridylamine and Hydrogenphosphate Ligands" ***Poster*** *presented at the 2nd PERCH Annual Scientific Congress,* Chonburi, Thailand. 11-14 May 2003. Poster presented distinguished achievement award.
8. C. Chailuecha, S. Youngme, C. Pakawatchai "Synthesis, Crystal structure, Spectroscopic and Magnetic Properties of Roof-shaped formato-bridged Dinuclear Copper(II) Compounds Containing the Di-2-pyridylamine Ligand" ***Poster*** *presented at the 2nd PERCH Annual Scientific Congress,* Chonburi, Thailand. 11-14 May 2003. Poster presented distinguished achievement award.
9. P. Phuengphai, S. Youngme, N. Chaichit "The coordination chemistry of mono(di-2-pyridylamine) copper(II) complexes with monovalent and divalent oxoanions: Crystal structure and spectroscopic and magnetic properties of dinuclear $[Cu(L)(\mu\text{-}H_2PO_4)(H_2PO_4)]_2$ and polynuclear $[Cu(L)(\mu_3\text{-}HPO_4)]_n$" ***Poster*** *presented at the 7th Symposium on Graduate Research KKU,* Khon Kaen, Thailand. 20 January 2004. Poster presented distinguished achievement award.
10. C. Chailuecha, S. Youngme, C. Pakawatchai "Synthesis, crystal structure, spectroscopic and magnetic properties of doubly- and triply-bridged dinuclear copper(II) compounds containing di-2-pyridylamine as a ligand" ***Poster*** *presented at the 7th Symposium on Graduate Research KKU,* Khon Kaen, Thailand. 20 January 2004.
11. P. Phuengphai, S. Youngme, N. Chaichit "Structural Diversity of Hydrogenphosphato-bridged Polynuclear Copper(II) Complexes Containing the Di-2-pyridylamine: Synthesis, Spectroscopic and Magnetic Properties" ***Oral*** *presented at the 3rd PERCH Annual Scientific Congress,* Chonburi, Thailand. 9-12 May 2004.
12. C. Chailuecha, S. Youngme, C. Pakawatchai "Synthesis, Crystal structure, Spectroscopic and Magnetic Properties of Dinuclear Triply-bridged Dinuclear Copper(II) Compounds Containing the Di-2-pyridylamine Ligand with Carboxylato Bridge" ***Oral*** *presented at the 3rd PERCH Annual Scientific Congress,* Chonburi, Thailand. 9-12 May 2004. Oral presented distinguished achievement award.

13. S. Youngme, N. Chaichit, C. Pakawatchai, A.L. Spek, J. Reedijk "Planar and Roof-shaped Hydroxo-bridged Dinuclear Copper(II) Complexes: Structures, Magnetic Properties and Phase Transitions" ***Invited speaker*** *at the 4th PERCH Annual Scientific Congress,* Chonburi, Thailand. 8-11 May 2005.

14. S. Youngme, J. Phatchimkun, N. Chaichit, G.A. van Albada, S. Tanase, J. Reedijk "The coordination Chemistry of mono(di-2-pyridylamine) copper(II) complexes with monovalent oxoanions: Crystal structure and magnetic properties of polynuclear [Cu(L)(μ-O_2CH)(OH_2)]$_n$(NO_3)$_n$" ***Oral*** *presented at* the 20th International Conference on Coordination and Bioinorganic Chemistry, Smolenice, Slovakia. 5-10 June 2005.

APPENDICES

APPENDIX IA

Crystal and Refinement Data for

$[Cu_2(dpyam)_4(\mu\text{-}C_2O_4)]X_2$, X = BF_4^- (I), ClO_4^- (II) and PF_6^- (III)

and $[Cu_2(dpyam)_2(\mu\text{-}C_2O_4)Y_2]$, Y = NO_3^-·DMSO (IV),

NO_3^-·DMF (V), Cl^- (VI) and Br^- (VII)

Table 1 Crystal and refinement data for complexes **I-V**

Complexes	I	II	III	IV	V
Molecular formula	$[Cu_2(dpyam)_4(\mu\text{-}C_2O4)](BF_4)_2(H_2O)_3$	$[Cu_2(dpyam)_4(\mu\text{-}C_2O_4)](ClO_4)_2(H_2O)_3$	$[Cu_2(dpyam)_4(\mu\text{-}C_2O_4)](PF_6)_2(H_2O)_2$	$[Cu_2(dpyam)_2(\mu\text{-}C_2O_4)NO_3)_2((CH_3)_2SO)_2]$	$[Cu_2(dpyam)_2(\mu\text{-}C_2O_4)(NO_3)_2(CH_3)_2NCOH)_2]$
Molecular weight	1126.5	1152.8	1223.86	837.76	412.85
T(K)	293(2)	293(2)	293(2)	297.76	293(2)
Crystal system	Triclinic	Triclinic	Monoclinic	Triclinic	Triclinic
Space group	P-1	P-1	$P2_1/c$	P-1	P-1
a (Å)	9.629(2)	9.599(2)	8.5712(2)	8.719(0)	8.353(2)
b (Å)	11.170(2)	11.206(2)	11.3170(2)	8.980692)	9.100(2)
c (Å)	12.381(2)	12.480(3)	25.8680(5)	11.421(0)	12.245(3)
α (°)	73.81(2)	73.22(3)	90	68.58(0)	72.035(4)
β (°)	78.15(2)	77.84(3)	82.6150(10)	77.79(0)	75.228(4)
γ (°)	76.59(2)	76.88(3)	90	80.58(0)	78.552(4)
V ($Å^3$)	1229.7(2)	1236.5(4)	2488.39	808.87(1)	848.8(4)
Z	1	1	2	1	2
D_{calc} ($g\ cm^{-3}$)	1.516	1.542	1.633	1.720	1.615
μ (*mm*)	0.956	1.046	1.025	3.495	1.330
F (000)	569	588	1236	428	422
Crystal size (mm)	0.33 x 0.45 x 0.75	0.30 x 0.42 x 0.45	0.25 x 0.30 x 0.43	0.35 x 0.35 x 0.22	0.303 x 0.253 x 0.106
Reflection collected	9078	4834	17857	3171	7532
Unique reflections	7711 (R_{int} = 0.0179)	4834 (R_{int} = 0.0000)	7076 (R_{int} = 0.0487)	2964 (R_{int} = 0.0281)	3939 (R_{int} = 0.0150)
Observed ref. [I>2σ(I)]	6519	4349	7695	2828	6045
Data/restraints /parameter	7711/3/679	4834/3/694	7076/2/474	2964/0/228	3939/0/373
Goodness-of-fit	1.020	1.076	1.139	1.247	1.061
Final R indices [I>2σ(I)]	R1 = 0.0464, wR_2 = 0.1401	R1 = 0.0383, wR_2 = 0.1079	R1 = 0.0606, wR_2 = 0.1480	R1 = 0.0512, wR_2 = 0.1363	R1 = 0.0407, wR_2 = 0.1120
R indices (all data)	R1 = 0.0547, wR_2 = 0.1497	R1 = 0.0442, wR_2 = 0.1170	R1 = 0.0878, wR_2 = 0.1614	R1 = 0.060747, wR_2 = 0.1615	R1 = 0.0459, wR_2 = 0.1161
Largest difference peak and hole ($e\ Å^{-3}$)	0.946 and – 0.455	0.854 and – 0.472	1.058 and – 0.424	0.968 and – 0.554	0.676 and – 0.494

$$R = \Sigma||F_o| - |F_c||/\Sigma|F_o||,\quad R_w = [\Sigma w\{|F_o| - |F_c|\}^2/w|F_o|^2]^{1/2}$$

APPENDIX IB

Selected Bond Lengths (Å) and Angles (°) for

$[Cu_2(dpyam)_4(\mu\text{-}C_2O_4)]X_2$, X = BF_4^- (I), ClO_4^- (II) and PF_6^- (III)

and $[Cu_2(dpyam)_2(\mu\text{-}C_2O_4)Y_2]$, Y = NO_3^-·DMSO (IV),

NO_3^-· DMF (V), Cl^- (VI) and Br^- (VII)

Table 2
Selected bond lengths (Å) and angles (°) with e.s.d.s. in parentheses of $[Cu_2(dpyam)_4(C_2O_4)](BF_4)_2(H_2O)_3$ **(I)** and $[Cu_2(dpyam)_4(C_2O_4)](ClO_4)_2(H_2O)_3$ **(II)**

	(I)	**(II)**
Bond lengths		
Cu(1)-N(1)	2.008(8)	2.020(9)
Cu(1)-N(2)	2.111(7)	2.136(8)
Cu(1)-N(4)	2.024(6)	2.000(8)
Cu(1)-N(5)	2.134(8)	2.095(8)
Cu(1)-O(1)	2.229(8)	2.141(10)
Cu(1)-O(2)	2.252(8)	2.305(9)
Cu(2)-N(7)	2.021(8)	2.010(9)
Cu(2)-N(8)	2.145(7)	2.141(9)
Cu(2)-N(10)	2.006(7)	2.025(8)
Cu(2)-N(11)	2.094(6)	2.107(8)
Cu(2)-O(3)	2.208(9)	2.225(9)
Cu(2)-O(4)	2.189(8)	2.229(8)
Cu(1)-Cu(2)	5.745(3)	5.752(3)
Bond angles		
N(1)-Cu(1)-N(4)	173.4(3)	175.4(3)
N(2)-Cu(1)-O(1)	170.7(3)	165.8(3)
N(5)-Cu(1)-O(2)	166.0(2)	171.4(3)
N(2)-Cu(1)-N(5)	97.1(3)	97.5(3)
O(1)-Cu(1)-O(2)	74.8(2)	74.7(3)
N(7)-Cu(2)-N(10)	175.5(3)	173.2(4)
N(8)-Cu(2)-O(3)	166.1(2)	168.9(3)
N(11)-Cu(2)-O(4)	170.1(3)	166.8(3)
N(8)-Cu(2)-N(11)	97.6(3)	97.3(3)
O(3)-Cu(2)-O(4)	73.9(3)	73.7(3)

Table 3
Selected bond lengths (Å) and angles (°) with e.s.d.s. in parentheses of $[Cu_2(dpyam)_4(C_2O_4)](PF_6)_2(H_2O)_2$ **(III)**

Cu(1)-N(4)	1.992(10)	Cu(1)-N(2)	1.995(9)
Cu(1)-O(1)	2.029(9)	Cu(1)-N(5)	2.049(7)
Cu(1)-N(1)	2.191(6)	Cu(1)-O(2)	2.424(6)
Cu(2)-N(8)	1.979(9)	Cu(2)-O(4)	2.025(8)
Cu(2)-N(7)	2.027(7)	Cu(2)-N(11)	2.098(8)
Cu(2)-N(10)	2.249(8)	Cu(2)-O(3)	2.448(8)
Cu(1)...Cu(2)	5.737(2)		

N(4)-Cu(1)-N(2)	93.0(4)	N(4)-Cu(1)–O(1)	174.7(3)
N(2)-Cu(1)-O(1)	86.6(4)	N(4)-Cu(1)-N(5)	87.1(3)
N(2)-Cu(1)-N(5)	170.4(3)	O(1)-Cu(1)-N(5)	92.5(3)
N(4)-Cu(1)-N(1)	96.8(3)	N(2)-Cu(1)-N(1)	87.4(3)
O(1)-Cu(1)-N(1)	88.4(3)	N(5)-Cu(1)-N(1)	102.1(3)
N(4)-Cu(1)-O(2)	99.7(3)	N(2)-Cu(1)-O(2)	88.6(3)
O(1)-Cu(1)-O(2)	75.0(3)	N(5)-Cu(1)-O(2)	82.0(3)
N(1)-Cu(1)-O(2)	163.1(3)	N(8)-Cu(2)–O(4)	90.9(3)
N(8)-Cu(2)-N(7)	88.7(4)	O(4)-Cu(2)–N(7)	173.8(3)
N(8)-Cu(2)-N(1)1	171.5(4)	O(4)-Cu(2)-N(11)	89.4(3)
N(7)-Cu(2)-N(11)	90.1(3)	N(8)-Cu(2)–N(10)	101.5(3)
O(4)-Cu(2)-N(10)	87.2(3)	N(7)-Cu92)-N(10)	98.9(4)
N(11)-Cu(2)-N(10)	87.0(3)	N(8)-Cu(2)–O(3)	79.9(4)
O(4)-Cu(2)-O(3)	75.0(2)	N(7)-Cu(2)-O(3)	98.8(3)
N(11)-Cu(2)-O(3)	91.9(3)	N(10)-Cu(2)-O(3)	162.2(3)

Table 4
Selected bond lengths (Å) and angles (°) with e.s.d.s. in parentheses of $[Cu_2(dpyam)_2(C_2O_4)(NO_3)_2((CH_3)_2SO)_2]$ **(IV)**

Bond lengths

Cu(1)-N(1)	1.986(2)	Cu(1)-N(2)	2.002(2)
Cu(1)-O(1)	1.998(2)	Cu(1)-O(2)	1.994(2)
Cu(1)-O(3)	2.331(2)	Cu(1)-O(4)	2.502(2)
Cu(1)-Cu(1A)	5.220(2)		

Bond angles

N(1)-Cu(1)-O(2)	92.3(2)	N(1)-Cu(1)-O(1)	174.3(8)
O(2)-Cu(1)-O(1)	82.2(7)	N(1)-Cu(1)-N(2)	93.3(2)
O(2)-Cu(1)-N(2)	170.9(3)	O(1)-Cu(1)-N(2)	91.8(7)
N(1)-Cu(1)-O(3)	88.2(6)	O(2)-Cu(1)-O(3)	93.5(7)
O(1)-Cu(1)-O(3)	93.5(5)	O(4)-Cu(1)-N(1)	86.6(7)
O(4)-Cu(1)-N(2)	85.5(7)	O(4)-Cu(1)-O(1)	91.7(7)
O(4)-Cu(1)-O(2)	87.7(7)	O(4)-Cu(1)-O(3)	74.8(7)

Symmetry code: A= -x, -y+1, -z.

Table 5
Selected bond lengths (Å) and angles (°) with e.s.d.s. in parentheses of $[Cu_2(dpyam)_2(\mu\text{-}C_2O_4)(NO_3)_2((CH_3)_2NCOH)_2]$ (V)

Cu(1)-N(2)	1.979(7)	Cu(1)-N(1)	1.990(6)
Cu(1)-O(2)	2.005(6)	Cu(1)-O(1)	2.012(6)
Cu(1)-O(5)	2.254(7)	Cu(2)-N(4)	1.956(7)
Cu(1)-O(10B)	2.786(2)	Cu(1)-O(8B)	2.679(2)
Cu(2)-N(5)	1.973(7)	Cu(2)-O(4)	1.978(5)
Cu(2)-O(3)	2.002(6)	Cu(2)-O(6)	2.295(7)
Cu(1)...Cu(2)	5.212(2)		

N(2)-Cu(1)-N(1)	90.8(3)	N(2)-Cu(1)-O(2)	173.1(3)
N(1)-Cu(1)-O(2)	92.1(2)	N(2)-Cu(1)-O(1)	93.2(2)
N(1)-Cu(1)-O(1)	170.4(3)	O(2)-Cu(1)-O(1)	82.9(2)
N(2)-Cu(1)-O(5)	89.2(3)	N(1)-Cu(1)-O(5)	92.7(3)
O(2)-Cu(1)-O(5)	96.8(2)	O(1)-Cu(1)-O(5)	96.1(3)
N(4)-Cu(2)-N(5)	92.1(3)	N(4)-Cu(2)-O(4)	170.6(3)
N(5)-Cu(2)-O(4)	92.8(2)	N(4)-Cu(2)-O(3)	91.0(3)
N(5)-Cu(2)-O(3)	169.2(3)	O(4)-Cu(2)-O(3)	82.8(2)
N(4)-Cu(2)-O(6)	90.0(3)	N(5)-Cu(2)-O(6)	93.0(3)
O(4)-Cu(2)-O(6)	97.8(2)	O(3)-Cu(2)-O(6)	97.4(3)

Symmetry code: B= x, y, z-1

APPENDIX IC

The Infrared Spectra for

$[Cu_2(dpyam)_4(\mu\text{-}C_2O_4)]X_2$, X = BF_4^- (I), ClO_4^- (II) and PF_6^- (III) and $[Cu_2(dpyam)_2(\mu\text{-}C_2O_4)Y_2]$, Y = NO_3^- DMSO (IV), NO_3^- DMF (V), Cl^- (VI) and Br^- (VII)

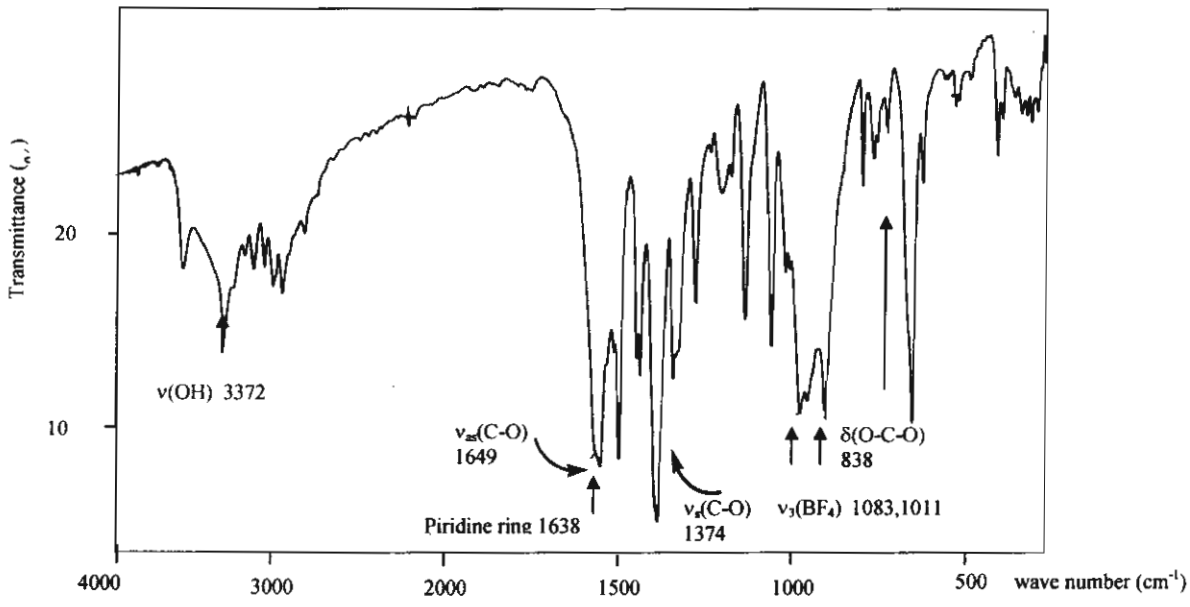

(a) The IR spectrum of $[Cu_2(dpyam)_4(\mu\text{-}C_2O_4)](BF_4)_2.3H_2O$ **(I)**

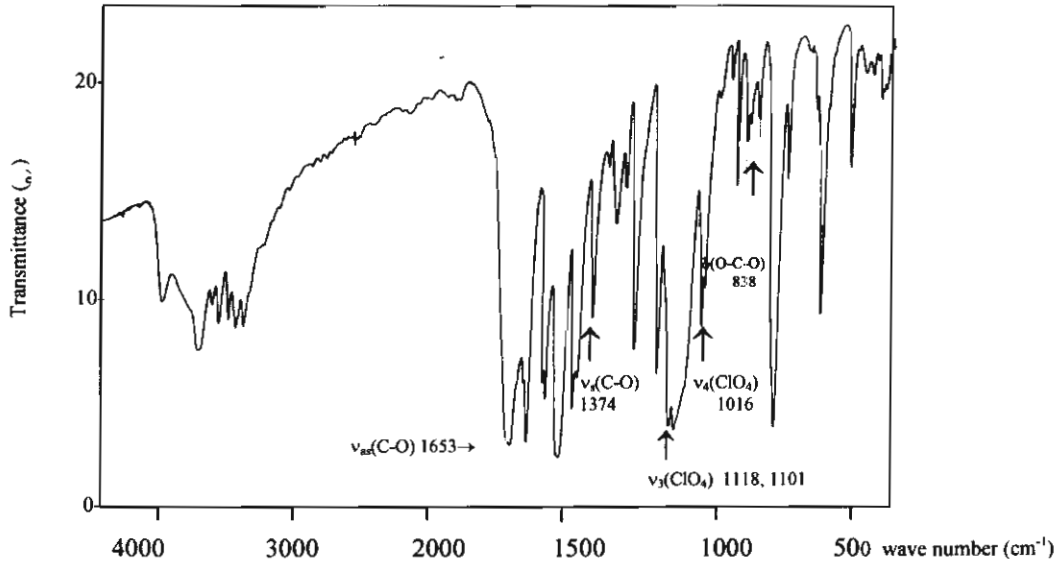

(b) The IR spectrum of $[Cu_2(dpyam)_4(\mu\text{-}C_2O_4)_2](ClO_4)_2.3H_2O$ **(II)**

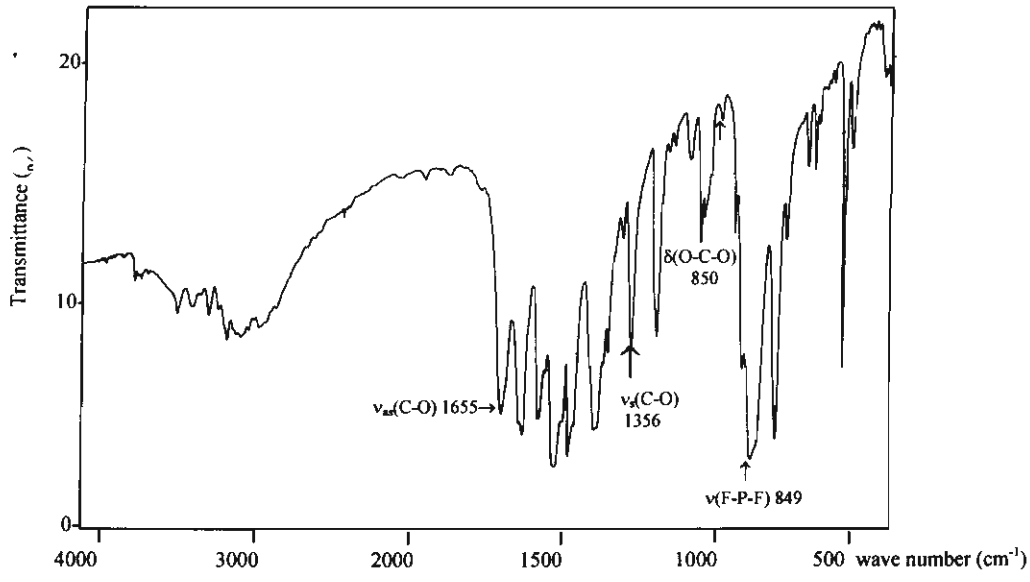

(c) The IR spectrum of $[Cu_2(dpyam)_4(\mu\text{-}C_2O_4)_2](PF_6)_2.2H_2O$ **(III)**

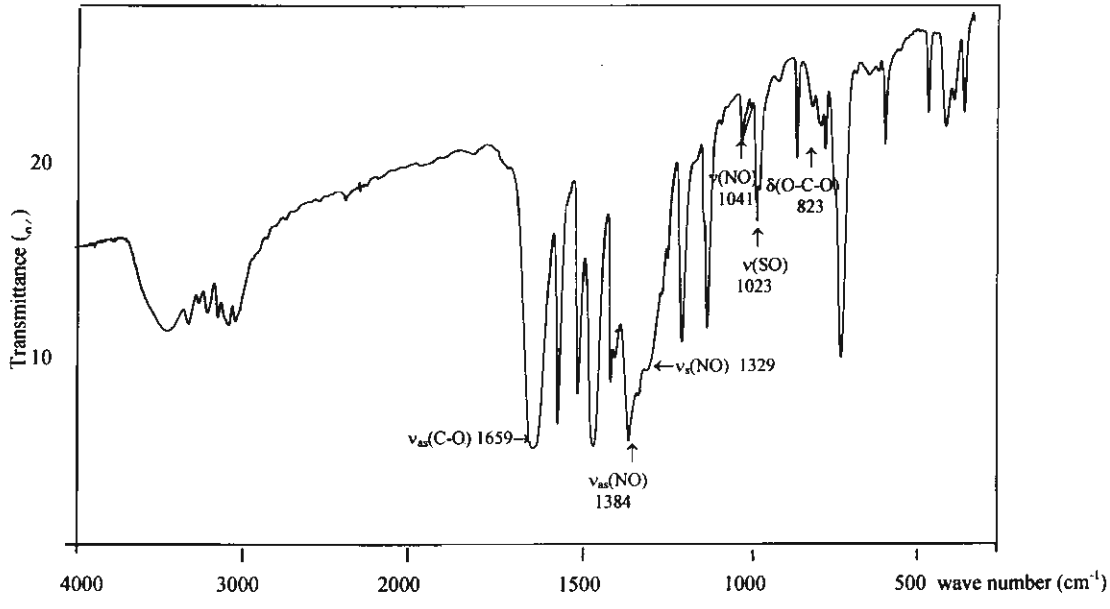

(d) The IR spectrum of $[Cu_2(dpyam)_2(\mu\text{-}C_2O_4)(NO_3)_2((CH_3)_2SO)_2)_2]$ **(IV)**

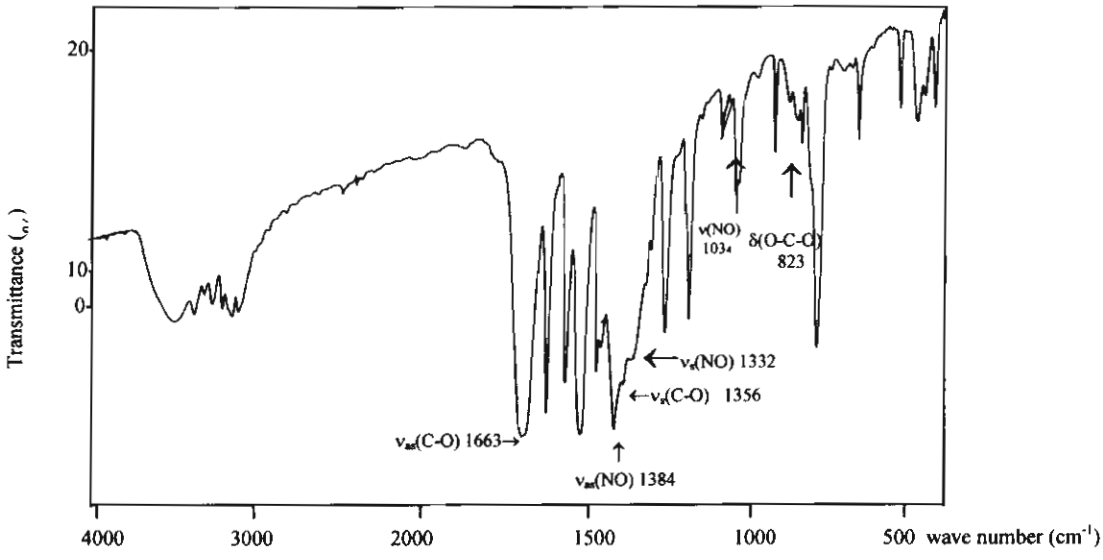

(e) The IR spectra of $[Cu_2(dpyam)_2(\mu\text{-}C_2O_4)(NO_3)_2(CH_3)_2NCOH)_2]$ **(V)**

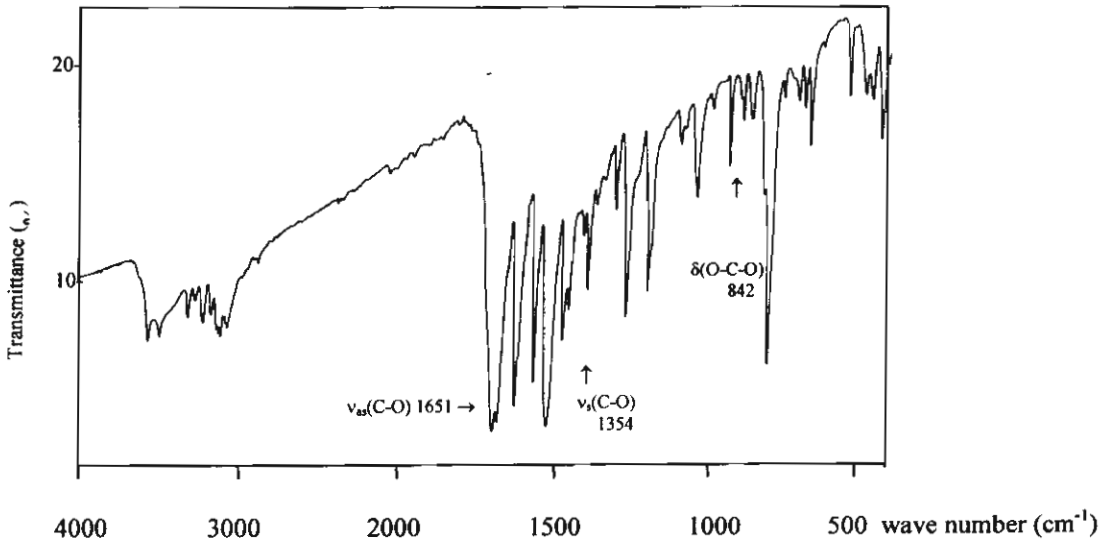

(f) The IR spectrum of $[Cu_2(dpyam)_2(\mu\text{-}C_2O_4)(Cl)_2]$ **(VI)**

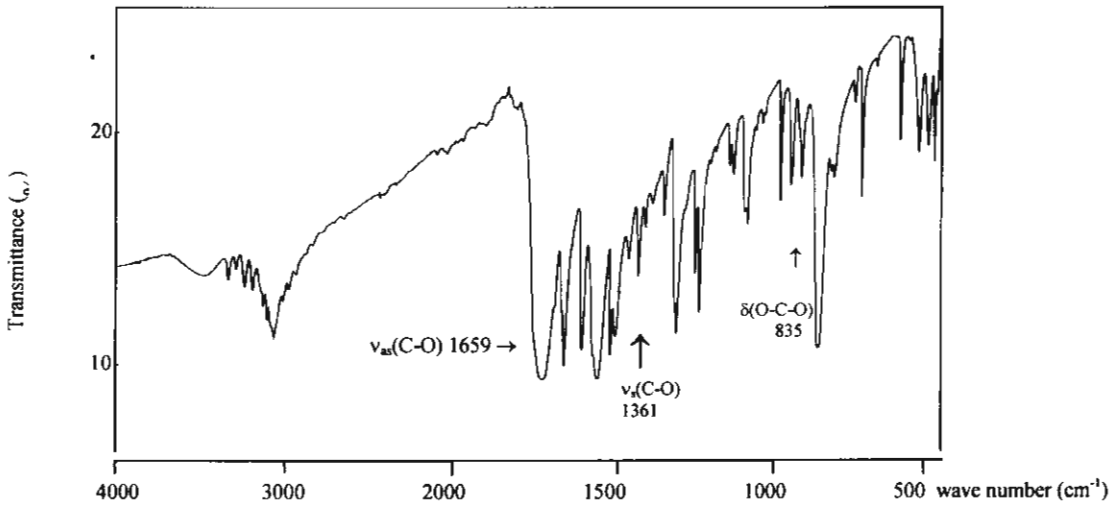

(g) The IR spectrum of $[Cu_2(dpyam)_2(\mu\text{-}C_2O_4)(Br)_2]$ **(VII)**

APPENDIX ID

The EPR Spectra for

$[Cu_2(dpyam)_4(\mu\text{-}C_2O_4)]X_2$, X = BF_4^- (I), ClO_4^- (II) and PF_6^- (III) and $[Cu_2(dpyam)_2(\mu\text{-}C_2O_4)Y_2]$, Y = NO_3^- DMSO (IV), NO_3^- DMF (V), Cl^- (VI) and Br^- (VII)

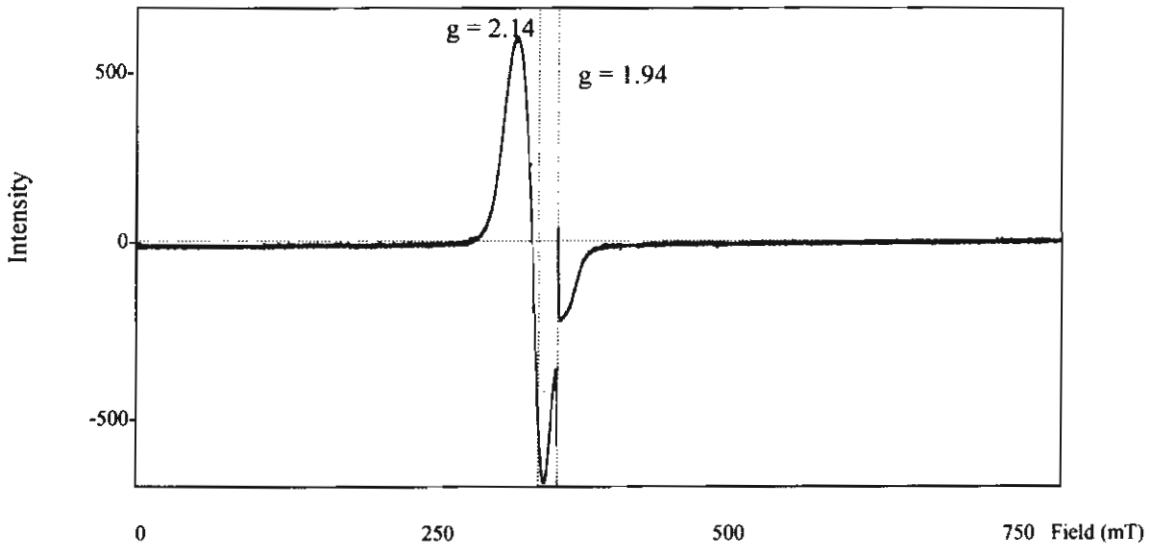

(a) The EPR spectrum at room temperature of $[Cu_2(dpyam)_4(\mu\text{-}C_2O_4)_2](BF_4)_2.3H_2O$ **(I)**

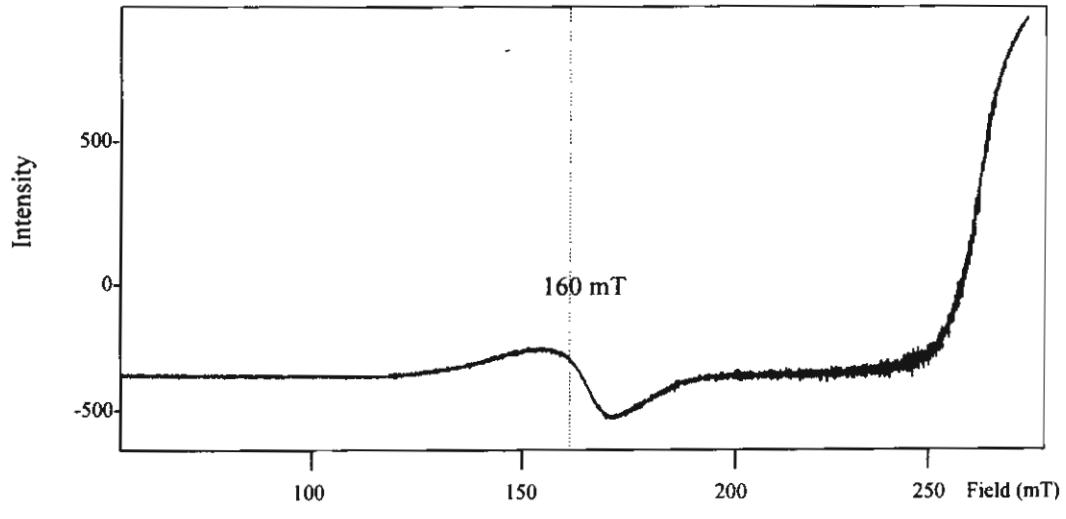

(b) The EPR spectrum at 77 K of $[Cu_2(dpyam)_4(\mu\text{-}C_2O_4)_2](BF_4)_2.3H_2O$ **(I)**

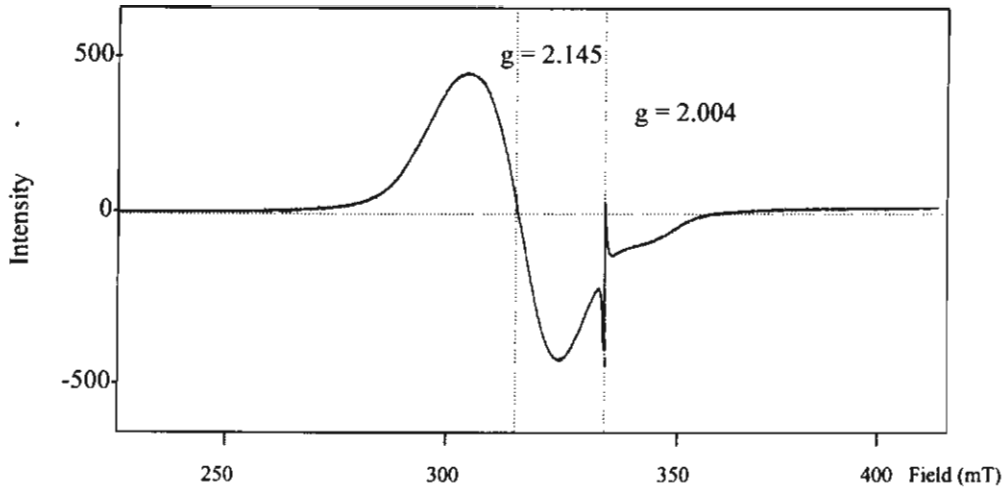

(c) The EPR spectrum at room temperature of $[Cu_2(dpyam)_4(\mu\text{-}C_2O_4)_2](ClO_4)_2.3H_2O$ **(II)**

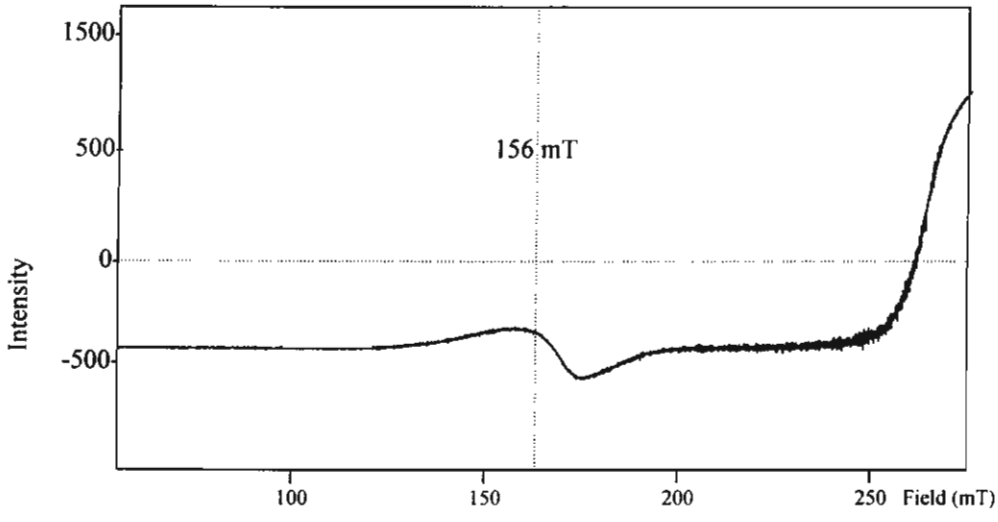

(d) The EPR spectrum at 77 K of $[Cu_2(dpyam)_4(\mu\text{-}C_2O_4)_2](ClO_4)_2.2H_2O$ **(II)**

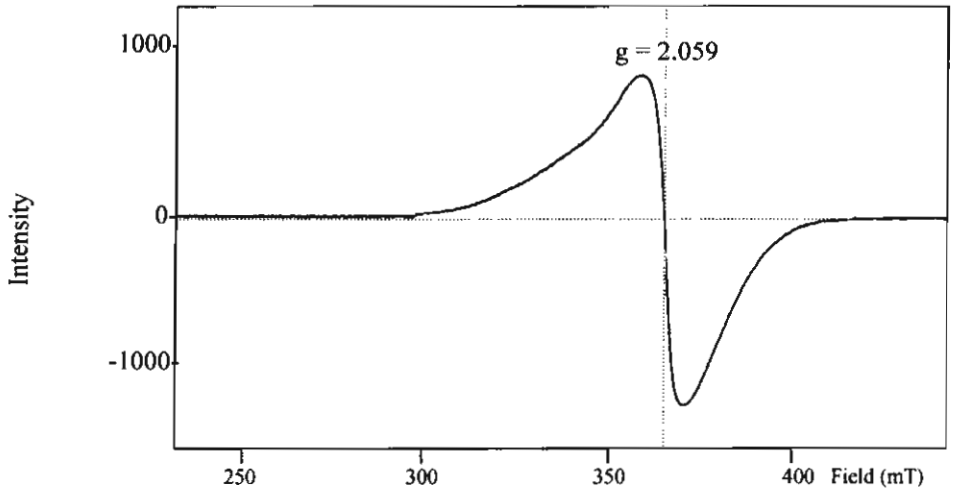

(e) The EPR spectrum at room temperature of $[Cu_2(dpyam)_4(\mu\text{-}C_2O_4)_2](PF_6)_2.2H_2O$ **(III)**

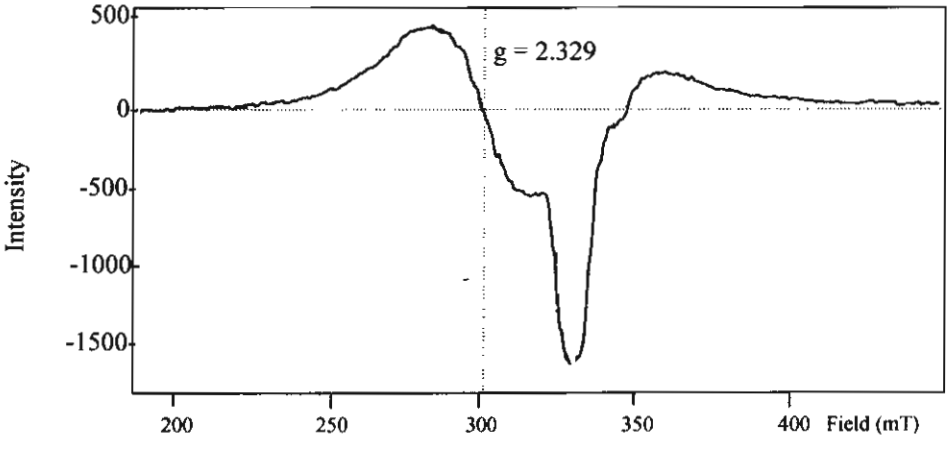

(f) The EPR spectrum at 77 K of $[Cu_2(dpyam)_4(\mu\text{-}C_2O_4)_2](PF_6)_2.2H_2O$ **(III)**

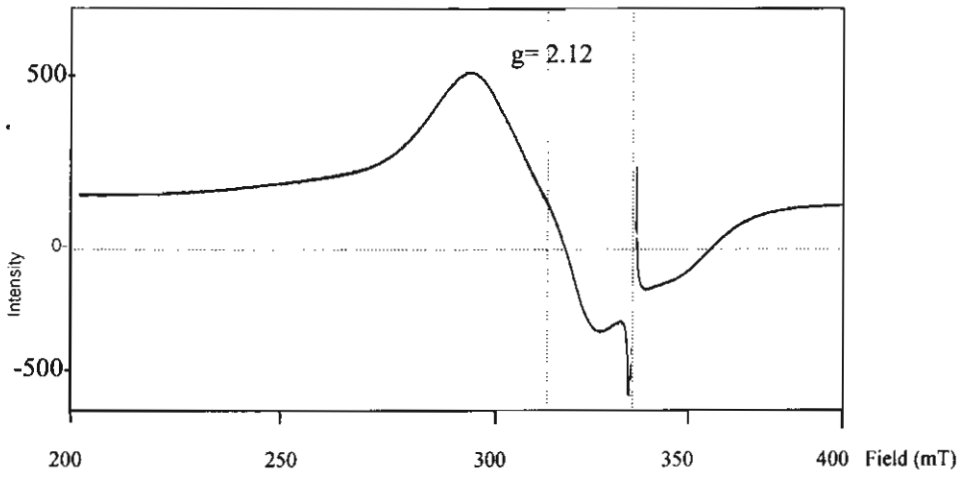

(g) The EPR spectrum at room temperature of $[Cu_2(dpyam)_2(C_2O_4)(NO_3)_2((CH_3)_2(SO)_2]$ **(IV)**

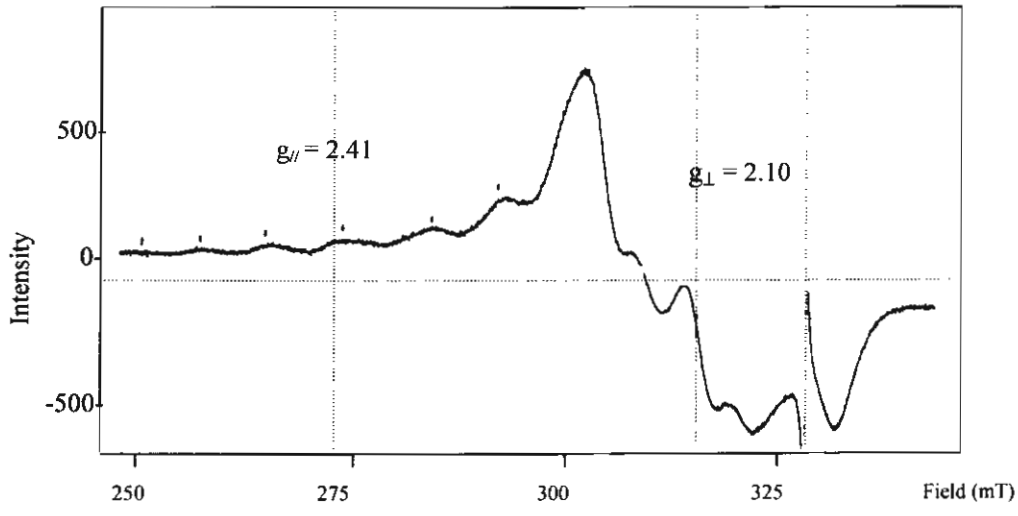

(h) The EPR spectrum at 77 K of $[Cu_2(dpyam)_2(C_2O_4)(NO_3)_2((CH_3)_2(SO)_2]$ **(IV)**

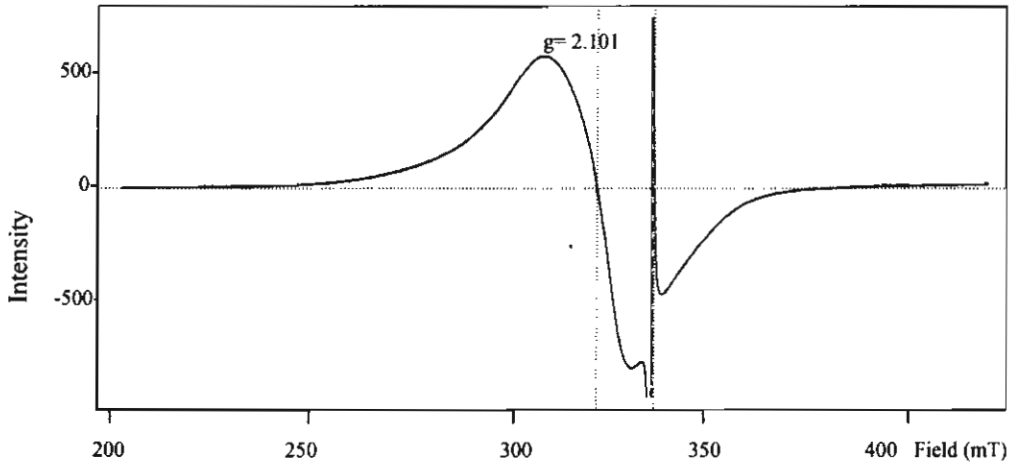

(i) The EPR spectrum at room temperature of $[Cu_2(dpyam)_2(\mu\text{-}C_2O_4)(NO_3)((CH_3)_2NCOH)_2]$ **(V)**

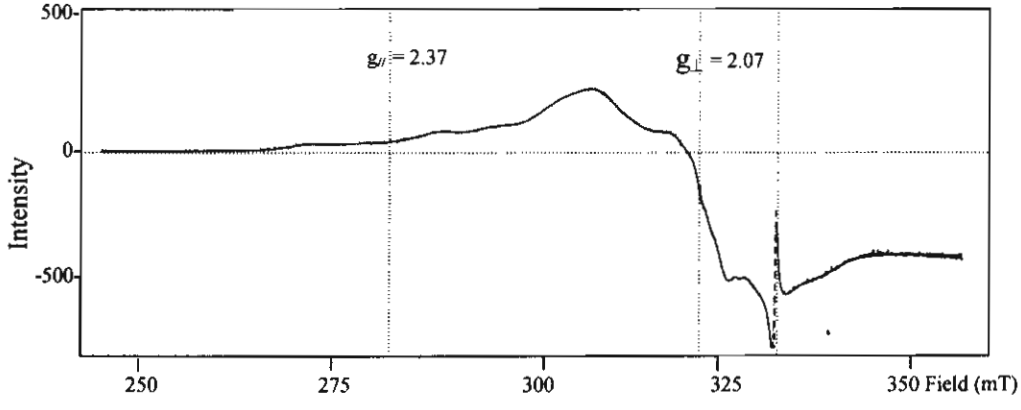

(j) The EPR spectrum at 77 K of $[Cu_2(dpyam)_2(\mu\text{-}C_2O_4)(NO_3)((CH_3)_2NCOH)_2]$ **(V)**

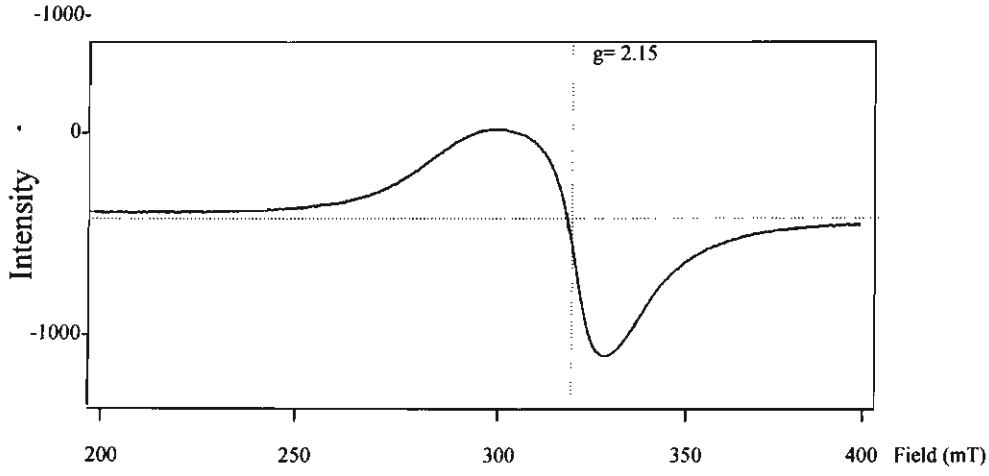

(k) The EPR spectrum at room temperature of $[Cu_2(dpyam)_2(\mu\text{-}C_2O_4)Cl_2]$ **(VI)**

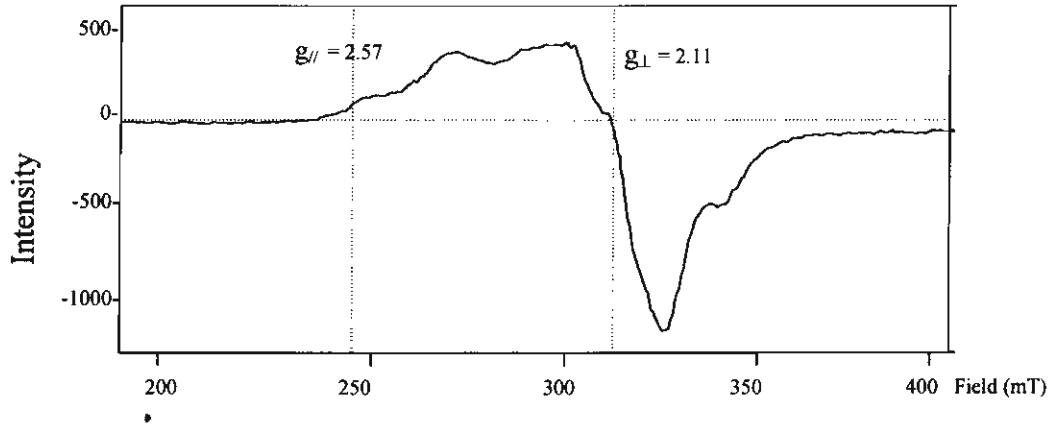

(l) The EPR spectrum at 77 K of $[Cu_2(dpyam)_2(\mu\text{-}C_2O_4)Cl_2]$ **(VI)**

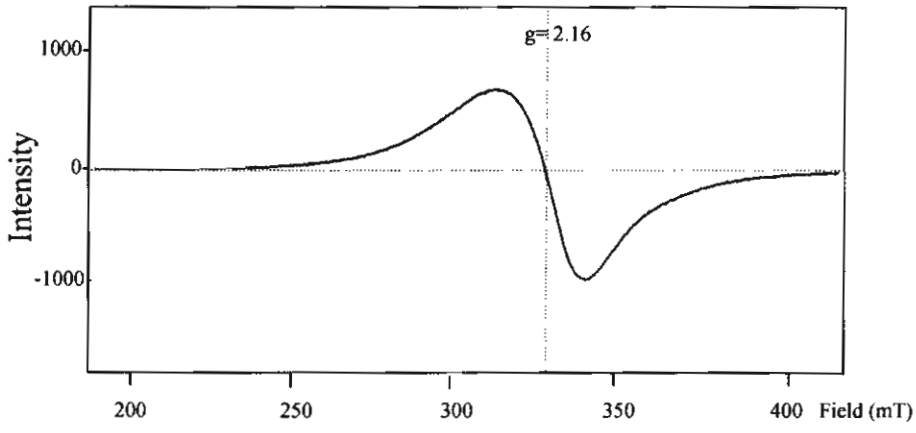

(m) The EPR spectrum at room temperature of $[Cu_2(dpyam)_2(\mu\text{-}C_2O_4)Br_2]$ **(VII)**

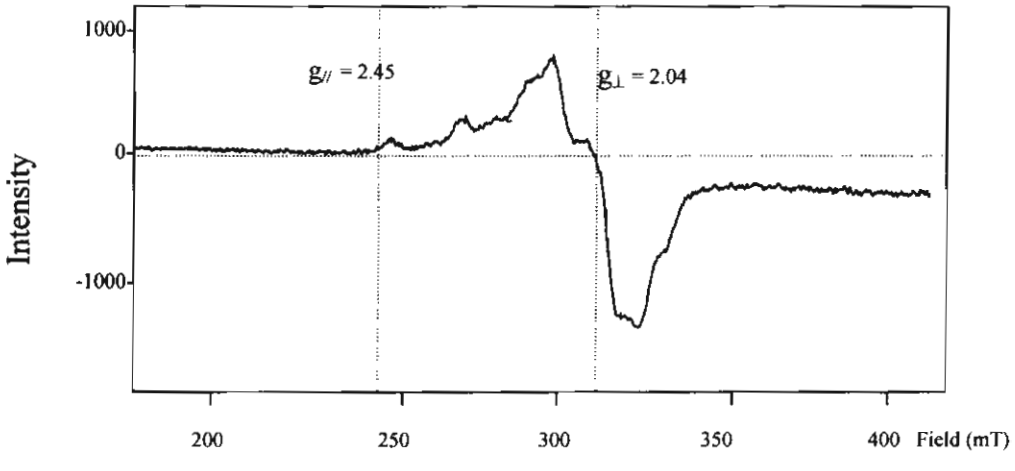

(n) The EPR spectrum at 77 K of $[Cu_2(dpyam)_2(\mu\text{-}C_2O_4)Br_2]$ **(VII)**

APPENDIX IIA

Crystal and Refinement Data for

$\{[Cu_3(dpyam)_3(\mu_3,\eta^3\text{-}HPO_4)(\mu_3,\eta^4\text{-}PO_4)(H_2O)](PF_6)\cdot 3H_2O\}_n$ (I)

$[Cu(dpyam)(\mu_2,\eta^3\text{-}HPO_4)]_n$ (II),

$[Cu(dpyam)(\mu_2,\eta^2\text{-}H_2PO_4)(H_2PO_4)]_2$ (III),

$[Cu_4(dpyam)_4(\mu_4,\eta^3\text{-}HPO_4)_2(\mu\text{-}Cl)_2](Cl)_2\cdot 6H_2O$ (IV),

$[Cu_4(dpyam)_4(\mu_4,\eta^3\text{-}HPO_4)_2(\mu\text{-}Br)_2](Br)_2\cdot 6H_2O$ (V) and

$[Cu_4(dpyam)_4(\mu_3,\eta^3\text{-}HPO_4)_2(NO_3)_2(H_2O)_2](NO_3)_2\cdot 2H_2O$ (VI)

Table 1 Crystal and refinement data for complexes **I-V**

Complexes	**I**	**II**	**III**	**IV**	**V**	**VI**
Formula weight	{[Cu_3(dpyam)$_3$ (μ_3,η^3 -HPO_4)(μ_3,η^4-PO_4) (H_2O)](PF_6)·3H_2O}$_n$ (**I**)	[Cu(dpyam)(μ_2,η^3-HPO_4)]$_n$ (**II**)	[Cu(dpyam) (μ_2,η^2-H_2PO_4) (H_2PO_4)]$_2$ (**III**)	[Cu_4(dpyam)$_4$(μ_4,η^3 -HPO_4)$_2$(μ-Cl)$_2$] (Cl)$_2$·6H_2O (**IV**)	[Cu_4(dpyam)$_4$(μ_4,η^3-HPO_4)$_2$(μ-Br)$_2$] (Br)$_2$·6H_2O (**V**)	[Cu_4(dpyam)$_4$(μ_3,η^3-HPO_4)$_2$(NO_3)$_2$ (H_2O)$_2$](NO_3)$_2$· 2H_2O (**VI**)
Molecular weight	1112.21	330.72	857.44	1380.85	1558.67	1451.02
T(K)	100(2) K	293(2)	293(2)	273(2)	273(2)	273(2)
Crystal system	Triclinic	Trigonal	Triclinic	monoclinic	monoclinic	monoclinic
Space group	P-1	P3/2	P-1	*Cm*	*Cm*	*C2/c*
a (Å)	7.4301(5)	9.6644(1)	8.0347(1)	16.3150(3)	16.4716(3)	28.4236(10)
b (Å)	15.9715(10)	9.6644(1)	10.0264(1)	48.2777(4)	49.3270(4)	9.7305(10)
c (Å)	17.4521(10)	10.6841(2)	10.5912(1)	12.5824(2)	12.6314(2)	22.7510(2)
α (°)	67.9970(10)	90	83.217(1)	90	90	90
β (°)	85.2240(10)	90	70.490(1)	125.9980(10)	126.2060(10)	118.183(10)
γ (°)	79.7430(10)	120	69.356(1)	90	90	90
V ($Å^3$)	1889.2(2) $Å^3$	864.21(2)	752.58(2)	8017.99(12)	8281.1(2)	5546.37(8)
Z	2	2	2	*4*	*4*	*8*
D_{calc} (*g* cm^{-3})	1.955 g.cm^{-3}	1.271	1.892	1.761	1.904	1.584
μ (mm)	1.907	1.365	1.712	1.908	4.548	1.650
F (000)	1122	334	434	4320	4752	2680
Crystal size (mm)	0.24 × 0.12 × 0.08	0.28 × 0.30 × 0.20	0.15 × 0.35 × 0.50	0.25 x 0.30 x 0.73	0.23 x 0.24 x 0.35	0.10 x 0.33 x 0.05
Reflection collected	16764	6496	5631	30204	31126	19678
Unique reflections	8741	3042	4101	17411	18172	7885
Observed ref. [I>2σ(I)]				11833		
Data/restraints /parameter	8741 / 0 / 712	3042/1/212	4101/0/269	17411 / 2 / 1306	18172/2/1085	7885/0/472
Goodness-of-fit	1.043	1.030	1.065	1.044	1.019	1.047
Final R indices	R1 = 0.0458,	*R1* = 0.0186	*R1* = 0.0261	R1 = 0.0364,	*R1* = 0.0796	*R1* = 0.0511
[I>2σ(I)]	wR2= 0.0903	*wR2* = 0.0451	*wR2* = 0.0752	wR2 = 0.0914	*wR2* = 0.01949	*wR2* = 0.0961
R indices (all data)	R1 = 0.0611, wR2= 0.0964	*R1* = 0.0192 *wR2* = 0.0452	*R1* = 0.0281 *wR2* = 0.0759	R1 = 0.0448, wR2 = 0.0981	*R1* = 0.11481 *wR2* = 0.2255	*R1* = 0.0977 *wR2* = 0.1144
Largest difference peak and hole (e $Å^{-3}$)	0.618,-0.508	0.252,-0.321	0.580,-0.509	1.981,-0.604	6.603,-1.298	0.956,-0.536

$$R = \Sigma||F_o| - |F_c||/\Sigma|F_o|, \quad R_w = [\Sigma w\{|F_o| - |F_c|\}^2/w|F_o|^2]^{1/2}$$

APPENDIX IIB

Selected Bond Lengths (Å) and Angles (°) for

$\{[Cu_3(dpyam)_3(\mu_3,\eta^3\text{-}HPO_4)(\mu_3,\eta^4\text{-}PO_4)(H_2O)](PF_6)\cdot 3H_2O\}_n$ (I)

$[Cu(dpyam)(\mu_2,\eta^3\text{-}HPO_4)]_n$ (II),

$[Cu(dpyam)(\mu_2,\eta^2\text{-}H_2PO_4)(H_2PO_4)]_2$ (III),

$[Cu_4(dpyam)_4(\mu_4,\eta^3\text{-}HPO_4)_2(\mu\text{-}Cl)_2](Cl)_2\cdot 6H_2O$ (IV),

$[Cu_4(dpyam)_4(\mu_4,\eta^3\text{-}HPO_4)_2(\mu\text{-}Br)_2](Br)_2\cdot 6H_2O$ (V) and

$[Cu_4(dpyam)_4(\mu_3,\eta^3\text{-}HPO_4)_2(NO_3)_2(H_2O)_2](NO_3)_2\cdot 2H_2O$ (VI)

Table 2 Selected bond lengths (Å) and angles (°) with e.s.d.s. in parentheses of $\{[Cu_3(dpyam)_3(\mu_3,\eta^3\text{-}HPO_4)(\mu_3,\eta^4\text{-}PO_4)(H_2O)](PF_6)\cdot 3H_2O\}_n$ **(I)**

Cu(3)-O(4A)	1.908(2)	Cu(3)-O(5)	1.924(2)
Cu(3)-N(8)	1.976(3)	Cu(3)-N(7)	1.985(3)
Cu(2)-O(2A)	1.920(2)	Cu(2)-O(7)	1.929(2)
Cu(2)-N(5)	1.978(3)	Cu(2)-N(4)	1.991(3)
Cu(1)-O(6)	1.942(2)	Cu(1)-O(1)	1.957(2)
Cu(1)-N(1)	2.008(3)	Cu(1)-N(2)	2.027(3)
Cu(1)-O(1W)	2.191(3)	P(2)-O(6)	1.515(2)
P(2)-O(8)	1.541(2)	P(2)-O(5)	1.547(2)
P(2)-O(7)	1.560(2)	P(1)-O(2)	1.516(2)
P(1)-O(4)	1.523(2)	P(1)-O(1)	1.524(2)
P(1)-O(3)	1.601(2)		
O(4A)-Cu(3)-O(5)	91.3(1)	O(4A)-Cu(3)-N(8)	148.0(1)
O(5)-Cu(3)-N(8)	94.4(1)	O(4A)-Cu(3)-N(7)	94.9(1)
O(5)-Cu(3)-N(7)	155.8(1)	N(8)-Cu(3)-N(7)	92.7(1)
O(2A)-Cu(2)-O(7)	98.7(1)	O(2A)-Cu(2)-N(5)	91.6(1)
O(7)-Cu(2)-N(5)	150.7(1)	O(2A)-Cu(2)-N(4)	140.3(1)
O(7)-Cu(2)-N(4)	97.1(1)	N(5)-Cu(2)-N(4)	92.1(1)
O(6)-Cu(1)-O(1)	97.3(1)	O(6)-Cu(1)-N(1)	91.9(1)
O(1)-Cu(1)-N(1)	166.9(1)	O(6)-Cu(1)-N(2)	132.8(1)
O(1)-Cu(1)-N(2)	91.6(1)	N(1)-Cu(1)-N(2)	89.0(1)
O(6)-Cu(1)-O(1W)	119.1(1)	O(1)-Cu(1)-O(1W)	85.4(1)
N(1)-Cu(1)-O(1W)	82.0(1)	N(2)-Cu(1)-O(1W)	107.7(1)
O(6)-P(2)-O(8)	111.2(1)	O(6)-P(2)-O(5)	108.9(1)
O(8)-P(2)-O(5)	108.8(1)	O(6)-P(2)-O(7)	110.4(1)
O(8)-P(2)-O(7)	107.6(1)	O(5)-P(2)-O(7)	109.9(1)
O(2)-P(1)-O(4)	113.0(1)	O(2)-P(1)-O(1)	112.4(1)
O(4)-P(1)-O(1)	114.3(1)	O(2)-P(1)-O(3)	102.6(1)
O(4)-P(1)-O(3)	105.1(1)	O(1)-P(1)-O(3)	108.3(1)

Table 3 Selected bond lengths (Å) and angles (°) with e.s.d.s. in parentheses of [Cu(dpyam)(μ_2,η^3-HPO_4)]$_n$ **(II)**

Cu(1)-O(4)	1.919(1)	Cu(1)-O(1)	1.946(1)
Cu(1)-N(1)	1.969(1)	Cu(1)-N(2)	1.994(1)
P(1)-O(3)	1.510(1)	P(1)-O(1)	1.519(1)
P(1)-O(4)A	1.531(1)	P(1)-O(2)	1.588(2)
Cu(1)-O(2)A	2.719(3)	Cu(1)-Cu(1)A	5.955(2)
O(4)-Cu(1)-O(1)	101.6(1)	O(4)-Cu(1)-N(1)	149.7(1)
O(1)-Cu(1)-N(1)	91.4(1)	O(4)-Cu(1)-N(2)	93.6(1)
O(1)-Cu(1)-N(2)	142.6(1)	O(1)-Cu(1)-N(2)	92.0(1)
O(3)-P(1)-O(1)	111.7(1)	O(3)-P(1)-O(4)A	111.1(1)
O(1)-P(1)-O(4)A	111.6(1)	O(3)-P(1)-O(2)	110.7(1)
O(1)-P(1)-O(2)	109.3(1)	O(4)A-P(1)-O(2)	101.9(1)

Symmetry code: A = –x+y+1, -x+1,z+1/3

Table 4 Selected bond lengths (Å) and angles (°) with e.s.d.s. in parentheses of $[Cu(dpyam)(\mu_2,\eta^2\text{-}H_2PO_4)(H_2PO_4)]_2$ **(III)**

Cu(1)-O(8A)	1.964(1)	Cu(1)-O(5)	1.987(1)
Cu(1)-N(1)	1.991(1)	Cu(1)-N(2)	1.997(1)
Cu(1)-O(1)	2.271(1)	P(1)-O(1)	1.512(1)
P(1)-O(3)	1.519(1)	P(1)-O(4)	1.558(1)
P(1)-O(2)	1.581(1)	P(2)-O(8)	1.506(1)
P(2)-O(5)	1.518(1)	P(2)-O(7)	1.558(1)
P(2)-O(6)	1.564(1)	Cu(1)-Cu(1)A	5.136(2)
O(8)A-Cu(1)-O(5)	89.7(1)	O(8)A-Cu(1)-N(1)	89.0(1)
O(5)-Cu(1)-N(1)	174.1(1)	O(8)A-Cu(1)-N(2)	167.0(1)
O(5)-Cu(1)-N(2)	91.8(1)	N(1)-Cu(1)-N(2)	88.1(1)
O(8)A-Cu(1)-O(1)	96.0(1)	O(5)-Cu(1)-O(1)	91.9(1)
N(1)-Cu(1)-O(1)	94.1(1)	N(2)-Cu(1)-O(1)	96.8(1)
O(1)-P(1)-O(3)	115.1(1)	O(1)-P(1)-O(4)	112.2(1)
O(3)-P(1)-O(4)	106.9(1)	O(1)-P(1)-O(2)	109.2(1)
O(3)-P(1)-O(2)	108.5(1)	O(4)-P(1)-O(2)	104.1(1)
O(8)-P(2)-O(5)	115.6(1)	O(8)-P(2)-O(7)	109.6(1)
O(5)-P(2)-O(7)	105.9(1)	O(8)-P(2)-O(6)	112.6(1)
O(5)-P(2)-O(6)	105.6(1)	O(7)-P(2)-O(6)	106.8(1)
P(2)-O(5)-Cu(1)	130.9(1)	P(1)-O(1)-Cu(1)	122.9(1)

Symmetry code: A = -x+1, -y+1, -z+1

Table 5 Selected bond lengths (Å) and angles (°) with e.s.d.s. in parentheses of $[Cu_4(dpyam)_4(\mu_4,\eta^3\text{-}HPO_4)_2(\mu\text{-}Cl)_2](Cl)_2\cdot 6H_2O$ **(IV)**

Cu(6)-N(17)	1.962(4)	Cu(6)-N(16)	1.965(4)
Cu(6)-O(9)	2.011(3)	Cu(6)-O(12)	2.021(3)
Cu(6)-Cl(4)	2.604(3)	Cu(6)-Cu(6A)	2.802(3)
Cu(5)-O(10)	1.947(3)	Cu(5)-O(13)	1.966(3)
Cu(5)-N(14)	1.993(4)	Cu(5)-N(13)	2.012(4)
Cu(5)-Cl(3)	2.560(3)	Cu(4)-N(10)	1.970(4)
Cu(4)-N(11)	1.982(4)	Cu(4)-O(7)	2.012(3)
Cu(4)-O(3)	2.026(3)	Cu(4)-Cl(2)	2.592(3)
Cu(3)-N(8)	1.971(4)	Cu(3)-N(7)	1.981(4)
Cu(3)-O(7)	2.012(3)	Cu(3)-O(3)	2.030(3)
Cu(3)-Cl(2)	2.598(3)	Cu(3)-Cu(4)	2.816(3)
Cu(2)-O(6)	1.950(3)	Cu(2)-O(2)	1.969(3)
Cu(2)-N(5)	1.996(4)	Cu(2)-N(4)	2.009(4)
Cu(2)-Cl(1)	2.556(3)	Cu(1)-O(5)	1.948(3)
Cu(1)-O(1)	1.965(3)	Cu(1)-N(1)	1.993(3)
Cu(1)-N(2)	2.001(4)	Cu(1)-Cl(1)	2.551(3)
P(3)-O(11)	1.565(4)	P(3)-O(10)	1.509(3)
P(3)-O(9)	1.553(5)	P(4)-O(12)	1.558(4)
P(4)-O(13)	1.512(3)	P(2)-O(6)	1.503(3)
P(4)-O(14)	1. 587(5)	P(2)-O(7)	1.560(3)
P(2)-O(5)	1.504(3)	P(1)-O(2)	1.499(3)
P(2)-O(8)	1.580(3)	P(1)-O(3)	1.563(3)
P(1)-O(1)	1.501(3)	Cu(5)-Cu(5A)	3.917(3)
P(1)-O(4)	1.584(3)	Cu(6)-Cu(6A)	2.802(1)
Cu(1)-Cu(2)	3.882(3)	Cu(5A)-Cu(6A)	5.232(3)
Cu(3)-Cu(4)	2.8163(6)	Cu(2)-Cu(4)	4.027(3)
N(17)-Cu(6)-N(16)	91.4(2)	O(10)-Cu(5)-O(13)	91.8(2)
N(16)-Cu(6)-O(9)	171.7(2)	O(10)-Cu(5)-N(14)	164.0(2)
N(17)-Cu(6)-O(12)	172.9(2)	O(13)-Cu(5)-N(13)	162.5(2)
O(9)-Cu(6)-O(12)	78.9(2)	N(14)-Cu(5)-N(13)	87.4(2)
N(10)-Cu(4)-N(11)	90.6(2)	O(6)-Cu(2)-O(2)	91.6(2)
N(11)-Cu(4)-O(7)	171.6(2)	O(6)-Cu(2)-N(5)	162.6(2)
N(10)-Cu(4)-O(3)	173.3(2)	O(2)-Cu(2)-N(4)	164.8(2)
O(7)-Cu(4)-O(3)	79.0(2)	N(5)-Cu(2)-N(4)	87.3(2)
N(8)-Cu(3)-N(7)	91.3(2)	O(5)-Cu(1)-O(1)	91.6(2)
N(7)-Cu(3)-O(7)	171.7(2)	O(5)-Cu(1)-N(1)	164.5(2)
N(8)-Cu(3)-O(3)	173.4(2)	O(1)-Cu(1)-N(2)	161.3(2)
O(7)-Cu(3)-O(3)	78.9(2)	N(1)-Cu(1)-N(2)	87.1(2)

Table 6 Selected bond lengths (Å) and angles (°) with e.s.d.s. in parentheses of $[Cu_4(dpyam)_4(\mu_4,\eta^3\text{-}HPO_4)_2(\mu\text{-}Br)_2](Br)_2\cdot 6H_2O$ **(V)**

Br(4)-Cu(6)	2.766(2)	O(10)- Cu(5)- N(13)	163.3(4)
Cu(6)- N(16)	1.960(9)	O(13)- Cu(5)- N(13)	87.9(4)
Cu(6)- N(17)	1.977(9)	N(14)- Cu(5)- N(13)	87.5(4)
Cu(6)- O(12)	2.039(8)	N(10)- Cu(4)- N(11)	90.9(4)
Cu(6)- O(9)	2.045(7)	N(10)- Cu(4)- O(7)	97.2(4)
Cu(6)- Cu(6A)	2.834(2)	N(11)- Cu(4)- O(7)	170.8(4)
Cu(5)- O(10)	1.937(9)	N(10)- Cu(4)- O(3)	174.2(4)
Cu(5)- O(13)	1.974(9)	N(10)- Cu(4)- Cu(3)	132.8(3)
Cu(5)- N(14)	2.008(10)	N(11)- Cu(4)- Cu(3)	130.6(3)
Cu(5)- N(13)	2.019(10)	O(5)- Cu(1)- N(1)	165.3(4)
Cu(5)- Br(3)	2.7077(19)	O(1)- Cu(1)- N(2)	162.3(4)
Cu(4)- N(10)	1.981(10)	O(2)- Cu(2)- O(6)	91.8(4)
Cu(4)- N(11)	1.998(10)	O(2)- Cu(2)- N(5)	88.6(4)
Cu(4)- O(7)	2.005(7)	O(6)- Cu(2)- N(5)	164.5(4)
Cu(4)- O(3)	2.029(8)	O(2)- Cu(2)- N(4)	164.9(4)
Cu(4)- Br(2)	2.7450(19)	N(8)- Cu(3)- O(7)	97.4(4)
Cu(4)- Cu(3)	2.8507(17)	N(8)- Cu(3)- N(7)	90.9(4)
Cu(1)- O(1)	1.974(7)	O(7)- Cu(3)- N(7)	170.8(4)
Cu(1)- O(5)	1.988(8)	N(8)- Cu(3)- O(3)	175.1(4)
Cu(1)- N(1)	2.003(10)	O(7)- Cu(3)- O(3)	78.6(3)
Cu(1)- N(2)	2.021(10)	N(7)- Cu(3)- O(3)	92.9(4)
Cu(1)- Br(1)	2.7154(19)	N(8)- Cu(3)- Cu(4)	132.8(3)
Cu(2)- O(2)	1.970(8)	O(7)- Cu(3)- Cu(4)	44.7(2)
Cu(2)- O(6)	1.979(8)	N(7)- Cu(3)- Cu(4)	130.0(3)
Cu(2)- N(5)	1.987(10)	O(3)- Cu(3)- Cu(4)	45.4(2)
Cu(2)- N(4)	2.023(9)	Cu(4)- Br(2)- Cu(3)	62.40(5)
Cu(2)- Br(1)	2.7199(19)	O(13)- P(4)- O(13A)	115.3(7)
Cu(3)- N(8)	1.984(10)	O(13)- P(4)- O(12)	111.3(4)
Cu(3)- O(7)	1.993(7)	O(13)- P(4)- O(14)	108.0(5)
Cu(3)- N(7)	2.005(10)	O(12)- P(4)- O(14)	101.9(7)
Cu(3)- O(3)	2.033(8)	O(10)- P(3)- O(10A)	115.8(7)
Cu(3)- Br(2)	2.7577(18)	O(10)- P(3)- O(9)	109.8(4)
P(4)- O(13)	1.506(8)	O(10)- P(3)- O(11)	110.3(4)
P(4)- O(12)	1.555(11)	O(9)- P(3)- O(11)	99.8(8)
P(4)- O(14)	1.612(12)	O(5)- P(2)- O(6)	116.7(6)
P(3)- O(10)	1.523(8)	O(5)- P(2)- O(7)	111.4(4)
P(3)- O(9)	1.529(11)	O(6)- P(2)- O(7)	110.6(5)
P(3)- O(11)	1.544(14)	O(5)- P(2)- O(8)	107.1(5)
P(2)- O(5)	1.475(8)	O(6)- P(2)- O(8)	106.3(5)
P(2)- O(6)	1.492(8)	O(7)- P(2)- O(8)	103.7(5)
P(2)- O(7)	1.589(9)	O(1)- P(1)- O(2)	117.9(5)
P(2)- O(8)	1.629(10)	O(1)- P(1)- O(4)	109.6(5)
P(1)- O(1)	1.497(7)	O(2)- P(1)- O(4)	109.5(5)
P(1)- O(2)	1.510(7)	O(2)- P(1)- O(3)	108.2(5)
P(1)- O(4)	1.533(10)	O(4)- P(1)- O(3)	102.3(6)
P(1)- O(3)	1.599(10)		
N(17)- Cu(6)- O(12)	173.1(4)		
N(16)- Cu(6)- O(9)	173.2(4)		
O(13)- Cu(5)- N(14)	165.0(4)		

Table 7 Selected bond lengths (Å) and angles (°) with e.s.d.s. in parentheses of $[Cu_4(dpyam)_4(\mu_3,\eta^3\text{-}HPO_4)_2(NO_3)_2(H_2O)_2](NO_3)_2\cdot 2H_2O$ **(VI)**

Cu(1)-O(6)	1.972(2)	Cu(1)-O(4)	1.968(2)
Cu(1)-N(1)	1.967(2)	Cu(1)-N(2)	2.001(3)
Cu(1)-O(7)	2.497(2)	Cu(2)-O(7)	1.933(2)
Cu(2)-N(5)	2.013(3)	Cu(2)-N(4)	1.979(3)
Cu(2)-O(10)	2.145(2)	Cu(2)-O(11)	2.152(3)
Cu(2)-O(9)	2.743(2)	Cu(1)...Cu(2)	4.136(2)
Cu(1)...Cu(2A)	4.895(2)	Cu(1)...Cu(1A)	4.560(2)
Cu(2)...Cu(2A)	7.833(2)	P(1)-O(7)	1.525(2)
P(1)-O(4A)	1.526(2)	P(1)-O(6)	1.542(2)
P(1)- O(5)	1.574(2)	N(8)-O(8)	1.233(4)
N(8)-O(9)	1.249(4)	N(8)-O(10)	1.283(3)
N(1)-Cu(1)-O(6)	161.7(1)	O(4)-Cu(1)-N(2)	142.4(1)
O(6)-Cu(1)-N(2)	95.3(1)	O(7)-Cu(2)-N(5)	90.6(1)
N(5)-Cu(2)-N(4)	89.6(1)	O(7)-Cu(2)-O(10)	91.8(1)
N(5)-Cu(2)-O(10)	137.5(1)	N(4)-Cu(2)-O(10)	95.5(1)
O(7)-Cu(2)-O(11)	86.4(1)	N(5)-Cu(2)-O(11)	131.1(1)
N(4)-Cu(2)-O(11)	84.7(1)		

A; –x +2, -y, -z +1

APPENDIX IIC

The Infrared Spectra for

$\{[Cu_3(dpyam)_3(\mu_3,\eta^3\text{-}HPO_4)(\mu_3,\eta^4\text{-}PO_4)(H_2O)](PF_6)\cdot 3H_2O\}_n$ (I)

$[Cu(dpyam)(\mu_2,\eta^3\text{-}HPO_4)]_n$ (II),

$[Cu(dpyam)(\mu_2,\eta^2\text{-}H_2PO_4)(H_2PO_4)]_2$ (III),

$[Cu_4(dpyam)_4(\mu_4,\eta^3\text{-}HPO_4)_2(\mu\text{-}Cl)_2](Cl)_2\cdot 6H_2O$ (IV),

$[Cu_4(dpyam)_4(\mu_4,\eta^3\text{-}HPO_4)_2(\mu\text{-}Br)_2](Br)_2\cdot 6H_2O$ (V) and

$[Cu_4(dpyam)_4(\mu_3,\eta^3\text{-}HPO_4)_2(NO_3)_2(H_2O)_2](NO_3)_2\cdot 2H_2O$ (VI)

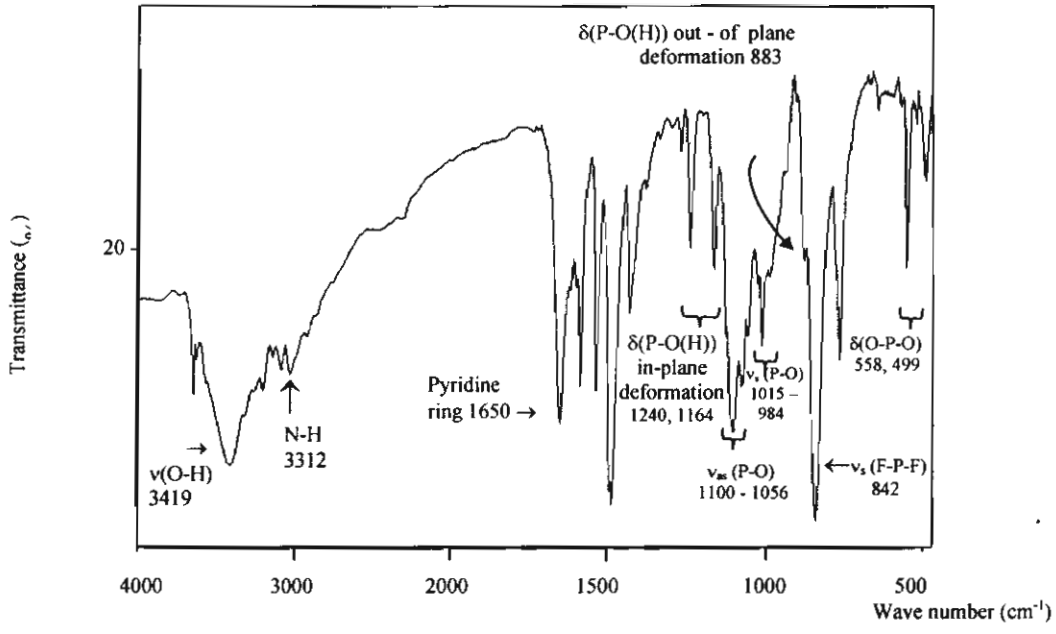

(a) The infrared spectrum of $\{[Cu_3(dpyam)_3(\mu_3,\eta^3\text{-}HPO_4)(\mu_3,\eta^4\text{-}PO_4)(H_2O)](PF_6)\cdot 3H_2O\}_n$ **(I)**

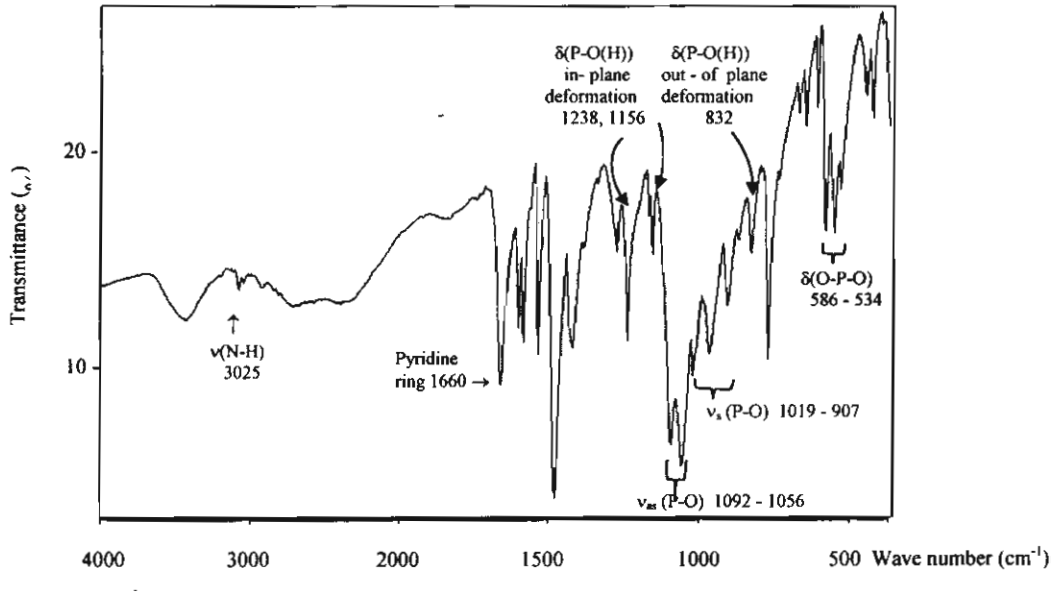

(b) The IR spectrum of $[Cu(dpyam)(\mu_2,\eta^3\text{-}HPO_4)]_n$ **(II)**

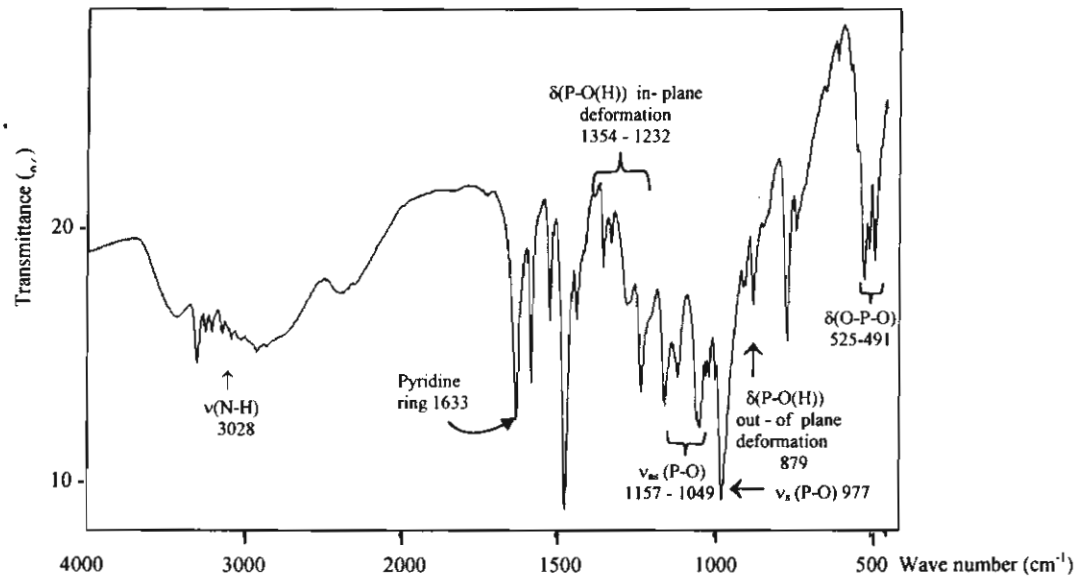

(c) The IR spectrum of $[Cu(dpyam)(\mu_2,\eta^2\text{-}H_2PO_4)(H_2PO_4)]_2$ **(III)**

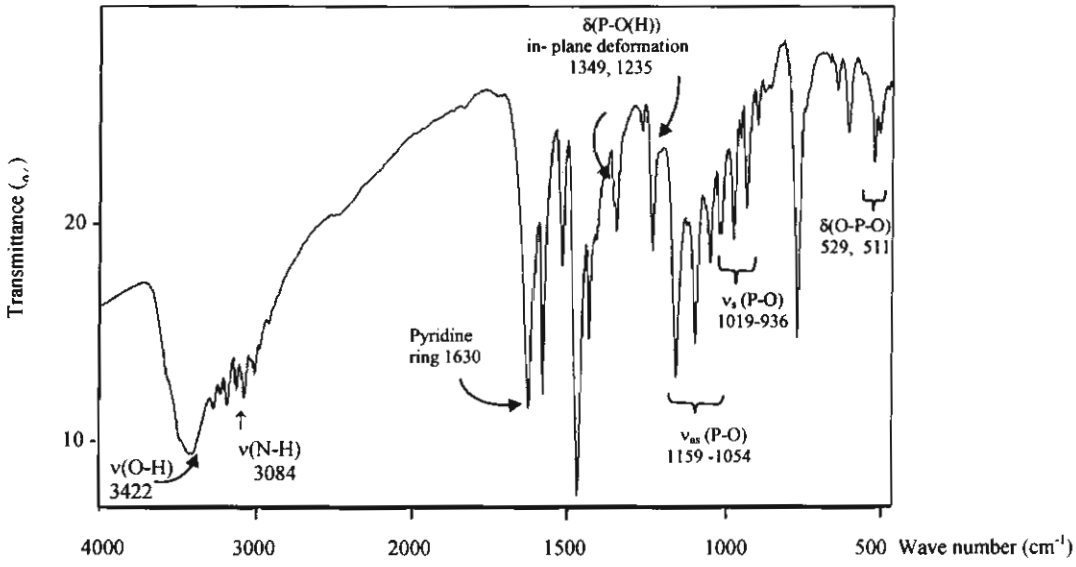

(d) The infrared spectrum of $[Cu_4(dpyam)_4(\mu_4,\eta^3\text{-}HPO_4)_2(\mu\text{-}Cl)_2](Cl)_2\cdot 6H_2O$ **(IV)**

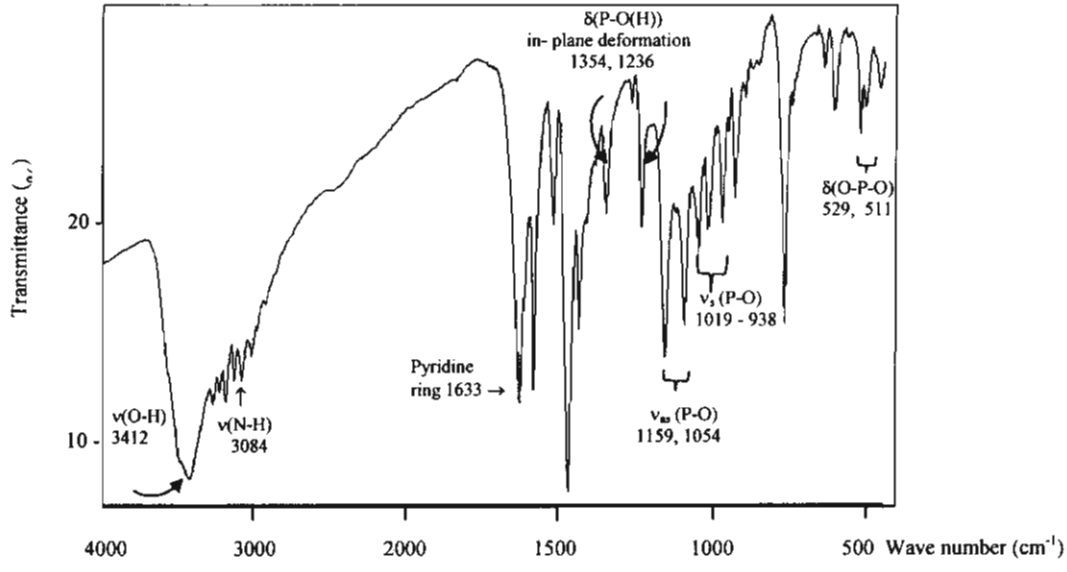

(e) The IR spectrum of $[Cu_4(dpyam)_4(\mu_4,\eta^3\text{-}HPO_4)_2(\mu\text{-}Br)_2](Br)_2{\cdot}6H_2O$ **(V)**

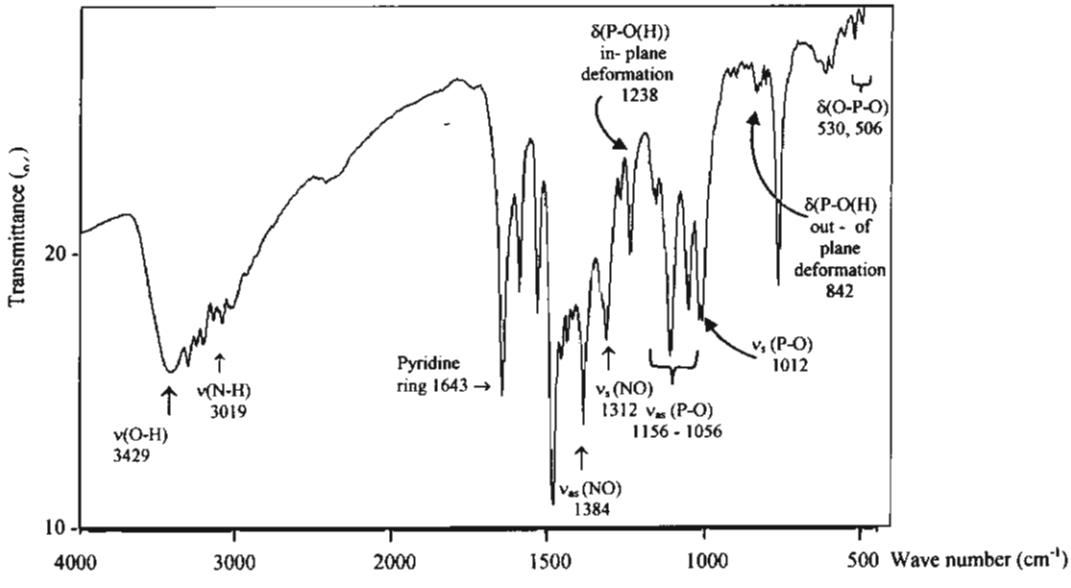

(f) The IR spectrum of $[Cu_4(dpyam)_4(\mu_3,\eta^3\text{-}HPO_4)_2(NO_3)_2(H_2O)_2](NO_3)_2{\cdot}2H_2O$ **(VI)**

APPENDIX IID

The Thermal Analysis for

$\{[Cu_3(dpyam)_3(\mu_3,\eta^3\text{-}HPO_4)(\mu_3,\eta^4\text{-}PO_4)(H_2O)](PF_6)\cdot 3H_2O\}_n$ (I)

$[Cu(dpyam)(\mu_2,\eta^3\text{-}HPO_4)]_n$ (II),

$[Cu(dpyam)(\mu_2,\eta^2\text{-}H_2PO_4)(H_2PO_4)]_2$ (III),

$[Cu_4(dpyam)_4(\mu_4,\eta^3\text{-}HPO_4)_2(\mu\text{-}Cl)_2](Cl)_2\cdot 6H_2O$ (IV),

$[Cu_4(dpyam)_4(\mu_4,\eta^3\text{-}HPO_4)_2(\mu\text{-}Br)_2](Br)_2\cdot 6H_2O$ (V) and

$[Cu_4(dpyam)_4(\mu_3,\eta^3\text{-}HPO_4)_2(NO_3)_2(H_2O)_2](NO_3)_2\cdot 2H_2O$ (VI)

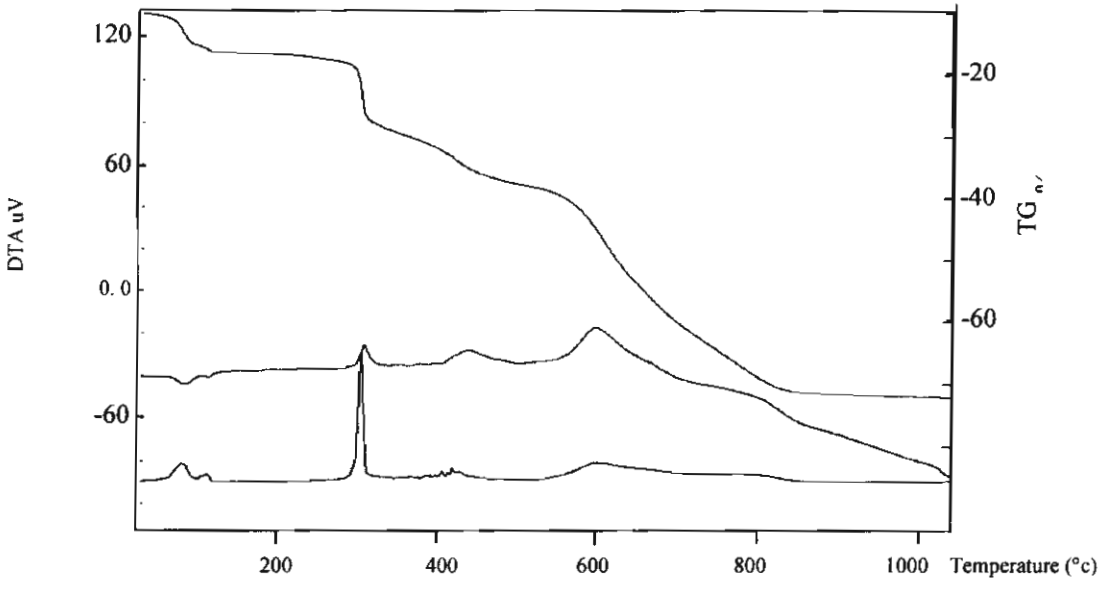

(a) The TG-DTA curve of $\{[Cu_3(dpyam)_3(\mu_3,\eta^3\text{-}HPO_4)(\mu_3,\eta^4\text{-}PO_4)(H_2O)](PF_6)\cdot 3H_2O\}_n$ **(I)**

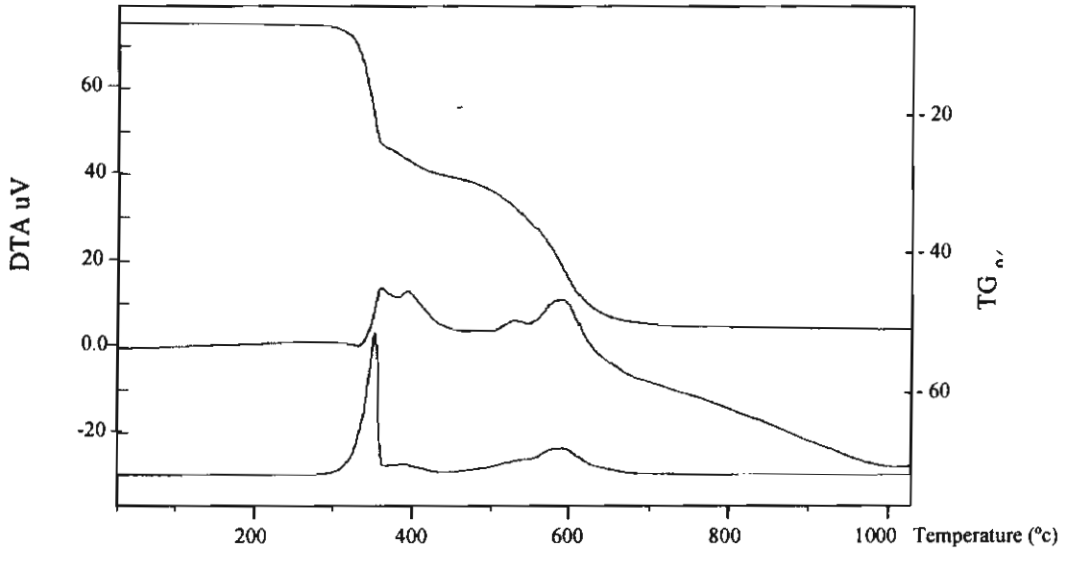

(b) The TG-DTA curve of $[Cu(dpyam)(\mu_2,\eta^3\text{-}HPO_4)]_n$ **(II)**

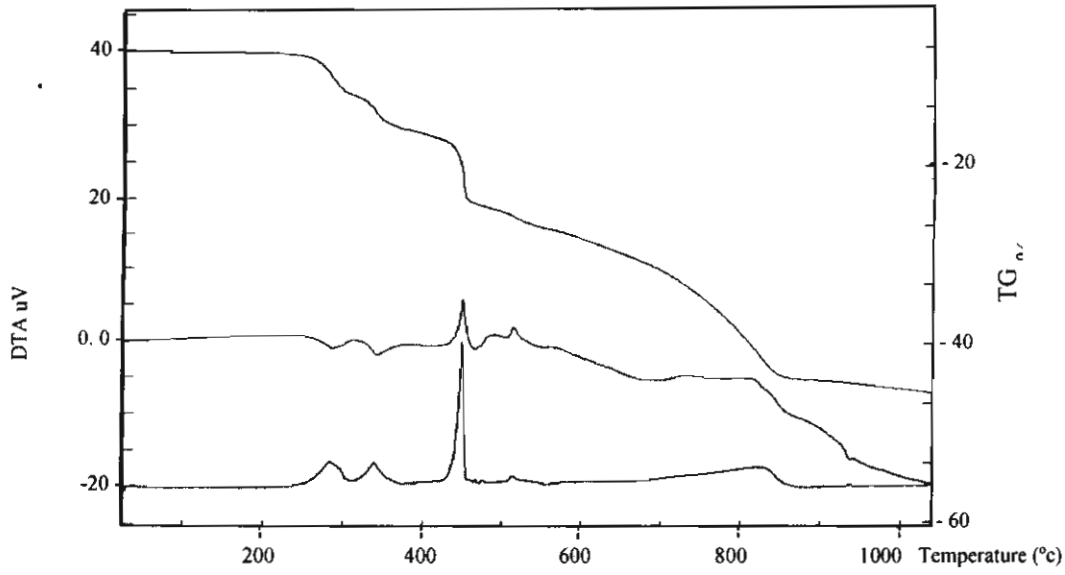

(c) The TG-DTA curve of $[Cu(dpyam)(\mu_2,\eta^2\text{-}H_2PO_4)(H_2PO_4)]_2$ **(III)**

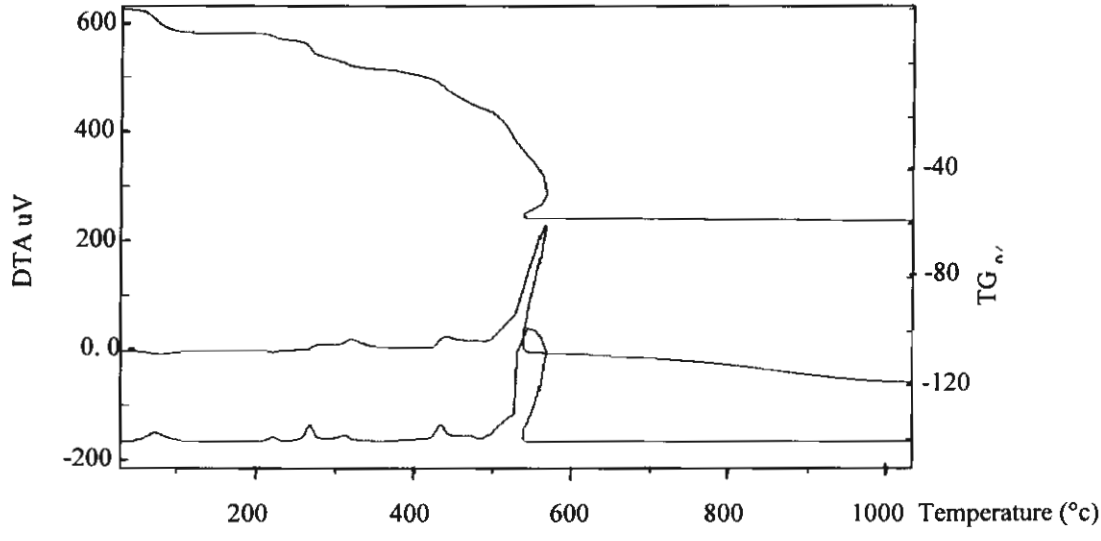

(d) The TG-DTA curve of $[Cu_4(dpyam)_4(\mu_4,\eta^3\text{-}HPO_4)_2(\mu\text{-}Cl)_2](Cl)_2{\cdot}6H_2O$ **(IV)**

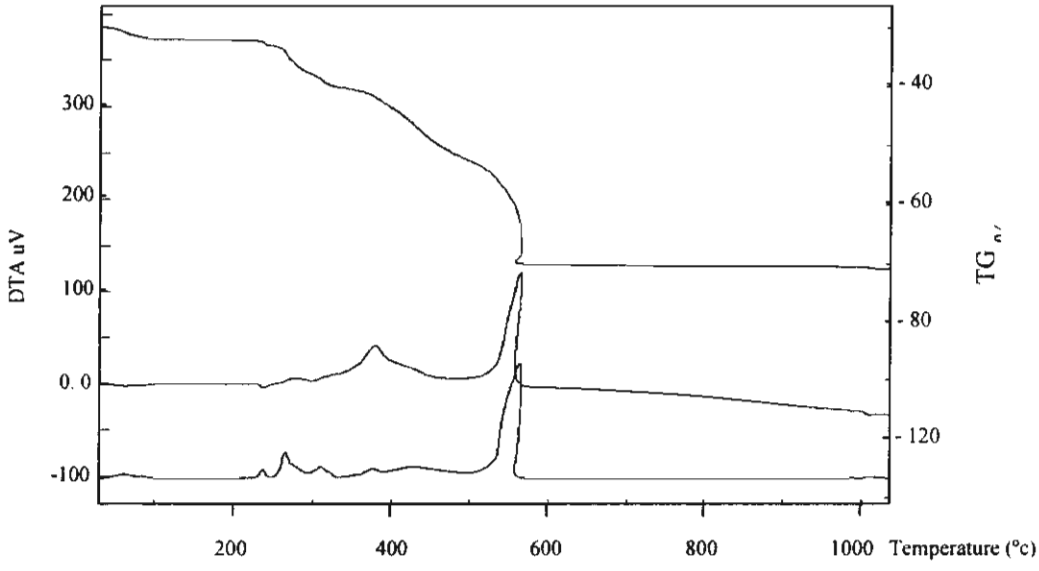

(e) The TG-DTA curve of $[Cu_4(dpyam)_4(\mu_4,\eta^3\text{-}HPO_4)_2(\mu\text{-}Br)_2](Br)_2 \cdot 6H_2O$ **(V)**

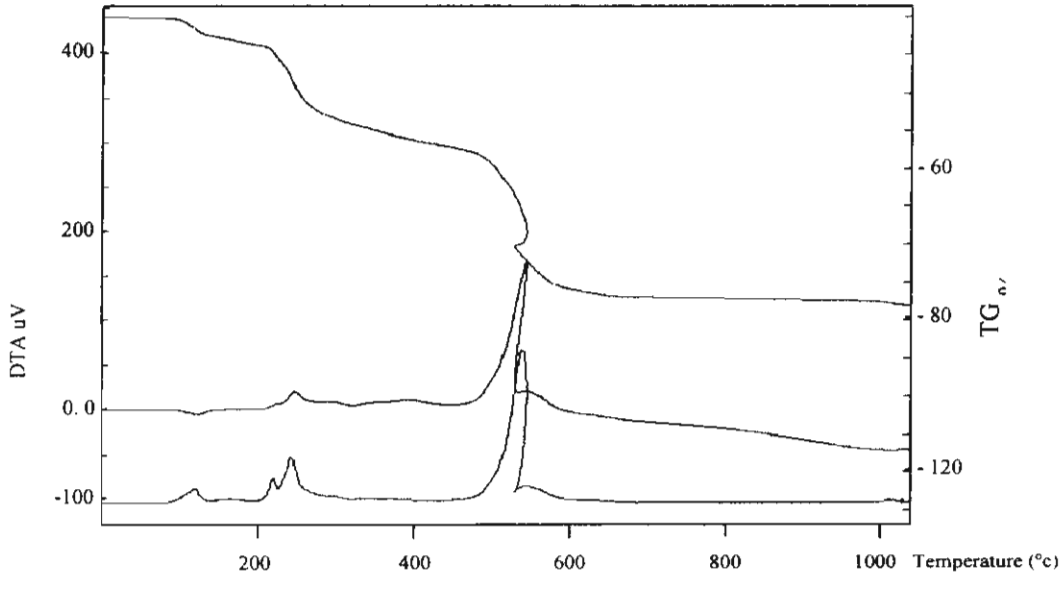

(f) The TG-DTA curve of $[Cu_4(dpyam)_4(\mu_3,\eta^3\text{-}HPO_4)_2(NO_3)_2(H_2O)_2](NO_3)_2 \cdot 2H_2O$ **(VI)**

APPENDIX IIE

The EPR Spectra for

$\{[Cu_3(dpyam)_3(\mu_3,\eta^3\text{-}HPO_4)(\mu_3,\eta^4\text{-}PO_4)(H_2O)](PF_6)\cdot 3H_2O\}_n$ (I)

$[Cu(dpyam)(\mu_2,\eta^3\text{-}HPO_4)]_n$ (II),

$[Cu(dpyam)(\mu_2,\eta^2\text{-}H_2PO_4)(H_2PO_4)]_2$ (III),

$[Cu_4(dpyam)_4(\mu_4,\eta^3\text{-}HPO_4)_2(\mu\text{-}Cl)_2](Cl)_2\cdot 6H_2O$ (IV) ,

$[Cu_4(dpyam)_4(\mu_4,\eta^3\text{-}HPO_4)_2(\mu\text{-}Br)_2](Br)_2\cdot 6H_2O$ (V) and

$[Cu_4(dpyam)_4(\mu_3,\eta^3\text{-}HPO_4)_2(NO_3)_2(H_2O)_2](NO_3)_2\cdot 2H_2O$ (VI)

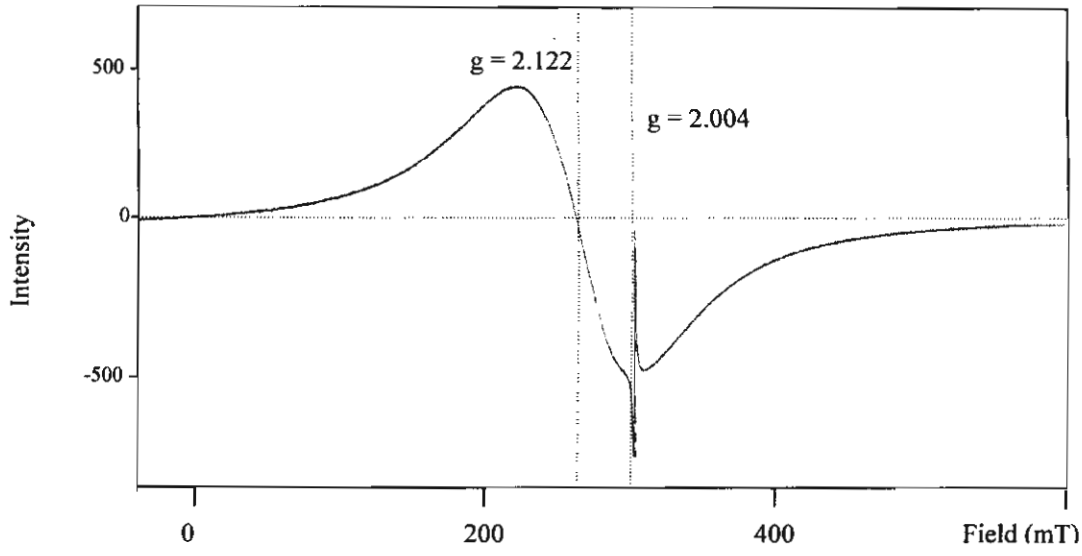

(a) The EPR spectrum at room temperature of $\{[Cu_3(dpyam)_3(\mu_3,\eta^3\text{-}HPO_4)(\mu_3,\eta^4\text{-}PO_4)(H_2O)](PF_6)\cdot 3H_2O\}_n$ **(I)**

(b)

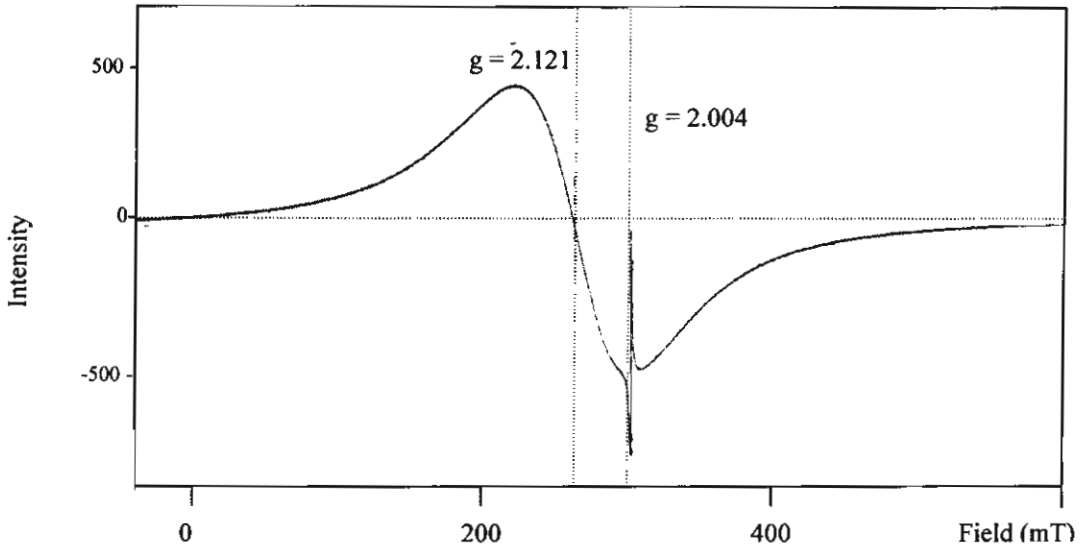

(b) The EPR spectrum at 77K of $\{[Cu_3(dpyam)_3(\mu_3,\eta^3\text{-}HPO_4)(\mu_3,\eta^4\text{-}PO_4)(H_2O)](PF_6)\cdot 3H_2O_n$ **(I)**

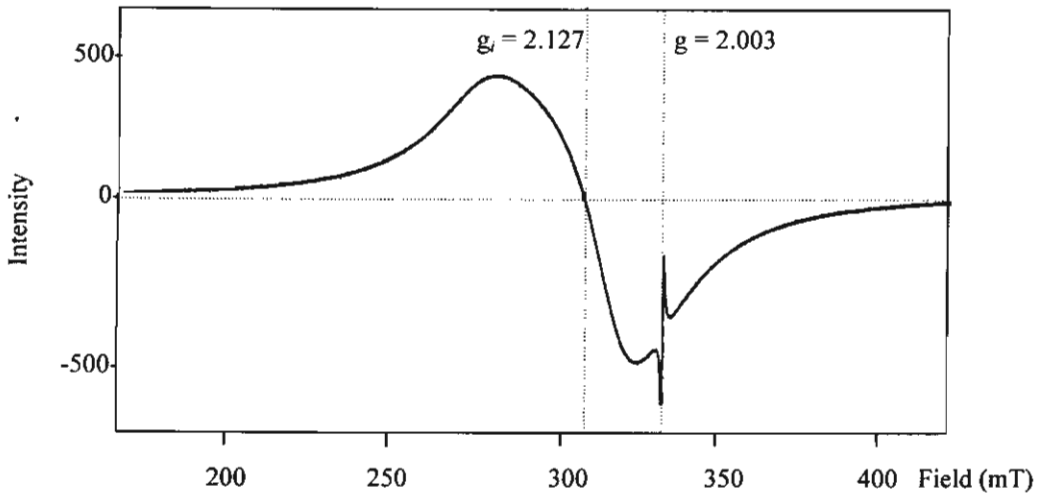

(c) The EPR spectrum at room temperature of $[Cu(dpyam)(\mu_2,\eta^3\text{-}HPO_4)]_n$ **(II)**

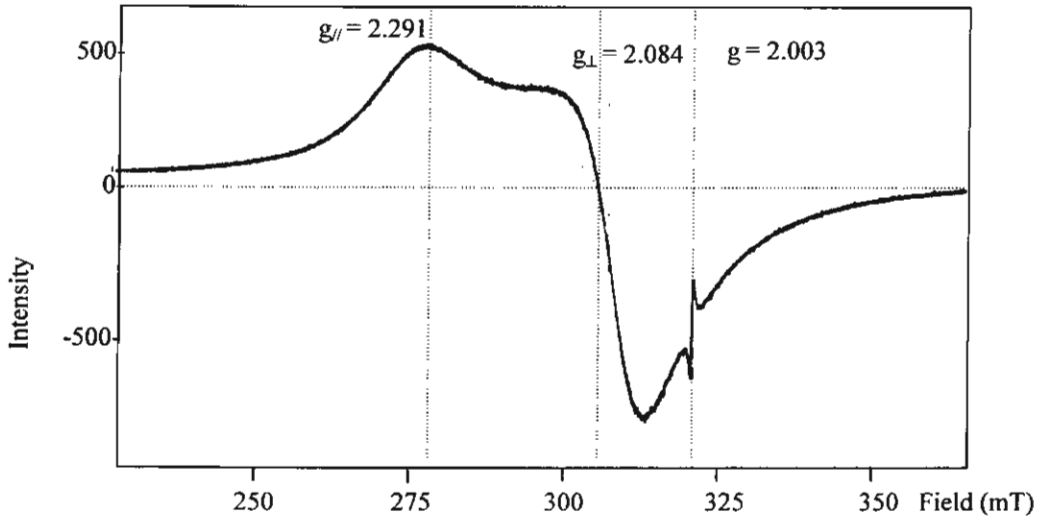

(d) The EPR spectrum at 77K of $[Cu(dpyam)(\mu_2,\eta^3\text{-}HPO_4)]_n$ **(II)**

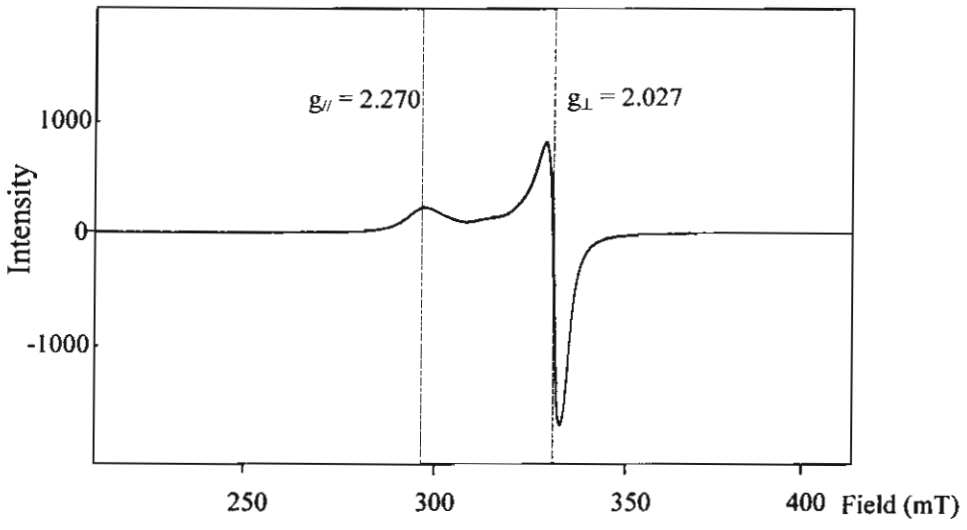

(e) The EPR spectrum at room temperature of $[Cu(dpyam)(\mu_2,\eta^2\text{-}H_2PO_4)(H_2PO_4)]_2$ **(III)**

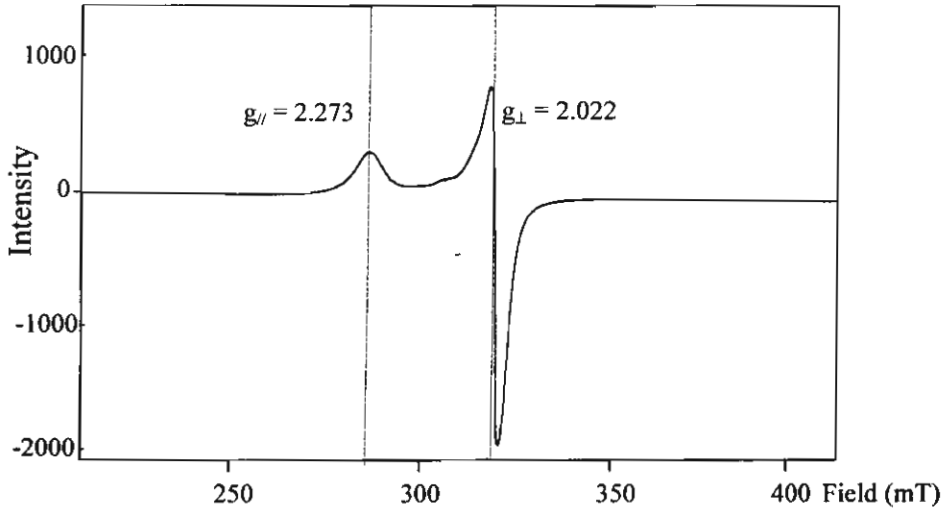

(f) The EPR spectrum at 77K of $[Cu(dpyam)(\mu_2,\eta^2\text{-}H_2PO_4)(H_2PO_4)]_2$ **(III)**

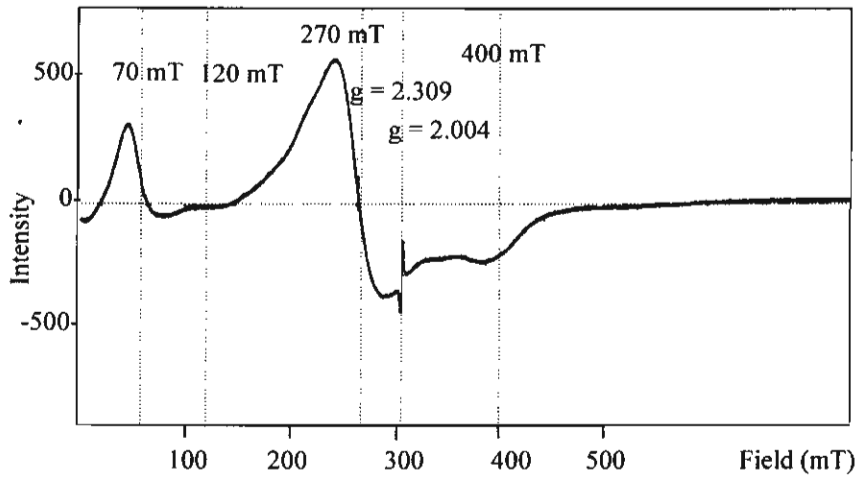

(g) The EPR spectrum at room temperature of $[Cu_4(dpyam)_4(\mu_4,\eta^3\text{-}HPO_4)_2(\mu\text{-}Cl)_2](Cl)_2{\cdot}6H_2O$ **(IV)**

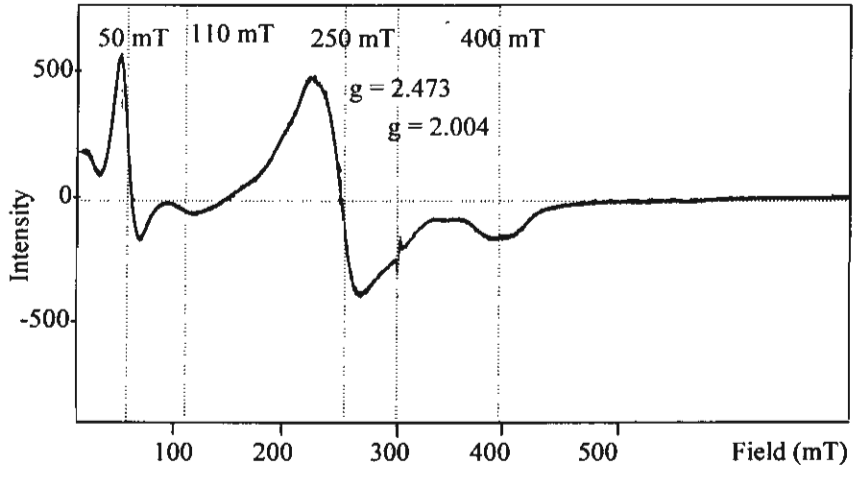

(h) The EPR spectrum at 77K of $[Cu_4(dpyam)_4(\mu_4,\eta^3\text{-}HPO_4)_2(\mu\text{-}Cl)_2](Cl)_2{\cdot}6H_2O$ **(IV)**

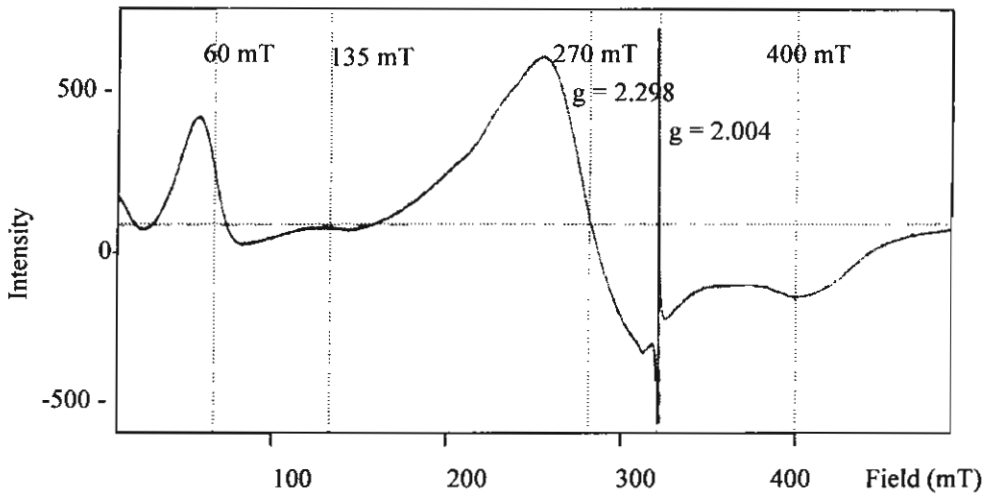

(i) The EPR spectrum at room temperature of $[Cu_4(dpyam)_4(\mu_4,\eta^3\text{-}HPO_4)_2(\mu\text{-}Br)_2](Br)_2{\cdot}6H_2O$ **(V)**

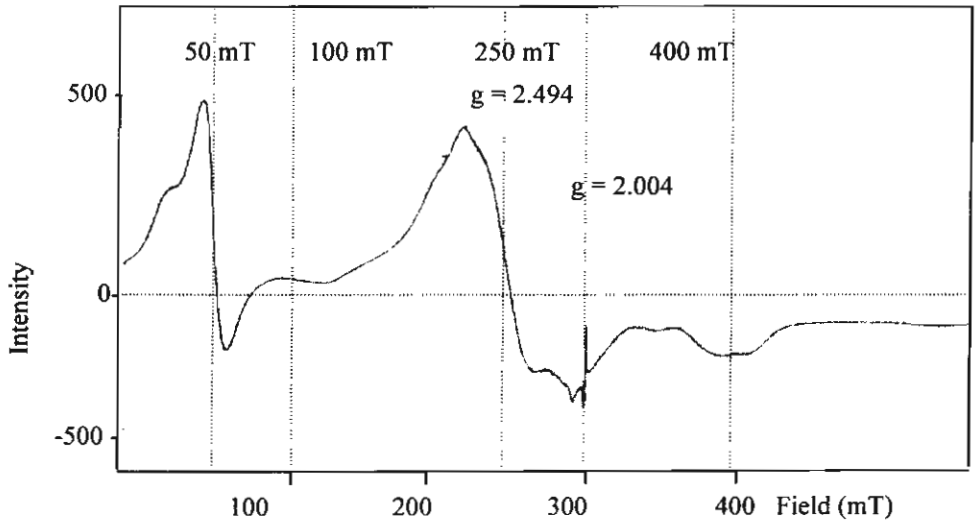

(j) The EPR spectrum at 77K of $[Cu_4(dpyam)_4(\mu_4,\eta^3\text{-}HPO_4)_2(\mu\text{-}Br)_2](Br)_2{\cdot}6H_2O$ **(V)**

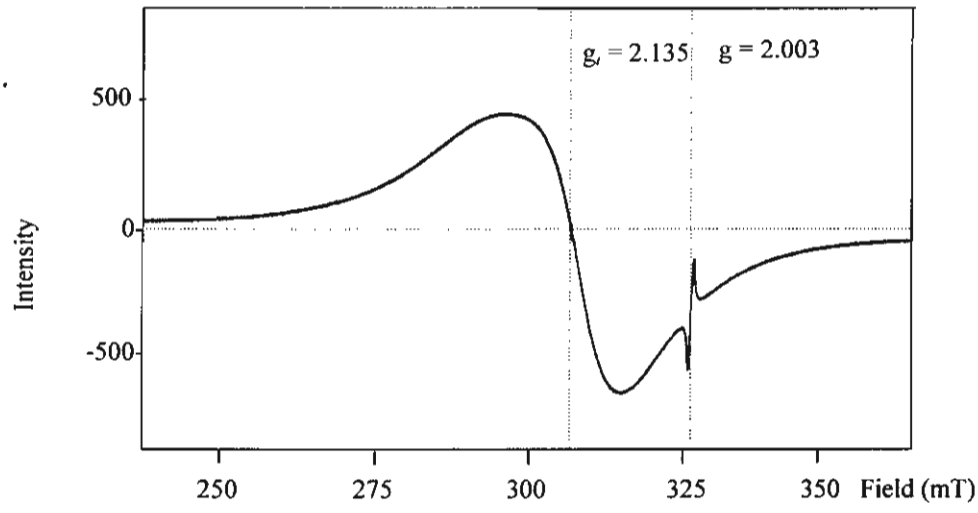

(k) The EPR spectrum at room temperature of $[Cu_4(dpyam)_4(\mu_3,\eta^3\text{-}HPO_4)_2(NO_3)_2(H_2O)_2](NO_3)_2{\cdot}2H_2O$ **(VI)**

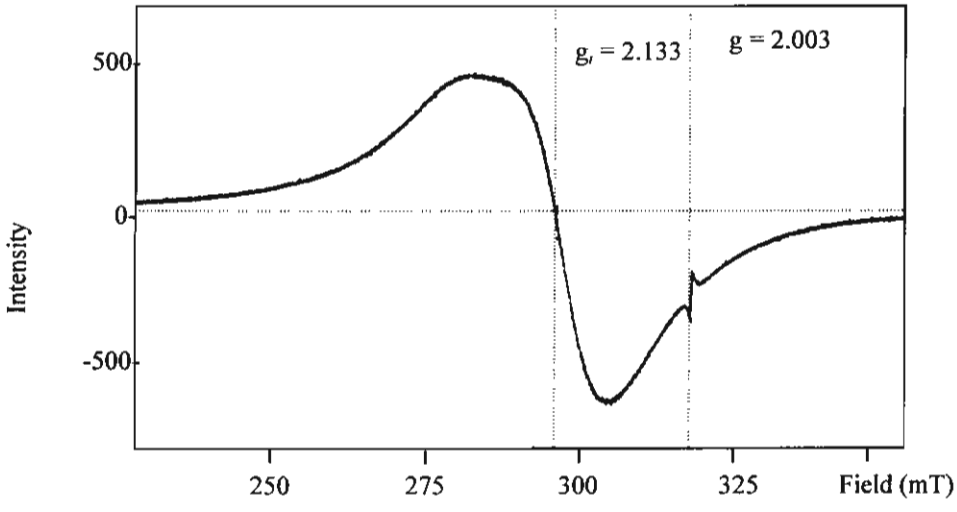

(l) The EPR spectrum at 77K of $[Cu_4(dpyam)_4(\mu_3,\eta^3\text{-}HPO_4)_2(NO_3)_2(H_2O)_2](NO_3)_2{\cdot}2H_2O$ **(VI)**

APPENDIX IIIA

Crystal and Refinement Data for

$[Cu_2(dpyam)_2(\mu\text{-}O_2CH)(\mu\text{-}OH)(\mu\text{-}OCH_3)](ClO_4)$ (I)

$[Cu_2(dpyam)_2(\mu\text{-}O_2CH)(\mu\text{-}OH)_2](ClO_4)\cdot H_2O$ (II)

$[Cu_2(dpyam)_2(\mu\text{-}O_2CH)(\mu\text{-}OOCH)(\mu\text{-}OH)](PF_6)$ (III)

$[Cu_2(dpyam)_2(\mu\text{-}O_2CH)(\mu\text{-}OH)(\mu\text{-}Cl)](ClO_4)\cdot 0.5H_2O$ (IV)

and $[Cu_2(dpyam)_2(\mu\text{-}O_2CH)(\mu\text{-}OH)(\mu\text{-}Cl)](PF_6)$ (V)

Table 1 Crystal and refinement data for complexes **I-V**

Complex	**I**	**II**	**III**	**IV**	**V**
Molecular Formula	$[Cu_2(dpyam)_2(\mu\text{-}O_2CH)(\mu\text{-}OH)(\mu\text{-}OCH_3)](ClO_4)$	$[Cu_2(dpyam)_2(\mu\text{-}O_2CH)(\mu\text{-}OH)_2](ClO_4).H_2O$	$[Cu_2(dpyam)_2(\mu\text{-}O_2CH)_2(\mu\text{-}OH)](PF_6)$	$[Cu_2(dpyam)_2(\mu\text{-}O_2CH)(\mu\text{-}OH)(\mu\text{-}Cl)](ClO_4).0.5H_2O$	$[Cu_2(dpyam)_2(\mu\text{-}O_2CH)(\mu\text{-}OH)(\mu\text{-}Cl)](PF_6)$
Molecular weight	661.99	665.98	721.50	675.43	771.94
Temperature/K	293(2)	293(2)	293(2)	293(2)	293(2)
Crystal system	Orthorhombic	Monoclinic	Orthorhombic	Orthorhombic	Orthorhombic
Space group	$Cmc2_1$	C2/m	$Cmc2_1$	$Cmc2_1$	$Cmc2_1$
a (Å)	16.7872(13)	14.3312(5)	17.011(43)	16.8229(3)	16.8665(1)
b (Å)	8.0793(7)	16.8446(7)	8.031(2)	7.8066(2)	7.829(1)
c (Å)	18.7410(15)	12.4728(5)	19.258(5)	19.2753(0)	19.4941(1)
α	90	90	90	90	90
β	90	120.97	90	90	90
γ	90	90	90	90	90
Volume/$Å^3$	2541.8(4)	2581.72(17)	2631.1(11)	2531.42(10)	2574.22(4)
Z	4	4	4	4	4
Density (calculated)/$g.cm^{-3}$	1.693	1.713	1.821	1.746	1.837
Absorption coefficient (μ)/mm^{-1}	1.837	1.813	1.767	1.946	1.900
F(000)	1312	1352	1448	1344	1424
Crystal size/mm	0.08x0.20x0.30	0.05x0.10x0.38	0.05x0.12x0.25	0.13x0.33x0.40	0.13x0.28x0.33
No. reflection collected	10804	9714	11030	9109	9380
No. unique reflections	3124 (R_{int}=0.0226)	3851 (R_{int}=0.0351)	3180 (R_{int}=0.0355)	3640 (R_{int}=0.0208)	3725 (R_{int}=0.0224)
Data/restraints/parameter	3124/1/206	3851/0/221	3180/1/234	3640/1/230	3725/1/234
GOF	1.095	1.022	1.022	1.007	1.033
Final R indices [I>2σ(I)]	R1=0.0571, wR2=0.1668	R1=0.0609, wR2=0.1571	R1=0.0515, wR2=0.1194	R1=0.0278, wR2=0.0707	R1=0.0387, wR2=0.1073
R indices (all data)	R1=0.0625, wR2=0.1734	R1=0.0936, wR2=0.1796	R1=0.0699, wR2=0.1296	R1=0.0322, wR2=0.0731	R1=0.0441, wR2=0.1115
Largest diff. peak and hole/$e.Å^{-3}$	0.979, -0.419	1.037, -0.884	0.669, -0.468	0.388, -0.373	0.651, -0.672

$$R = \Sigma||F_o| - |F_c||/\Sigma|F_o|, \quad R_w = [\Sigma w\{|F_o| - |F_c|\}^2/w|F_o|^2]^{1/2}$$

APPENDIX IIB

Selected Bond Lengths (Å) and Angles (°) for

$[Cu_2(dpyam)_2(\mu\text{-}O_2CH)(\mu\text{-}OH)(\mu\text{-}OCH_3)](ClO_4)$ (I)

$[Cu_2(dpyam)_2(\mu\text{-}O_2CH)(\mu\text{-}OH)_2](ClO_4)\cdot H_2O$ (II)

$[Cu_2(dpyam)_2(\mu\text{-}O_2CH)(\mu\text{-}OOCH)(\mu\text{-}OH)](PF_6)$ (III)

$[Cu_2(dpyam)_2(\mu\text{-}O_2CH)(\mu\text{-}OH)(\mu\text{-}Cl)](ClO_4)\cdot 0.5H_2O$ (IV) and

$[Cu_2(dpyam)_2(\mu\text{-}O_2CH)(\mu\text{-}OH)(\mu\text{-}Cl)](PF_6)$ (V)

Table 1 Selected bond lengths (Å) and angles (°) with e.s.d.s. in parentheses for $[Cu_2(dpyam)_2(\mu\text{-}O_2CH)(\mu\text{-}OH)(\mu\text{-}OCH_3)](ClO_4)$ **(I)**

Cu(1)-N(1)	1.961(4)	Cu(1)-O(2)	2.169(5)
Cu(1)-N(2)	2.010(4)	Cu(1)-O(3)	2.175(3)
Cu(1)-O(1)	1.918(4)	Cu(1)-Cu(1A)	3.023(1)
O(2)-C(12)	1.196(1)	O(3)-C(11)	1.257(4)
O(1)-Cu(1)-O(2)	81.9(2)	N(1)-Cu(1)-Cu(1A)	138.2(1)
O(1)-Cu(1)-O(3)	88.5(2)	N(1)-Cu(1)-N(2)	91.1(2)
O(1)-Cu(1)-N(1)	173.8(1)	N(2)-Cu(1)-O(2)	133.0(3)
O(1)-Cu(1)-N(2)	93.7(2)	N(2)-Cu(1)-O(3)	135.7(2)
O(1)-Cu(1)-Cu(1A)	38.0(1)	N(2)-Cu(1)-Cu(1A)	125.3(1)
O(2)-Cu(1)-O(3)	91.1(2)	Cu(1)-O(1)-Cu(1A)	104.0(3)
O(2)-Cu(1)-Cu(1A)	45.8(1)	Cu(1)-O(2)-Cu(1A)	88.3(2)
O(3)-Cu(1)-Cu(1A)	79.7(1)	C(11)-O(3)-Cu(1)	126.5(3)
N(1)-Cu(1)-O(2)	95.6(2)	O(3)-C(11)-O(3A)	126.6(6)
N(1)-Cu(1)-O(3)	86.9(2)		

Symmetry code: A = -x, y, z

Table 2 Selected bond lengths [Å] and angles [°] with e.s.d.s. in parentheses of $[Cu_2(dpyam)_2(\mu\text{-}O_2CH)(\mu\text{-}OH)_2](ClO_4).H_2O$ **(II)**

Cu(1)-N(1)	2.003(3)	Cu(1)-O(2)	1.952(3)
Cu(1)-N(2)	2.005(3)	Cu(1)-O(3)	2.345(3)
Cu(1)-O(1)	1.955(3)	Cu(1)-Cu(1A)	2.9027(10)
O(1)-Cu(1)-O(2)	79.55(13)	N(1)-Cu(1)-O(2)	156.04(16)
O(1)-Cu(1)-O(3)	89.07(15)	N(1)-Cu(1)-O(3)	102.81(13)
O(1)-Cu(1)-N(1)	95.88(13)	N(1)-Cu(1)-N(2)	91.92(15)
O(1)-Cu(1)-N(2)	172.20(13)	N(2)-Cu(1)-O(2)	93.28(13)
O(2)-Cu(1)-O(3)	100.62(14)	N(2)-Cu(1)-O(3)	89.25(13)
C(11)-O(3)-Cu(1)	124.4(3)	O(3)-C(11)-O(3A)	127.6(6)
Cu(1)-O(1)-Cu(1A)	95.89(17)	Cu(1)-O(2)-Cu(1A)	96.09(17)

Symmetry code: A = -x+2, y, z

Table 3 Selected bond lengths [Å] and angles [°] with e.s.d.s. in parentheses of $[Cu_2(dpyam)_2(\mu\text{-}O_2CH)(\mu\text{-}OOCH)(\mu\text{-}OH)](PF_6)$ **(III)**

Cu(1)-N(1)	1.972(4)	Cu(1)-O(2)	2.144(6)
Cu(1)-N(2)	2.029(4)	Cu(1)-O(4)	2.200(3)
Cu(1)-O(1)	1.934(5)	Cu(1)-Cu(1A)	3.113(5)
Cu(1)-O(3)	2.246(5)		
O(1)-Cu(1)-O(2)	78.2(2)	N(1)-Cu(1)-O(2)	100.5(2)
O(1)-Cu(1)-O(4)	96.6(2)	N(1)-Cu(1)-O(4)	87.2(1)
O(1)-Cu(1)-N(1)	173.6(2)	N(1)-Cu(1)-N(2)	91.7(1)
O(1)-Cu(1)-N(2)	93.3(2)	N(2)-Cu(1)-O(2)	138.3(3)
O(2)-Cu(1)-O(4)	89.7(3)	N(2)-Cu(1)-O(4)	130.9(1)
C(12)-O(4)-Cu(1)	127.4(4)	O(4)-C(12)-O(4A)	127.5(7)
Cu(1)-O(1)-Cu(1A)	107.2(4)	Cu(1)-O(2)-Cu(1A)	93.1(4)

Symmetry code: A = -x+2, y, z

Table 4 Selected bond lengths [Å] and angles [°] with e.s.d.s. in parentheses of $[Cu_2(dpyam)_2(\mu\text{-}O_2CH)(\mu\text{-}OH)(\mu\text{-}Cl)](ClO_4)\cdot 0.5H_2O$ **(IV)**

Cu(1)-N(1)	1.975(1)	Cu(1)-O(1)	1.916(2)
Cu(1)-N(2)	2.027(2)	Cu(1)-O(2)	2.158(1)
Cu(1)-Cl(1)	2.478(2)	Cu(1)-Cu(1A)	3.036(1)
O(1)-Cu(1)-N(1)	173.8(1)	N(1)-Cu(1)-Cl(1)	96.4(1)
O(1)-Cu(1)-N(2)	94.1(1)	N(1)-Cu(1)-Cu(1A)	138.0(1)
O(1)-Cu(1)-O(2)	88.1(1)	N(2)-Cu(1)-O(2)	133.6(1)
O(1)-Cu(1)-Cl(1)	82.5(1)	N(2)-Cu(1)-Cl(1)	119.1(1)
O(1)-Cu(1)-Cu(1A)	37.6(1)	N(2)-Cu(1)-Cu(1A)	126.3(1)
O(2)-Cu(1)-Cl(1)	107.2(1)	Cu(1)-O(1)-Cu(1A)	104.8(1)
O(2)-Cu(1)-Cu(1A)	79.4(1)	Cu(1)-Cl(1)-Cu(1A)	75.6(1)
N(1)-Cu(1)-N(2)	91.7(1)	C(11)-O(2)-Cu(1)	126.8(1)
N(1)-Cu(1)-O(2)	86.4(1)	O(2)-C(11)-O(2 A)	127.1(3)

Symmetry code: A = -x+2, y, z

Table 5 Selected bond lengths [Å] and angles [°] with e.s.d.s. in parentheses of $[Cu_2(dpyam)_2(\mu\text{-}O_2CH)(\mu\text{-}OH)(\mu\text{-}Cl)](PF_6)$ **(V)**

Cu(1)-N(1)	2.031(3)	Cu(1)-O(1)	2.183(2)
Cu(1)-N(2)	1.983(2)	Cu(1)-O(2)	1.918(2)
Cu(1)-Cl(1)	2.451(1)	Cu(1)-Cu(1A)	3.061(5)
O(1)-Cu(1)-N(1)	130.6(1)	N(1)-Cu(1)-Cl(1)	124.1(1)
O(1)-Cu(1)-N(2)	86.7(1)	N(2)-Cu(1)-O(2)	173.8(1)
O(1)-Cu(1)-O(2)	87.3(1)	N(2)-Cu(1)-Cl(1)	97.7(1)
O(1)-Cu(1)-Cl(1)	104.8(1)	Cu(1)-O(2)-Cu(1A)	105.9(1)
O(2)-Cu(1)-Cl(1)	82.3(1)	Cu(1)-Cl(1)-Cu(1A)	77.2(1)
N(1)-Cu(1)-N(2)	91.8(1)	C(11)-O(1)-Cu(1)	127.5(2)
N(1)-Cu(1)-O(2)	93.2(1)	O(1)-C(11)-O(1A)	126.5(4)

Symmetry code: A = -x+1, y, z

APPENDIX IIIC

The infrared spectra for

$[Cu_2(dpyam)_2(\mu\text{-}O_2CH)(\mu\text{-}OH)(\mu\text{-}OCH_3)](ClO_4)$ (I)

$[Cu_2(dpyam)_2(\mu\text{-}O_2CH)(\mu\text{-}OH)_2](ClO_4)\cdot H_2O$ (II)

$[Cu_2(dpyam)_2(\mu\text{-}O_2CH)(\mu\text{-}OOCH)(\mu\text{-}OH)](PF_6)$ (III)

$[Cu_2(dpyam)_2(\mu\text{-}O_2CH)(\mu\text{-}OH)(\mu\text{-}Cl)](ClO_4)\cdot 0.5H_2O$ (IV)

$[Cu_2(dpyam)_2(\mu\text{-}O_2CH)(\mu\text{-}OH)(\mu\text{-}Cl)](PF_6)$ (V) and

$[Cu_2(dpyam)_2(\mu\text{-}O_2CH)(\mu\text{-}OH)(\mu\text{-}Cl)](BF_4)$ (VI)

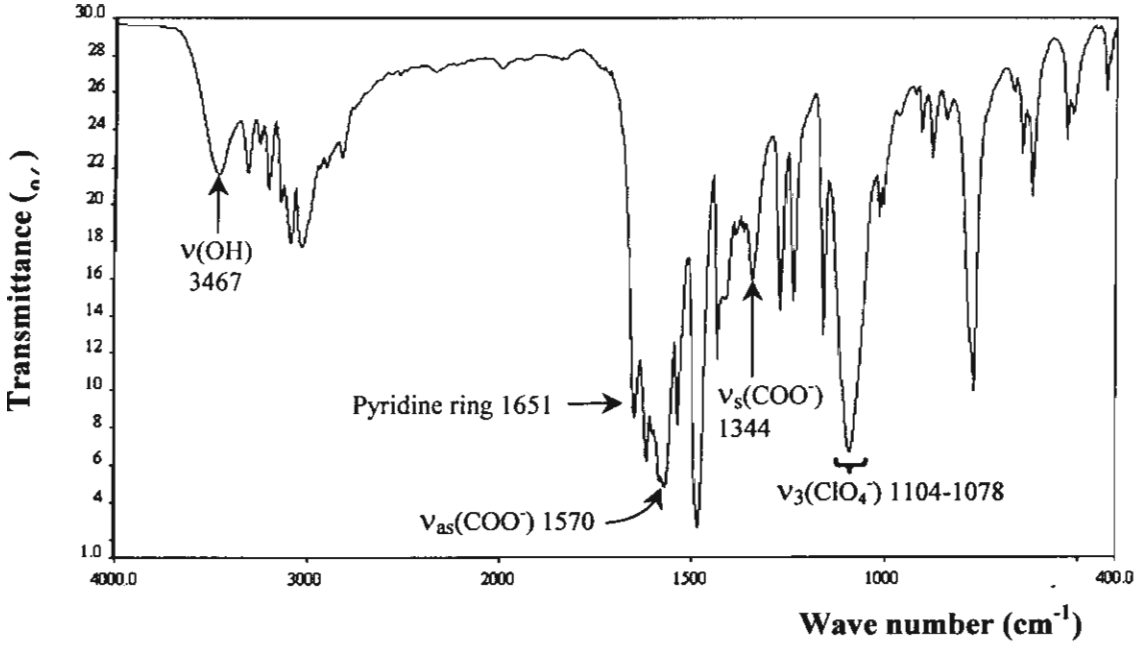

(a) IR spectrum of $[Cu_2(dpyam)_2(\mu\text{-}O_2CH)(\mu\text{-}OH)(\mu\text{-}OCH_3)](ClO_4)$ **(I)**

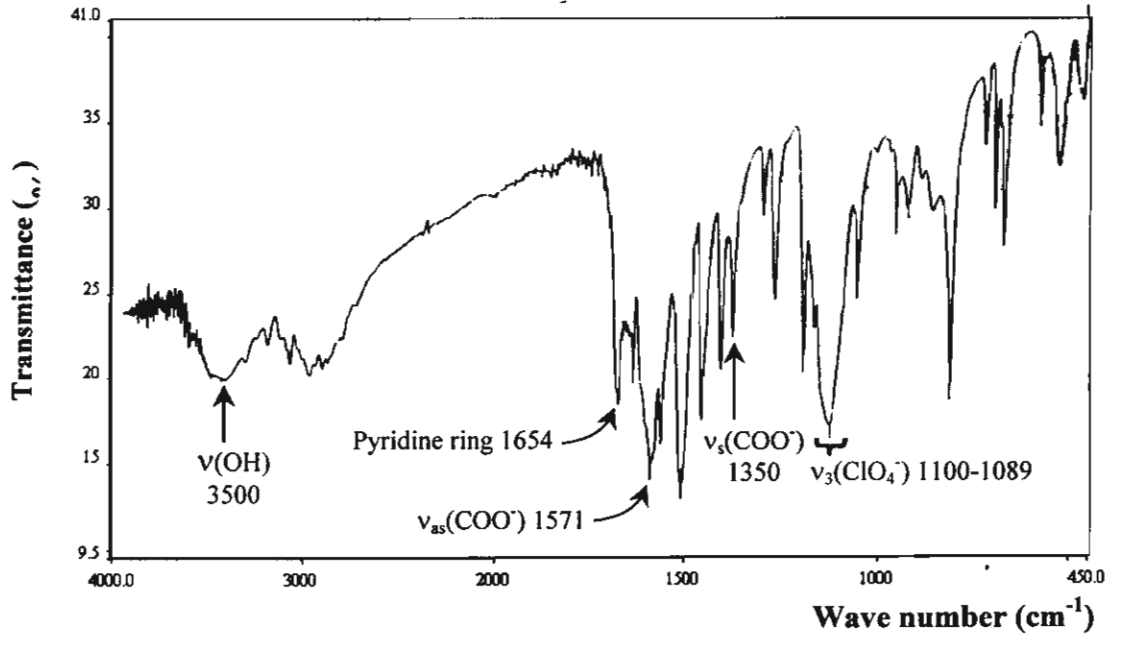

(b) IR spectrum of $[Cu_2(dpyam)_2(\mu\text{-}O_2CH)(\mu\text{-}OH)_2](ClO_4)\cdot H_2O$ **(II)**

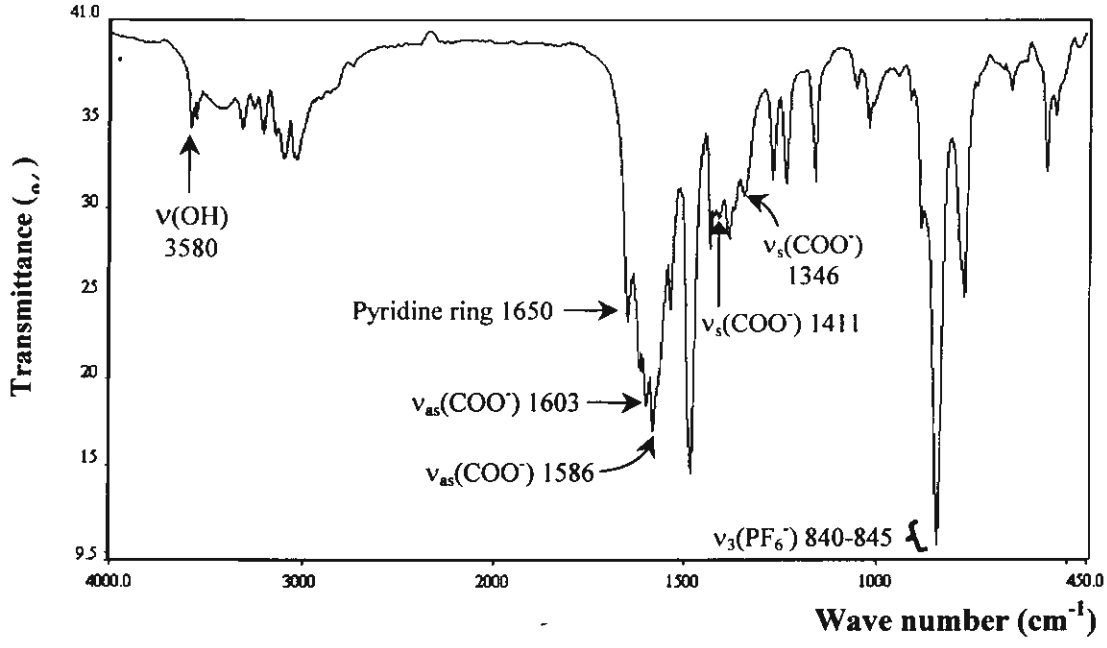

(c) IR spectrum of $[Cu_2(dpyam)_2(\mu\text{-}O_2CH)(\mu\text{-}OOCH)(\mu\text{-}OH)](PF_6)$ **(III)**

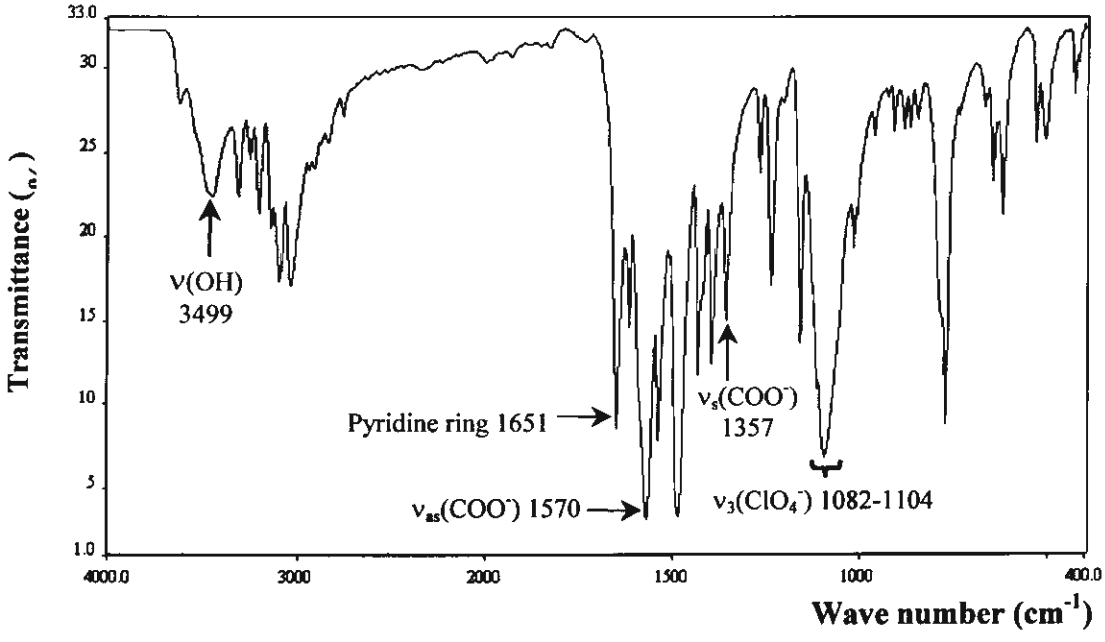

(d) IR spectrum of $[Cu_2(dpyam)_2(\mu\text{-}O_2CH)(\mu\text{-}OH)(\mu\text{-}Cl)](ClO_4)\cdot 0.5H_2O$ **(IV)**

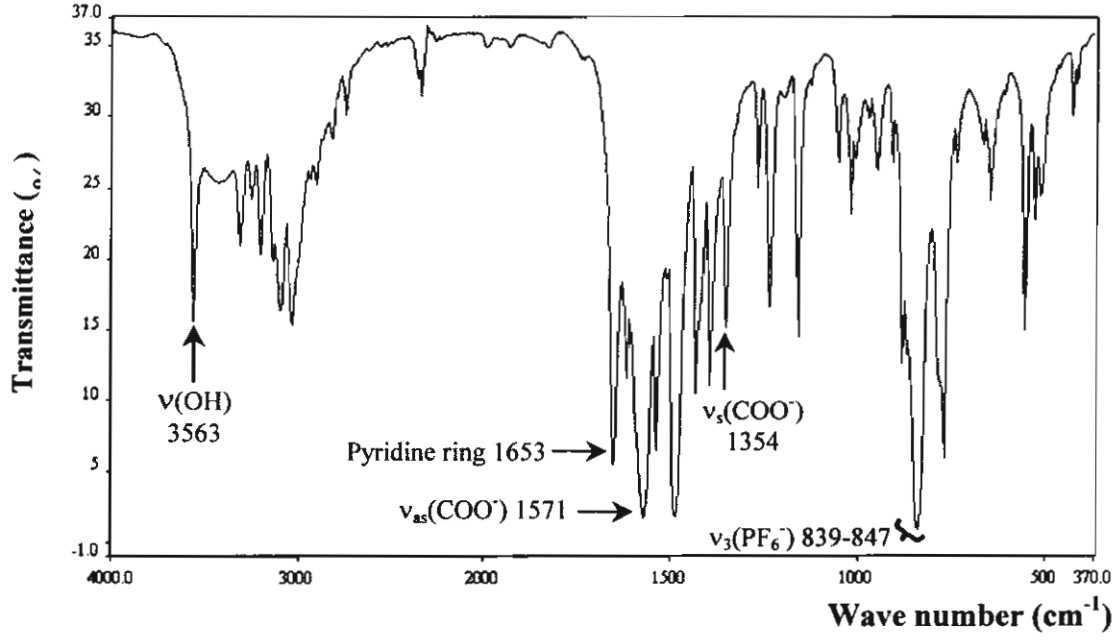

(e) IR spectrum of $[Cu_2(dpyam)_2(\mu\text{-}O_2CH)(\mu\text{-}OH)(\mu\text{-}Cl)](PF_6)$ **(V)**

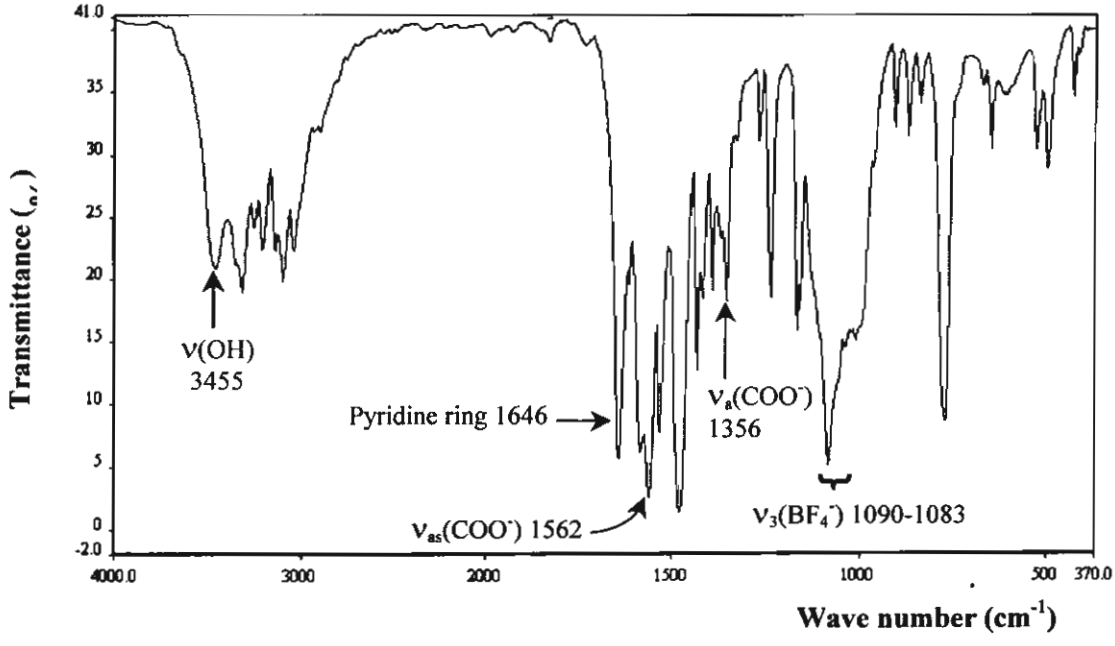

(f) IR spectrum of $[Cu_2(dpyam)_2(\mu\text{-}O_2CH)(\mu\text{-}OH)(\mu\text{-}Cl)](BF_4)$ **(VI)**

APPENDIX IIID

The EPR spectra for

$[Cu_2(dpyam)_2(\mu\text{-}O_2CH)(\mu\text{-}OH)(\mu\text{-}OCH_3)](ClO_4)$ (I)

$[Cu_2(dpyam)_2(\mu\text{-}O_2CH)(\mu\text{-}OH)_2](ClO_4)\cdot H_2O$ (II)

$[Cu_2(dpyam)_2(\mu\text{-}O_2CH)(\mu\text{-}OOCH)(\mu\text{-}OH)](PF_6)$ (III)

$[Cu_2(dpyam)_2(\mu\text{-}O_2CH)(\mu\text{-}OH)(\mu\text{-}Cl)](ClO_4)\cdot 0.5H_2O$ (IV)

$[Cu_2(dpyam)_2(\mu\text{-}O_2CH)(\mu\text{-}OH)(\mu\text{-}Cl)](PF_6)$ (V)

and $[Cu_2(dpyam)_2(\mu\text{-}O_2CH)(\mu\text{-}OH)(\mu\text{-}Cl)](BF_4)$ (VI)

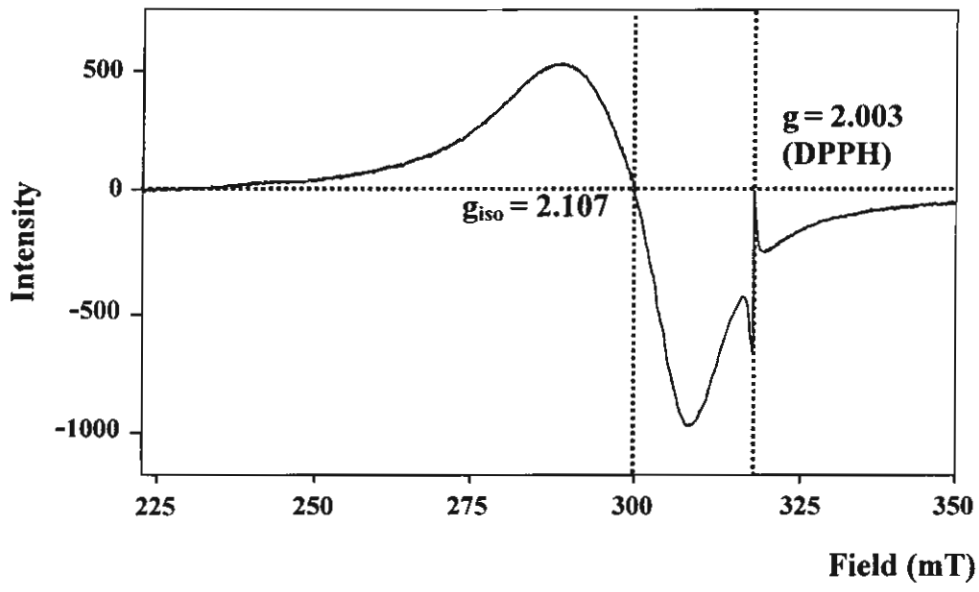

(a) The EPR spectrum at room temperature of $[Cu_2(dpyam)_2(\mu\text{-}O_2CH)(\mu\text{-}OH)(\mu\text{-}OCH_3)](ClO_4)$ **(I)**

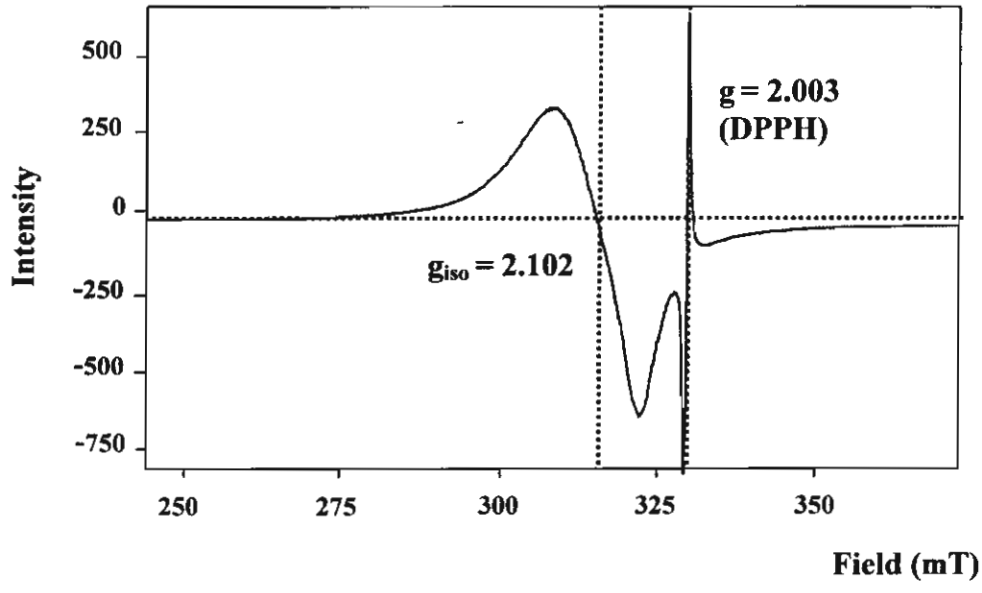

(b) The EPR spectrum at 77 K of $[Cu_2(dpyam)_2(\mu\text{-}O_2CH)(\mu\text{-}OH)(\mu\text{-}OCH_3)](ClO_4)$ **(I)**

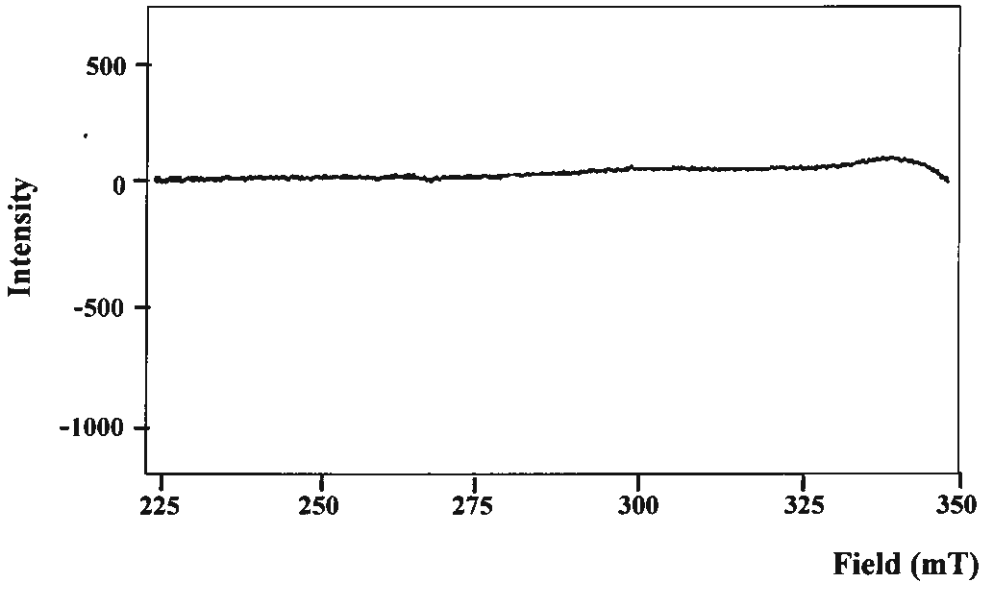

(c) The EPR spectrum at room temperature of $[Cu_2(dpyam)_2(\mu\text{-}O_2CH)(\mu\text{-}OH)_2](ClO_4)\cdot H_2O$ **(II)**

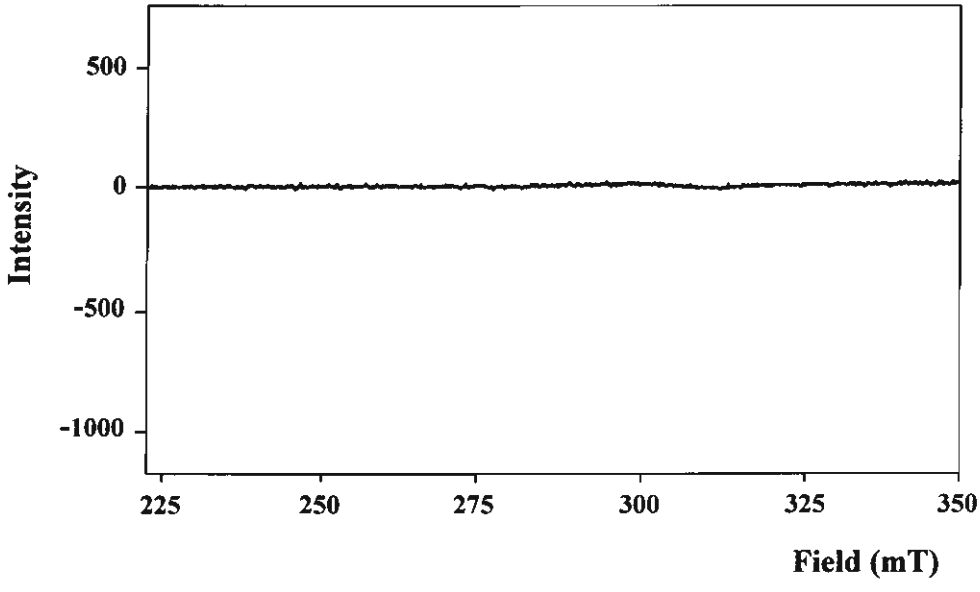

(d) The EPR spectrum at 77 K of $[Cu_2(dpyam)_2(\mu\text{-}O_2CH)(\mu\text{-}OH)_2](ClO_4)\cdot H_2O$ **(II)**

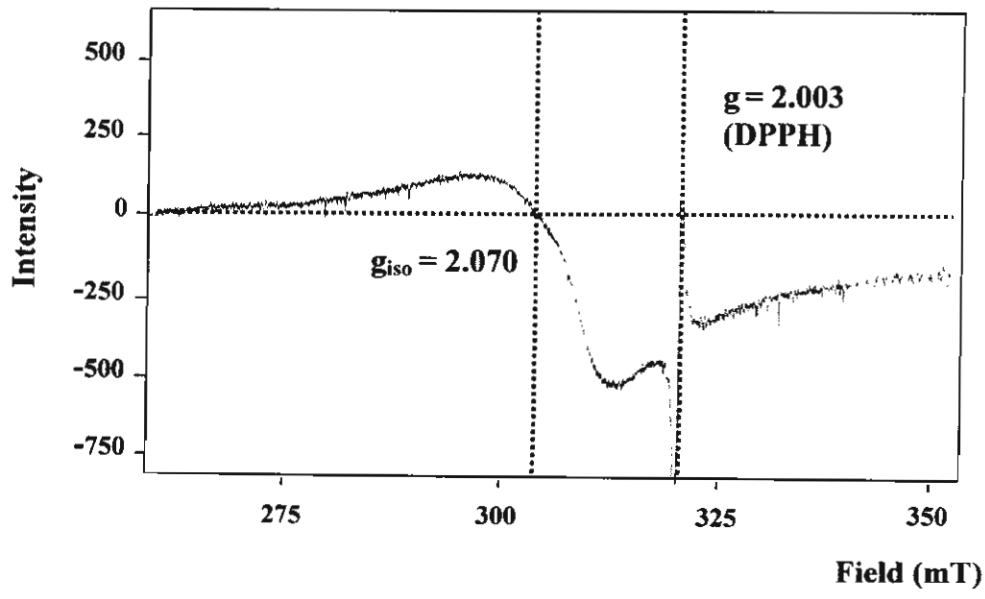

(e) The EPR spectrum at room temperature of $[Cu_2(dpyam)_2(\mu\text{-}O_2CH)(\mu\text{-}OOCH)(\mu\text{-}OH)](PF_6)$ **(III)**

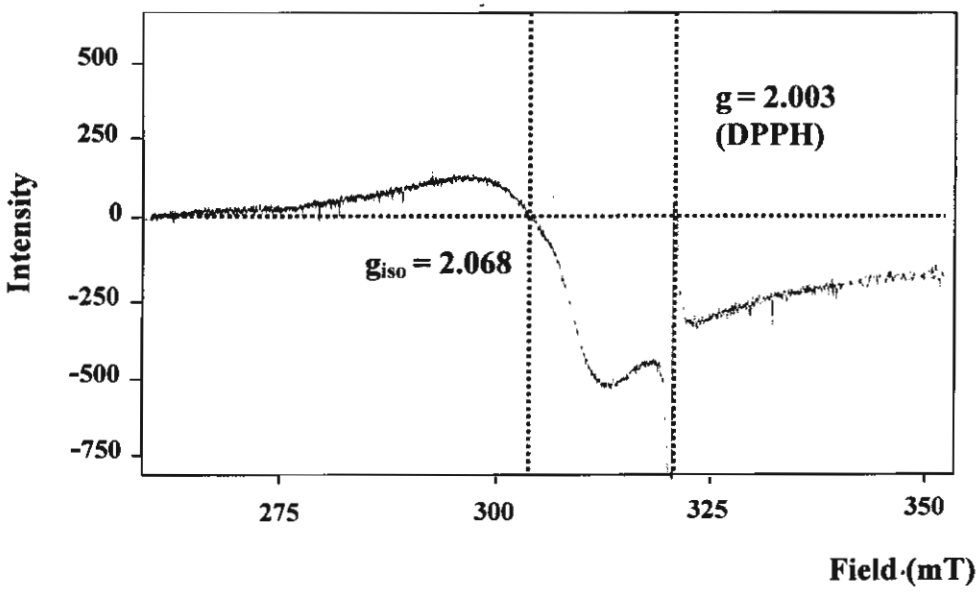

(f) The EPR spectrum at 77 K of $[Cu_2(dpyam)_2(\mu\text{-}O_2CH)(\mu\text{-}OOCH)(\mu\text{-}OH)](PF_6)$ **(III)**

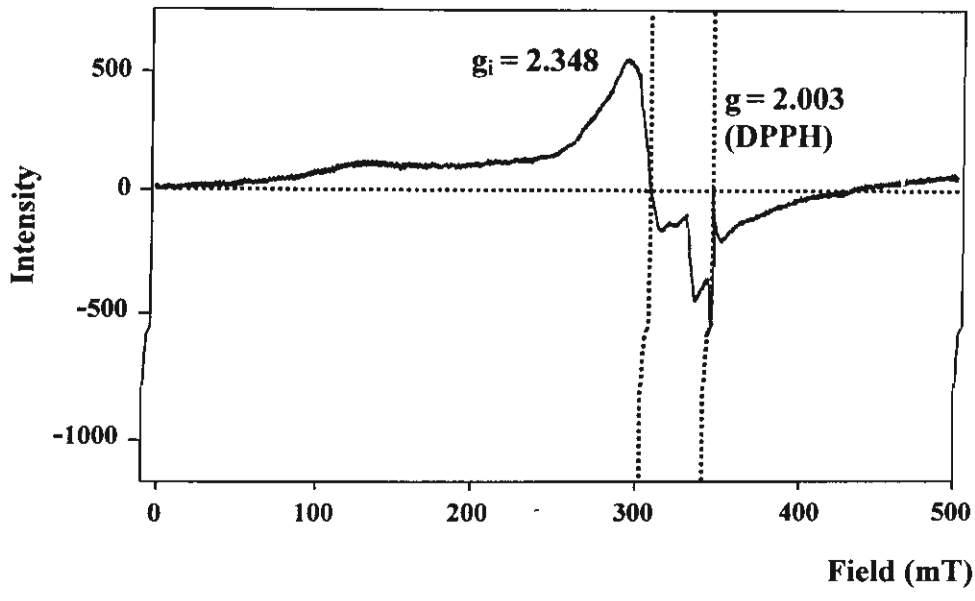

(g) The EPR spectrum at room temperature of $[Cu_2(dpyam)_2(\mu\text{-}O_2CH)(\mu\text{-}OH)(\mu\text{-}Cl)](ClO_4)\cdot 0.5H_2O$ **(IV)**

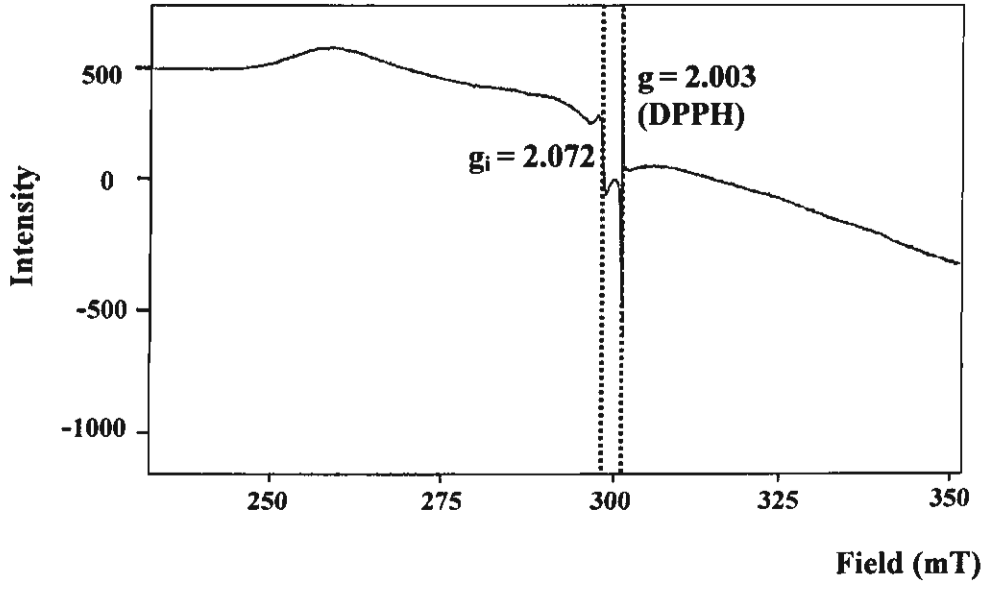

(h) The EPR spectrum at 77 K of $[Cu_2(dpyam)_2(\mu\text{-}O_2CH)(\mu\text{-}OH)(\mu\text{-}Cl)](ClO_4)\cdot 0.5H_2O$ **(IV)**

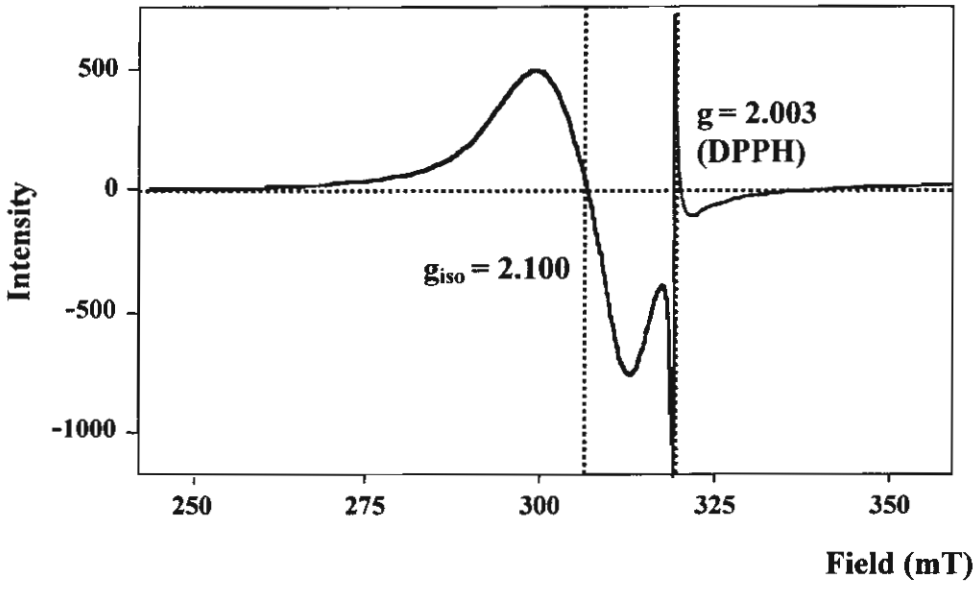

(i) The EPR spectrum at room temperature of $[Cu_2(dpyam)_2(\mu\text{-}O_2CH)(\mu\text{-}OH)(\mu\text{-}Cl)](PF_6)$ (V)

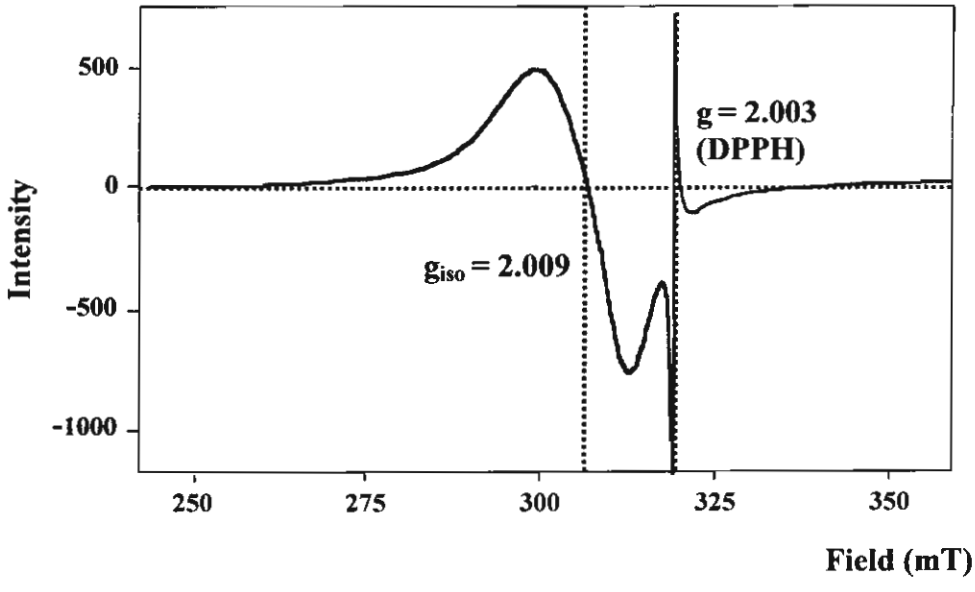

(j) The EPR spectrum at 77 K of $[Cu_2(dpyam)_2(\mu\text{-}O_2CH)(\mu\text{-}OH)(\mu\text{-}Cl)](PF_6)$ (V)

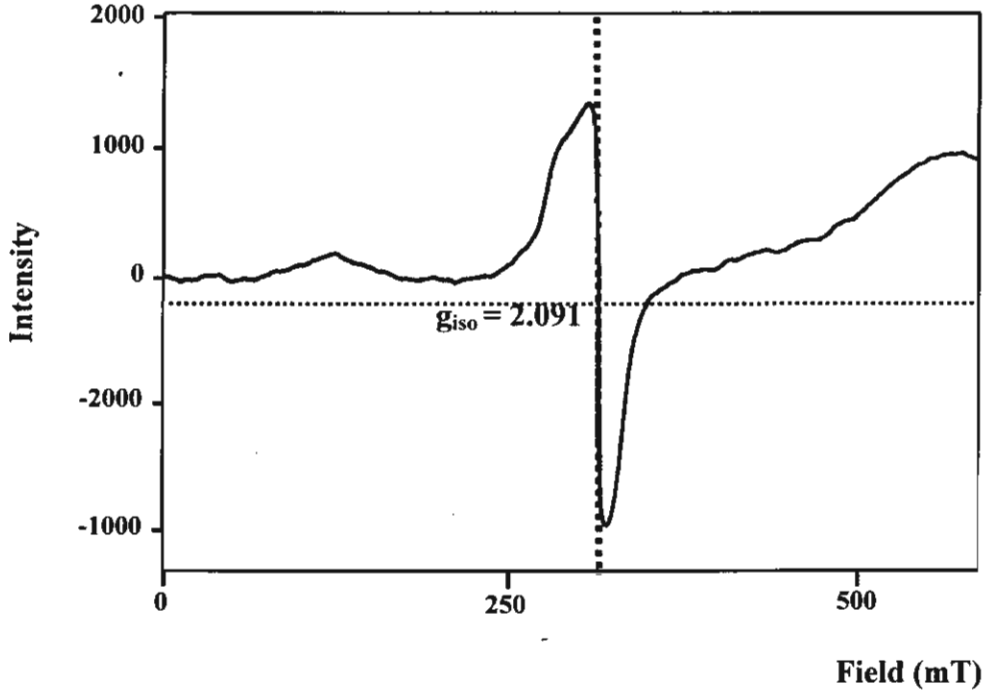

(k) The EPR spectrum at room temperature of $[Cu_2(dpyam)_2(\mu\text{-}O_2CH)(\mu\text{-}OH)(\mu\text{-}Cl)](BF_4)$ **(VI)**

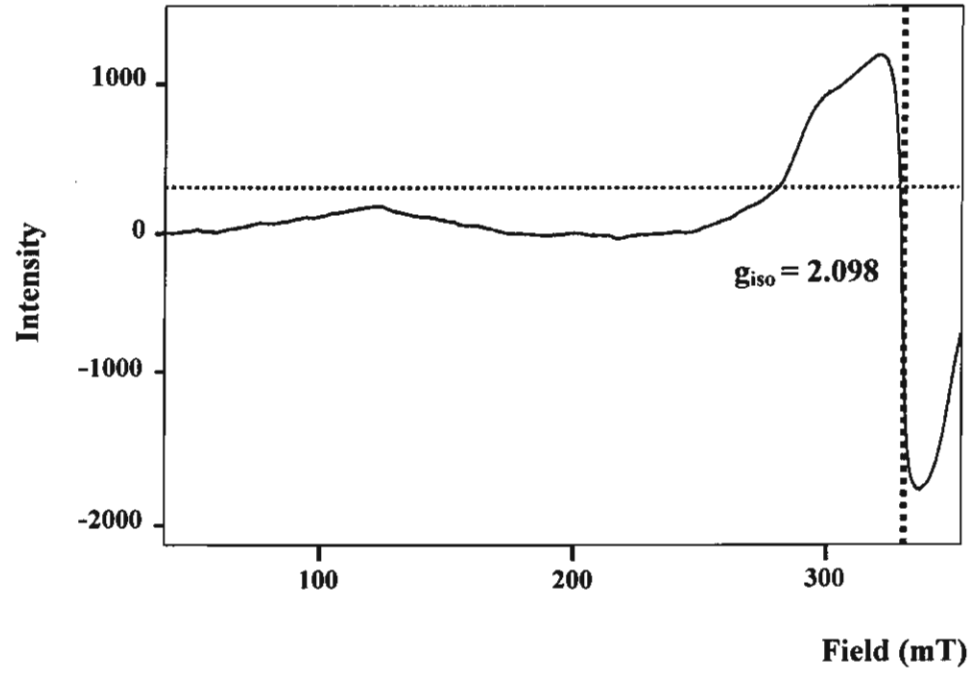

(l) The EPR spectrum at 77 K of $[Cu_2(dpyam)_2(\mu\text{-}O_2CH)(\mu\text{-}OH)(\mu\text{-}Cl)](BF_4)$ **(VI)**

APPENDIX IV

PUBLICATION PAPERS

PUBLICATION PAPERS OF PART I

Available online at www.sciencedirect.com
SCIENCE DIRECT®
Inorganica Chimica Acta 353 (2003) 119–128
Inorganica Chimica Acta
www.elsevier.com/locate/ica

Synthesis, spectroscopic characterization, X-ray crystal structure and magnetic properties of oxalato-bridged copper(II) dinuclear complexes with di-2-pyridylamine

Sujittra Youngme [a,*], Gerard A. van Albada [d], Narongsak Chaichit [b], Pimprapun Gunnasoot [a], Palangpon Kongsaeree [c], Ilpo Mutikainen [e], Olivier Roubeau [d], Jan Reedijk [d], Urho Turpeinen [e]

[a] Department of Chemistry, Faculty of Science, Khon Kaen University, Khon Kaen 40002, Thailand
[b] Department of Physics, Faculty of Science and Technology, Thammasat University Rangsit, Pathumthani 12121, Thailand
[c] Department of Chemistry, Faculty of Science, Mahidol University, Bangkok 10400, Thailand
[d] Gorlaeus Laboratories, Leiden Institute of Chemistry, Leiden University, P.O. Box 9502, 2300 RA Leiden, The Netherlands
[e] Department of Chemistry, Laboratory of Inorganic Chemistry, P.O. Box 55 (A.I.Virtasen aukio 1), 00014 University of Helsinki, Helsinki, Finland

Received 28 October 2002; accepted 4 February 2003

Abstract

The syntheses and characterization of a series of dinuclear μ-oxalato copper(II) complexes of the general type $[(NN)_{1\text{ or }2}Cu(C_2O_4)Cu(NN)_{1\text{ or }2}]^{2+}$, where NN = didentate dpyam (di-2-pyridylamine) ligand, are described. The crystal structures of three representative complexes have been determined. The dinuclear-oxalate bridged compounds $[Cu(dpyam)_4(C_2O_4)](ClO_4)_2(H_2O)_3$ **(1)** and $[Cu_2(dpyam)_4(C_2O_4)](BF_4)_2(H_2O)_3$ **(2)** crystallize in the non-centrosymmetric triclinic space group $P\bar{1}$ which are isomorphous and isostructural. The compound $[Cu_2(dpyam)_2(C_2O_4)(NO_3)_2((CH_3)_2SO)_2]$ **(3)** crystallizes in the centrosymmetric monoclinic space group $P\bar{1}$ with all Cu-oxalate contacts in the equatorial plane. All three complexes contain six-coordinate copper centres bridged by planar bis-didentate oxalate groups from the equatorial position of one chromophore to the equatorial position of the other one. Both chromophores in **1** and **2** exhibit the compressed octahedral Cu(II) geometry, while **3** displays an elongated octahedral Cu(II) environment. The IR, ligand field and EPR measurements are in agreement with the structures found. The magnetic susceptibility measurements, measured from 5 to 280 K, revealed a very weak ferromagnetic interaction between the Cu(II) atoms for compound **1** and **2**, with a singlet–triplet energy gap (J) of 2.42 and 3.38 cm^{-1}, for compounds **1** and **2**, respectively. Compound **3** has a strong antiferromagnetic interaction with a J of -305.1 cm^{-1}, in agreement with coplanarity of the magnetic orbitals.

Keywords: Copper(II) complexes; Crystal structures; μ-Oxalato dimers; Magnetic properties; EPR

1. Introduction

In the past decades, there has been a great deal of interest in the magneto-structural studies of transition metal atoms [1–40] with polyatomic bridging ligands both in the experimental and theoretical points of view. The oxalate ion is well known to be an appropriate bridging ligand to design magnetic materials and many oxalato-bridged complexes have been prepared and characterized [2–36]. Eight different bridging modes (Scheme 1) have been observed for the oxalato group in the oxalato copper(II) complexes [1–4].

A number of dinuclear copper complexes with an oxalato bridge, generally formulated as $[(NN)Cu(\mu\text{-}C_2O_4)Cu(NN)]X_n$, where NN is a chelating ligand, and X is a counter anion or a solvent molecule, have been structurally characterized [5–14,36]. Analysis of the structural factors that influence the magnitude of the magnetic interactions allowed to tune the value of the singlet–triplet energy gap (J values) in oxalato-bridged dinuclear Cu(II) complexes from approximately 0 to approximate -400 cm^{-1} by playing on the nature of

* Corresponding author. Fax: +66-43-243-338.
E-mail address: sujittra@kku.ac.th (S. Youngme).

0020-1693/03/$ - see front matter © 2003 Elsevier B.V. All rights reserved.
doi:10.1016/S0020-1693(03)00207-X

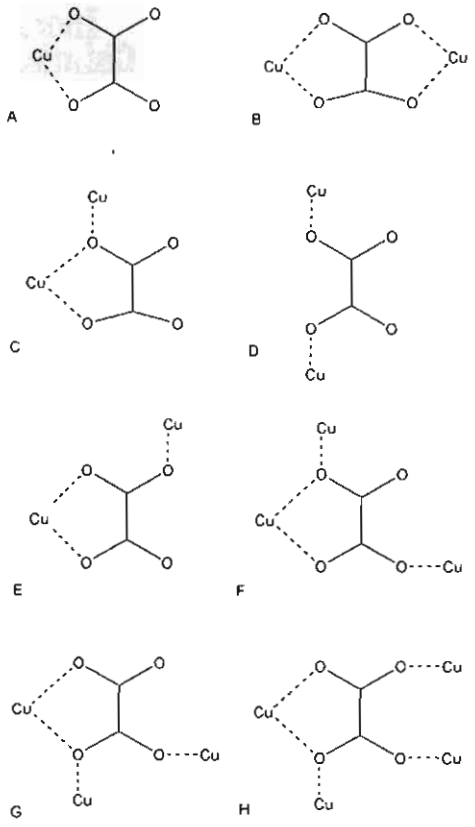

Scheme 1. Different coordination modes of oxalate ligands known for oxalato copper (II) complexes.

the terminal ligand (tridentate and/or didentate nitrogen donors) or of the counter ions, taking advantage of the plasticity effect of the Cu(II) coordination sphere [5,19,21]. Previous theoretical and experimental works [5,6,16–21] have revealed that the exchange interaction between the copper ions propagated through the oxalate bridge is strongly dependent on the geometry around the copper ions, sensitive to the orientation of the magnetic orbital of each Cu(II) relative to the oxalate plane and the bridging mode of the oxalate group. The actual role of this ligand modification is to realign the metal magnetic orbital relative to the oxalate σ orbital as the magnetic exchange pathway is dominated by interactions between the metal $d_{x^2-y^2}$ orbitals and the oxalate σ orbitals.

In most cases, the copper ions present a square-pyramidal structure with two oxygen atoms of oxalate bridge and two nitrogen atoms of the diamine occupying the base of the pyramid and the counter anion or a solvent molecule occupying the axial position. Some compounds present an additional bond to X, giving rise to elongated octahedral coordination. In the literature compounds have been reported which have a square-pyramidal and elongated octahedral geometries in which one of the oxalate oxygen atoms is in the basal plane and the other oxygen is apical [4,5,10,12–14,19] and others having a trigonal-bipyramidal geometry around the copper atoms [15].

It is extremely difficult to control the value of structural parameters during the synthetic process and great difficulties are faced to establish the magneto-structural correlation. In order to extend the investigation by modifying the terminal ligand to the more flexible, nitrogen donor didentate dpyam ligand, we now describe the synthesis, the crystal structure, and the magnetic properties of three new μ-oxalato Cu(II) complexes, $[Cu_2(dpyam)_4(C_2O_4)](ClO_4)_2(H_2O)_3$ (1), $[Cu_2(dpyam)_4(C_2O_4)](BF_4)_2(H_2O)_3$ (2) and $[Cu_2(dpyam)_2(C_2O_4)(NO_3)_2((CH_3)_2SO)_2]$ (3). The ligand dipyam has been selected primarily because of the fact that it also has a N–H H-bond donor function that might interfere with the oxalate bridging ligand.

2. Experimental

2.1. Reagents and physical measurements

All reagents are commercial grade materials and were used without further purification. Elemental analyses(C, H, N) were performed by the Microanalytical Service of Science and Technological Research Equipment Centre, Chulalongkorn University on Perkin–Elmer PE2400 CHNS/O Analyzer. Copper content was determined on atomic absorption spectrophotometer.

IR spectra were recorded with a Biorad FTS-7/PC FTIR spectrophotometer as KBr pellets/and or as Nujol mulls in the 4000–450 cm^{-1} spectral range. Solid-state (diffuse reflectance) electronic spectra were recorded as polycrystalline samples on a Perkin–Elmer Lambda2S spectrophotometer over the range 8000–18 000 cm^{-1}. X-band powder EPR spectra were obtained on a JEOL RE2x electron spin resonance spectrometer using DPPH ($g = 2.0036$) as a standard. Magnetic susceptibility measurements (5–280 K) were carried out using a Quantum Design MPMS-5 5T SQUID magnetometer (measurements carried out at 1000 Gauss). Data were corrected for magnetization of the sample holder and for diamagnetic contributions, which were estimated from the Pascal constants.

2.2. Syntheses

Caution! Although the perchlorate salt described in this work do not appear to be sensitive to shock. This material, like all perchlorate salts can be potentially explosive with organic solvents. Only a small amount of material should be prepared, and it should be handled with caution.

2.2.1. $[Cu_2(dpyam)_4(\mu\text{-}C_2O_4)](ClO_4)_2(H_2O)_3$ (1)

Compound **1** was prepared by adding a hot methanol solution (40 ml) of dpyam (0.342 g, 2.0 mmol) to a hot aqueous solution (60 ml) of $Cu(ClO_4)_2$ (0.371 g, 1.0 mmol). The mixture was heated at approximately 70 °C with continuous stirring for 10 min, then solid $Na_2C_2O_4$ (0.134 g, 1.0 mmol) was added. The resulting hot solution was filtered off to remove any impurities. After standing at room temperature (r.t.) for a week, green needle-like crystals of **1** were obtained. Yield approximately 75%. *Anal.* Calc. for $C_{42}H_{42}Cl_2Cu_2N_{12}O_{15}$: C, 43.76; H, 3.67; Cu, 11.03; N, 14.58. Found: C, 43.69; H, 3.60; Cu, 11.10; N, 14.61%.

2.2.2. $[Cu_2(dpyam)_4(\mu\text{-}C_2O_4)](BF_4)_2(H_2O)_3$ (2)

A solution containing dpyam (0.342 g, 2.0 mmol) in ethanol (20 ml) and $Na_2C_2O_4$ (0.068 g, 0.5 mmol) in water (10 ml) was added to a solution of $Cu(BF_4)_2$ (0.237 g, 1 mmol) in water (10 ml). The resulting green solution was allowed to evaporate at r.t. After 2 weeks, green crystals of $[Cu_2(dpyam)_4(\mu\text{-}C_2O_4)](BF_4)_2(H_2O)_3$ (**2**) were obtained which were filtered off, washed with water and were dried in air. Yield approximately 60%. *Anal.* Calc. for $C_{42}H_{42}B_2Cu_2F_8N_{12}O_7$: C, 44.74; H, 3.76; Cu, 11.27; N, 14.90. Found: C, 44.82; H, 3.68; Cu, 11.33; N, 14.85%.

2.2.3. $[Cu_2(dpyam)_2(\mu\text{-}C_2O_4)(NO_3)_2((CH_3)_2SO)_2]$ (3)

Compound **3** was prepared by adding a hot dimethylsulfoxide (10 ml) of dpyam (0.342 g, 2.0 mmol) to hot aqueous solution containing $Cu(NO_3)_2(H_2O)_{2.5}$ (0.465 g, 2.0 mmol) and $H_2C_2O_4$ (0.126 g, 1 mmol) in dimethylsulfoxide (23 ml). The green solution was allowed to evaporate at r.t. After a week, green crystals of $[Cu_2(dpyam)_2(\mu\text{-}C_2O_4)(NO_3)_2(dmso)_2]$ (**3**) formed which were filtered off, washed with mother liquor and air-dried. Yield approximately 95%. *Anal.* Calc. for $C_{26}H_{30}Cu_2N_8O_{12}S_2$: C, 37.27; H, 3.61; Cu, 15.17; N, 13.37. Found: C, 37.34; H, 3.55; Cu, 15.12; N, 13.44%.

2.3. Crystallography

Reflection data for **1** were collected using an Enraf–Nonius MACH3 diffractometer with Mo Kα radiation($\lambda = 0.70183$ Å) at 298 K. An absorption correction was performed by using the Psi-scan program, which resulted in transmission coefficients ranging from 0.917 to 1.000. The structure was solved by direct methods using SHELXS-97 [40] and refined by the least-squares method F^2_{obs} using SHELXL-97 [41]. The non-hydrogen atoms were located on the E map or successive Fourier difference syntheses and anisotropically refined. All other hydrogen atoms were geometrically fixed and allowed to ride on the attached atoms except the water hydrogen atoms, which could not be located at all. One of the perchlorate groups showed disorder which was resolved in two sets with occupancies of 0.5 for both conformers.

Reflection data for **2** were collected at 298 K on a 1K Bruker SMART CCD area-detector diffractometer using graphite monochromated Mo Kα radiation ($\lambda =$ 0.71073 Å) at a detector distance of 4.5 cm and swing angle of −35°. A hemisphere of the reciprocal space was covered by combination of three sets of exposures; each set had a different ϕ angle (0, 88, 180°) and each exposure of 10 s covered 0.3° in ω. Data reduction and cell refinements were performed using the program SAINT [42]. An empirical absorption correction by using the SADABS [43] program was applied, which resulted in transmission coefficients ranging from 0.659 to 1.000. The structure was solved by direct methods and refined by full-matrix least-squares method on F^2_{obs} with anisotropic thermal parameters for all non-hydrogen atoms using the SHELXTL-PC V 5.03 software package [44]. All hydrogen atoms were geometrically fixed and allowed to ride on the attached atoms. Two BF_4^- groups and three water molecules are disordered with site occupancies of 0.5 for both conformers. The hydrogen atoms of the lattice water molecules could not be located at all.

A crystal of compound **3** was selected and mounted to a glass fiber using the oil-drop method. Data were collected on a Rigaku AFC-7S diffractometer (graphite-monochromated Mo Ka radiation, ω–2θ scans). The intensity data were corrected for Lp, for absorption (psi-scan absorption correction) and extinction. The structures were solved by direct methods. The programs TEXSAN [45], SHELXS-97 [50], SHELXL-97 [41] were used for data reduction, structure solution and structure refinement, respectively. Refinement of F^2 was done against all reflections. The weighted R factor, wR, and goodness of fit S are based on F^2. Conventional R factors, R, are based on F, with F set to zero for negative F^2. All non-H atoms were refined anisotropically. The H atoms were introduced in calculated positions and refined with fixed geometry with respect to their carrier atoms.

The molecular graphics were created by using SHELXTL-PC [44]. The crystal and refinement details for compounds **1**–**3** are listed in Table 1.

3. Results and discussion

3.1. Description of $[Cu_2(dpyam)_4(C_2O_4)]X_2(H_2O)_3$ ($X=(ClO_4)$ (1) and (BF_4) (2))

The structures of **1** and **2** are made up of oxalate bridged non-centrosymmetric dinuclear cations $[(dpyam)_2Cu(C_2O_4)Cu(dpyam)_2]^{2+}$, non-coordinating ClO_4^- and BF_4^- anions and water molecules of crystallization. The structures are depicted in Figs. 1

Table 1
Crystal and refinement data for complexes **1**, **2** and **3**

Complex	**1**	**2**	**3**
Molecular formular	$[Cu_2(dpyam)_4(C_2O_4)](ClO_4)_2(H_2O)_3$	$[Cu_2(dpyam)_4(C_2O_4)](BF_4)_2(H_2O)_3$	$[Cu_2(dpyam)_2(C_2O_4)NO_3)_2((CH_3)_2SO)_2$
Molecular weight	1152.8	1126.5	837.76
T (K)	293(2)	293(2)	297.76
Crystal system	triclinic	triclinic	triclinic
Space group	P_1	P_1	$P\bar{1}$
a (Å)	9.599(2)	9.629(2)	8.719(0)
b (Å)	11.206(2)	11.170(2)	8.980(9)
c (Å)	12.480(3)	12.381(2)	11.421(0)
α (°)	73.22(3)	73.81(2)	68.58(0)
β (°)	77.84(3)	78.15(2)	77.79(0)
γ (°)	76.88(3)	76.59(2)	80.58(0)
V (Å^3)	1236.5(4)	1229.7(2)	808.87(1)
Z	1	1	1
D_{calc} (g cm^{-3})	1.542	1.516	1.720
μ (mm)	1.046	0.956	3.495
F (000)	588	569	428
Crystal size (mm)	0.30 × 0.42 × 0.45	0.33 × 0.45 × 0.75	0.35 × 0.35 × 0.22
Reflection collected	4834	9078	3171
Unique reflections	4834 ($R_{int} = 0.0000$)	7711 ($R_{int} = 0.0179$)	2964 ($R_{int} = 0.0281$)
Observed ref. [$I > 2\sigma(I)$]	4349	6519	2828
Data/restraints/parameter	4834/3/694	7711/3/679	2964/0/228
Goodness-of-fit	1.076	1.020	1.247
Final R indices [$I > 2\sigma(I)$]	$R_1 = 0.0383$, $wR_2 = 0.1079$	$R_1 = 0.0464$, $wR_2 = 0.1401$	$R_1 = 0.0512$, $wR_2 = 0.1363$
R indices (all data)	$R_1 = 0.0442$, $wR_2 = 0.1170$	$R_1 = 0.0547$, $wR_2 = 0.1497$	$R_1 = 0.060747$, $wR_2 = 0.1615$
Largest difference peak and hole (e Å^{-3})	0.854, −0.472	0.946, −0.455	0.968, −0.554

and **2** together with the numbering scheme. Selected bond distances and angles are listed in Table 2.

Compounds **1** and **2** are found to be isomorphous and isostructural, the copper coordination spheres in both complexes display a identical environment. Each copper atom in **1** and **2** has a compressed rhombic octahedral coordination geometry with the equatorial plane formed by two nitrogen atoms from a dpyam ligand and two oxalate–oxygen atoms (Cu–N distances vary from 2.095(8) to 2.141(9) Å and from 2.094(6) to 2.145(7) Å, for **1** and **2** respectively, while Cu–O distances vary

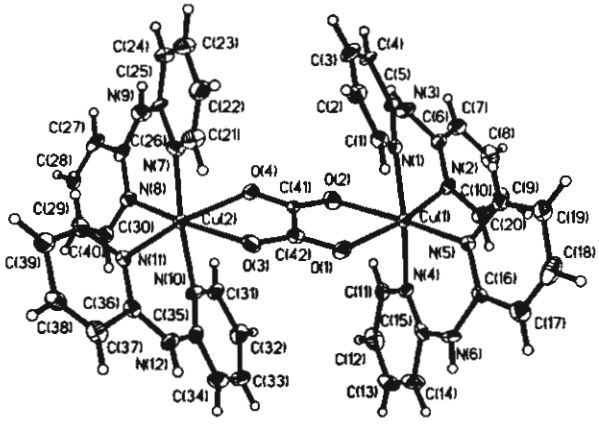

Fig. 1. ORTEP 50% probability plot of the cation in $[Cu(dpyam)_4(C_2O_4)](ClO_4)_2(H_2O)_3$ (**1**)

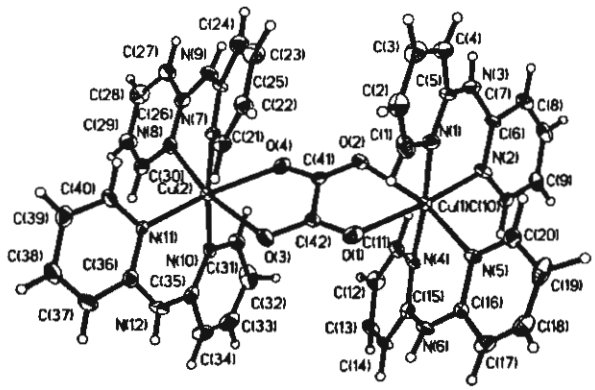

Fig. 2. ORTEP 50% probability plot of the cation in $[Cu_2(dpyam)_4(C_2O_4)](BF_4)_2(H_2O)_3$ (**2**)

from 2.141(10) to 2.305(9) and from 2.189(8) to 2.252(8), for **1** and **2**, respectively). The axial positions are occupied by the other nitrogen atoms of the dpyam ligand (Cu–N distances vary from 2.000(8) to 2.025(8) and from 2.006(7) to 2.024(6) Å, for **1** and **2**, respectively), resulting in the rather unique $CuN_2O_2N_2'$ (4+2) chromophore. This axially-compressed octahedral (2+4) geometry is uncommon as most of other dinuclear μ-oxalatodicopper(II) complexes found in literature have five-coordinate geometries. This geometry has only been previously observed in the dinuclear oxalato-bridged Cu^{II} complexes with a tetradentate terminal ligand [11].

Table 2
Selected bond lengths (Å) and angles (°) with e.s.d.s. in parentheses of $[Cu_2(dpyam)_4(C_2O_4)](ClO_4)_2(H_2O)_3$ (1) and $[Cu_2(dpyam)_4(C_2O_4)](BF_4)_2(H_2O)_3$ (2)

	(1)	(2)
Bond lengths		
Cu(1)–N(1)	2.020(9)	2.008(8)
Cu(1)–N(2)	2.136(8)	2.111(7)
Cu(1)–N(4)	2.000(8)	2.024(6)
Cu(1)–N(5)	2.095(8)	2.134(8)
Cu(1)–O(1)	2.141(10)	2.229(8)
Cu(1)–O(2)	2.305(9)	2.252(8)
Cu(2)–N(7)	2.010(9)	2.021(8)
Cu(2)–N(8)	2.141(9)	2.145(7)
Cu(2)–N(10)	2.025(8)	2.006(7)
Cu(2)–N(11)	2.107(8)	2.094(6)
Cu(2)–O(3)	2.225(9)	2.208(9)
Cu(2)–O(4)	2.229(8)	2.189(8)
Cu(1)–Cu(2)	5.752(3)	5.745(3)
Bond angles		
N(1)–Cu(1)–N(4)	175.4(3)	173.4(3)
N(2)–Cu(1)–O(1)	165.8(3)	170.7(3)
N(5)–Cu(1)–O(2)	171.4(3)	166.0(2)
N(2)–Cu(1)–N(5)	97.5(3)	97.1(3)
O(1)–Cu(1)–O(2)	74.7(3)	74.8(2)
N(7)–Cu(2)–N(10)	173.2(4)	175.5(3)
N(8)–Cu(2)–O(3)	168.9(3)	166.1(2)
N(11)–Cu(2)–O(4)	166.8(3)	170.1(3)
N(8)–Cu(2)–N(11)	97.3(3)	97.6(3)
O(3)–Cu(2)–O(4)	73.7(3)	73.9(3)

This geometry arise due to the flexible nature of the dpyam ligand compared to the bpy, phen or other didentate chelate ligands which are found to have a square-pyramidal structure with the counter anion or solvent molecule occupying the axial position and the general formula of $[(NN)Cu(\mu\text{-}C_2O_4)Cu(NN)]X_n$, (in which X = counter anion or solvent molecule) [5–14]. Some compounds of this formula present an additional bond to X, giving rise to an axially-elongated octahedral geometry [5–10]. In addition, the compounds **1** and **2** are two rare examples of 2+4 compressed rhombic coordination resulting from a pseudo Jahn–Teller effect. As in almost all the cases of observed Jahn–Teller compression examined in detail to date, the apparent compression is due to dynamic interconversion between two of the possible axial elongations [51,52].

For compound **1**, the lattice is similarity further stabilized by hydrogen bonding between the amine-N and O_{ClO4} (N···O distances 3.059–3.334 Å) and O_{water} (N···O distances 2.828–2.843 Å) and between the O_{water} and O_{ClO4} (O···O distance 3.094 Å) and $O_{oxalate}$ (O···O distance 3.002 Å).

For compound **2**, the lattice is stabilized by hydrogen bonding between the amine-N and F_{BF4} (N···F distances 2.974–3.189 Å) and O_{water} (N···O distances 2.750–2.923 Å)

3.2. Description of $[Cu_2(dpyam)_2(C_2O_4)(NO_3)_2((CH_3)_2SO)_2]$ (3)

The structure of **3** consists of centrosymmetric $[Cu_2(dpyam)_2(\mu\text{-}C_2O_4)(NO_3)_2((CH_3)_2SO)_2]$ molecules. This unit is depicted in Fig. 3 together with the numbering scheme. Selected bond distances and angles are listed in Table 3.

The geometry around the copper atom can be considered as an elongated tetragonal octahedral environment with the equatorial plane formed by two nitrogen atoms of dpyam ligand and two oxygen atoms of the oxalate bridge (Cu–N/O distances vary from 1.986(2) to 2.002(2) Å), with the axial sites occupied by an oxygen atom of the nitrato group (Cu–O 2.502(2) Å) and the oxygen atom of the dimethylsulfoxide group (Cu–O 2.331(2) Å]. The copper–copper distance is 5.220(2) Å. The axial O_2NO–Cu–$OS(CH_3)_2$ angle is 174.8(7)° and the four donor atoms on the equatorial plane are not perfectly planar, showing a small tetrahedral distortion, with a dihedral angle of 7.2° formed between the O–Cu–O and N–Cu–N planes. The copper atoms are displaced by 0.0770 Å from the basal planes toward O(4).

The lattice is further stabilized by hydrogen bonding between the amine-N and an O_{NO3} of a neighbouring unit with a distance of 2.8551 Å, resulting in a polymeric chain.

3.3. Structure comparisons

The compounds **1** and **2** are found to be isomorphous and isostructural, and have compressed rhombic octahedral $CuN_2O_2N'_2$ chromophores. The most similarity to the stereochemistry of both complexes are found in the oxalato-bridged dimers $[Cu_2(bispicen)_2(C_2O_4)]$-

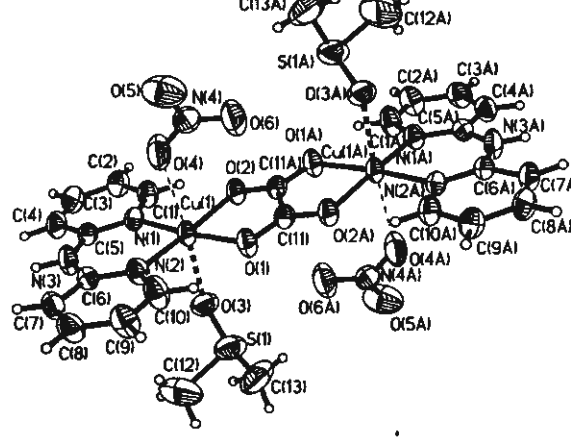

Fig. 3. ORTEP 50% probability plot of $[Cu_2(dpyam)_2(C_2O_4)(NO_3)_2((CH_3)_2SO)_2]$ (3) Atoms with an 'A' are generated by an inversion centre.

Table 3
Selected bond lengths (Å) and angles (°) with e.s.d.s. in parentheses for $[Cu_2(dpyam)_2(C_2O_4)(NO_3)_2((CH_3)_2SO)_2]$ (3)

Bond lengths			
Cu(1)–N(1)	1.986(2)	Cu(1)–N(2)	2.002(2)
Cu(1)–O(1)	1.998(2)	Cu(1)–O(2)	1.994(2)
Cu(1)–O(3)	2.331(2)	Cu(1)–O(4)	2.502(2)
Cu(1)–Cu(1A)	5.220(2)		
Bond angles			
N(1)–Cu(1)–O(2)	92.3(2)	N(1)–Cu(1)–O(1)	174.3(8)
O(2)–Cu(1)–O(1)	82.2(7)	N(1)–Cu(1)–N(2)	93.3(2)
O(2)–Cu(1)–N(2)	170.9(3)	O(1)–Cu(1)–N(2)	91.8(7)
N(1)–Cu(1)–O(3)	88.2(6)	O(2)–Cu(1)–O(3)	93.5(7)
O(1)–Cu(1)–O(3)	93.5(5)	O(4)–Cu(1)–N(1)	86.6(7)
O(4)–Cu(1)–N(2)	85.5(7)	O(4)–Cu(1)–O(1)	91.7(7)
O(4)–Cu(1)–O(2)	87.7(7)	O(4)–Cu(1)–O(3)	74.8(7)

Symmetry code: A = $-x, -y+1, -z$.

$(ClO_4)_2$ (**9**), $[Cu_2(bispicMe_2en)_2(C_2O_4)](ClO_4)_2$ (**10**), which have the compressed octahedral $CuN_2O_2N_2'$ chromophores (see Table 4). Related complexes are $[Cu_2(bpy)_2(C_2O_4)(NO_3)_2(H_2O)_2]$ (**4**), $[Cu_2(mpym)_2(C_2O_4)(NO_3)_2(H_2O)_2]$ (**5**), $[Cu_2(deen)_2(C_2O_4)(ClO_4)_2(H_2O)_2]$ (**6**),and $[Cu_2(tacn)_2(C_2O_4)(ClO_4)_2]$ (**7**) (Table 4), which have an elongated octahedral $CuN_2O_2O'O''$ and CuN_3O_2O chromophores, respectively, similar to the $CuN_2O_2O'O''$ chromophore geometry of **3**. There is some similarity to other dinuclear μ-oxalato dicopper(II) complexes which exhibit a square-pyramidal structure with two oxygen atoms of oxalate bridge and two nitrogen atoms of the diamine occupying the base of the pyramid and the counter anion or a solvent molecule occupying the axial position [12–14]. There are some differences to the elongated octahedral complex $[Cu_2(bpca)_2(C_2O_4)(H_2O)_2](H_2O)_2$ (**8**) involving the oxalato-bridged occupying axial and equatorial coordination sites and the trigonal bipyramidal complex $[Cu_2(Et_5dien)_2(C_2O_4)](BPh_4)_2]$ (in which Et_5dien is 1,1,4,7,7-pentaethylenetriamine) [15].

The coordination around the Cu ion of **1**, **2** can be best described as an axially-compressed octahedral (2+4) geometry [11], and differs from those of **3**, **4**, **5**, **6**, **7** which have an axially-elongated octahedral (4+2) geometry [5–10].

3.4. IR and electronic spectra

3.4.1. IR spectra

The IR spectra of **1** and **2** display characteristic bands of the asymmetric oxalate bridging ligand [6,8–10]: $\nu_{asym\ (C-O)}$ at 1647s, $\nu_{sym\ (C-O)}$ at 1375m and $\delta_{(O-C-O)}$ at 843m cm^{-1} for **1**; $\nu_{asym\ (C-O)}$ at 1642s, $\nu_{sym\ (C-O)}$ at 1370m and $\delta_{(O-C-O)}$ at 845m cm^{-1} for **2**. The ClO_4^- group vibration near 1100 cm^{-1} splitting into three sharp peaks at 1090s, 1116s and 1142s cm^{-1} and the BF_4^- group vibration near 1100 cm^{-1} splitting into a sharp

Table 4
Structural data and magnetic properties for 10 selected oxalato-bridged Cu(II) complexes

Compound[a]	Donor set	Geometry[b]	Oxalato-bridged Coordination	d_{Cu-Cu} (Å)	Dihedral angle[c]	Mode of magnetic interaction	J (cm^{-1})	Ref.
$[Cu_2(dpyam)_4(C_2O_4)](ClO_4)_2(H_2O)_3$ (**1**)	$O_2N_2N_2'$	com. Oct	eq–eq	5.752	11.3/11.3	c	2.42	this work
$[Cu_2(dpyam)_4(C_2O_4)](BF_4)_2(H_2O)_3$ (**2**)	$O_2N_2N_2'$	com. Oct	eq–eq	5.745	11.4/11.0	c	3.38	this work
$[Cu_2(dpyam)_2(C_2O_4)(NO_3)_2(DMSO)_2]$ (**3**)	$O_2N_2O'O$	elong. Oct	eq–eq	5.22	7	a	−305	this work
$[Cu_2(bpy)_2(C_2O_4)(NO_3)_2(H_2O)_2]$ (**4**)	$O_2N_2O'O''$	elong. Oct	eq–eq	5.143	4.6	a	−382	[5]
$[Cu_2(mpym)_2(C_2O_4)(NO_3)_2(H_2O)_2]$ (**5**)	$O_2N_2O'O''$	elong. Oct	eq–eq	5.217	d	a	−142	[7]
$[Cu_2(deen)_2(C_2O_4)(ClO_4)_2(H_2O)_2]$ (**6**)	$O_2N_2O'O''$	elong. Oct	eq–eq	d	3.88	a	−300	[8]
$[Cu_2(tacn)_2(C_2O_4)(ClO_4)_2]$ (**7**)	O_2N_3O'	elong. Oct	eq–eq	5.176	d	a	−41	[9]
$[Cu_2(bpca)_2(C_2O_4)(H_2O)_2](H_2O)_2$ (**8**)	O_2N_3O'	elong. Oct	ax–eq	5.631	d	b	1.1	[10]
$[Cu_2(bispicen)_2(C_2O_4)](ClO_4)_2$ (**9**)	$O_2N_2N_2'$	com. Oct	eq–eq	5.608	d	c	2.3	[11]
$[Cu_2(bispicMe_2en)_2(C_2O_4)](ClO_4)_2$ (**10**)	$O_2N_2N_2'$	com. Oct	eq–eq	5.494	d	c	2.14	[11]

[a] dpyam = di-2-pyridylamine; bpy = 2,2′-dipyridine; mpym = meripirizole; deen = *N*,*N*-diethylethane-1,2-diamine; tacn = 1,4,7-triazacyclononane; bpca = bis(2-pyridylmethyl)1-3,3-propanediamine; bispicen = *N*,*N*′-bis(2-pyridylmethyl)-1,2-ethanediamine; bispicMe2en = N,N′-bis(2-pyridylmethyl)-N-N-dimethyl-1,2-ethanediamine.
[b] com.Oct = compressed octahedral; elong. Oct = elongated octahedral.
[c] Dihedral angle between the basal and oxalate planes.
[d] Not reported.

peak at 1075 cm^{-1} and a shoulder at approximately 1055 cm^{-1}, indicates ClO_4^- ions in **1** and BF_4^- ions in **2** involved hydrogen bonding [46,47].

Compound **3** displays the characteristic bands of the symmetric oxalate bridging ligand $\nu_{asym(C-O)}$ at 1650s, $\nu_{sym(C-O)}$ at 1370m and $\delta_{(O-C-O)}$at 840m cm^{-1}. The bands observed at 1380s, 1320s,1080m cm^{-1} suggest monodentate coordination of the nitrate ion [6] and the SO stretching appear at approximately 1023w cm^{-1}, indicative of the presence of the dimethylsulfoxide ligand in **3** [48].

3.4.2. Electronic spectra

The electronic reflectance spectra of **1** and **2** consist of two clearly resolved peaks at 14 050 and 8800 cm^{-1} for **1** and 13 970 and 8700 cm^{-1} for **2**. These spectra are consistent with the compressed rhombic octahedral stereochemistry and assigned to be the $d_{x^2-y^2} \rightarrow d_{z^2}$ and the d_{xz}, d_{xy}, $d_{yz} \rightarrow d_{z^2}$ transitions. That of **3** has a broad peak center at 14700 cm^{-1}, with a poorly resolved shoulder to low energy at approximately 10600 cm^{-1}, corresponding to the elongated octahedral geometry. This suggests the assignment of the bands as the d_{xz}, d_{yz}, $d_{xy} \rightarrow d_{x^2-y^2}$ and $d_{z^2} \rightarrow d_{x^2-y^2}$ transitions, respectively.

3.5. EPR and Magnetic properties

The room temperature X-band powder EPR spectra of compounds **1** and **2** display a broad absorption centered around g of 2.14. At the high-field side (g = approximately 1.94) a small shoulder is observed which is due to a signal from the triplet state with a very small zero-field splitting. No half-field signal was observed at RT.

Both compounds were also measured as solids at 77 K, in which cases the signal appears as more resolved with non-split signals at $g_\perp = 2.10$, $g_\parallel = 2.27$ for **1** and $g_\perp = 2.10$, $g_\parallel = 2.33$ for **2**, corresponding to the pattern of Cu(II) in an elongated geometry, $g_\parallel > g_\perp > 2.0$ with the $d_{x^2-y^2}$ ground state. This suggest that the apparent compressed geometry at room temperature could be caused by a dynamic Jahn–Teller effect [51,52]. This is because compounds **1** and **2** adopt the time averaged structure found crystallographically which arise due to the short time scale of the X-ray technique, but the EPR spectra at 77 K are related to the underlying static axial elongated chromophore [51,52]. Also the half-field signal at approximately 1600 G, corresponding to $\Delta M = \pm 2$ transition was observed, which indicates that indeed a weak interaction between two Cu(II) ions within these compounds is present.

Compound **3**, measured as a powdered solid displays at RT an asymmetric broad resonance with a center at $g = 2.12$. The observed triplet signal is not resolved, apparently due to exchange narrowing resulting from nearby triplet molecules in the lattice. At 77 K a weak resolved signal is observed, with bands assigned for H_{z1} at 2691 G, H_{x1y1} at 3014 G, H_{x2y2} at 3218 G and H_{z2} at 3316 G. On the low field side of the $\Delta M = \pm 1$ signal of compound **3** a seven-line Cu hyperfine resonance centered at $g = 2.44$, with an average spacing of 88 G, is observed. The seventh line of this pattern is obscured by the intense signal of the perpendicular component. Such a seven-line pattern, is evidence for the parallel $\Delta M = \pm 1$ transition and indicative for a small zero-field splitting parameter, D [49,50,53–56]. No half-field signal was observed in this case. So the observed signal is typical for triplet Cu(II) dinuclear in an isolated state with D = approximately 0.03 cm^{-1} [49,50].

From the magnetic susceptibility (vide infra) at 77 K the compound is almost diamagnetic, so the observed resonances are likely to originate from a small paramagnetic impurity and a small amount of triplet signal thermally accessible at 77 K.

The exchange interaction between the copper ions via the oxalate bridge is known to be strongly dependent on the geometry around the Cu ions, the orientation of the magnetic orbitals in respect to the oxalate plane and the bridging mode of the oxalate group, which favours the antiferromagnetic interaction [5,6,16–21]. This interaction is weakened by structural distortions, such as the displacement of the copper atom out of the basal plane, the non-planarity of the Cu–ox–Cu framework and the tetrahedral distortion of the basal plane.

In compounds **1** and **2** the short Cu–L bonds result in magnetic orbitals that do not coincide with the oxalate ligand plane and therefore any significant antiferromagnetic interaction is not present. Instead a weak ferromagnetic interaction is seen and this agrees well to related systems from literature [10,11].

The magnetic susceptibility of the powdered compounds were measured from 5 to 280 K. At 280 K μ_{eff} is 2.62 μ_B for **1** (2.64 μ_B for **2**) which agrees well with the spin-only value of Cu(II) calculated for two uncoupled spin = 1/2 centres. Upon cooling these values are staying almost constant between about 2.64 and 2.61 μ_B until at about 50 K it raises gradually to reach 2.77 μ_B at 5 K for **1** (2.80 μ_B for **2**). This is typical for a very weak ferromagnetically coupled Cu(II) dinuclear compound. To reproduce this behaviour the theoretical expression of the magnetic susceptibility of spin = 1/2 dimer, arising from the hamiltonian $H = -J\ S_1 \cdot S_2$, has been considered, including possible intermolecular interactions, in the molecular-field approximation ([53], p. 132): $\chi_m = (2Ng^2\beta^2)[kT-(2\ zJ'/(3+\exp(-J/kT)))]^{-1}\ [3+\exp(-J/kT)]^{-1}\ (1-p)+\chi_p p$ where J is the singlet–triplet energy gap (negative value for antiferromagetic and positive value for ferromagnetic interaction) and N, g, β, k and T have their usual meanings. The parameter p denotes the molar fraction of paramagnetic impurity in the sample ([53], p. 107) and zJ' the interaction between neighbouring dinuclear identities.

Minimisation of the expression $R = \Sigma(\chi_{obs} - \chi_{calc})^2/\Sigma \chi^2_{obs}$, resulted in the best-fit parameters $J = 2.42$ cm^{-1}, $g = 2.12$ and zJ' and $p = 0$ with $R = 4.8 \times 10^{-4}$ for compound **1** (see Fig. 4(a)) and $J = 3.38$ cm^{-1}, $g = 2.10$ and zJ' and $p = 0$ with $R = 2.8 \times 10^{-3}$ for compound **2** (see Fig. 4(b)), which confirms the ferromagnetic type of the intradimer interaction.

The dinuclear unit is slightly folded in a chair from and the dihedral angles between the basal and the oxalate planes and the Cu–Cu distance are 5.752 Å in **1** and 5.745 Å in **2**. The magnetic orbitals are perpendicular to the oxalate plane, so the overlap of the Cu(II) orbitals do not coincide with the oxalate σ orbitals. This situation is corresponding to the coordinate *mode c* (Scheme 2) and consequently (as in fact the value of the exchange coupling (J) in a Cu(II) dimer is decomposed in two terms, of which one is antiferromagnetic (J_{AF}) and the other is ferromagnetic (J_F) according to $J = J_{AF} + J_F$)) when the antiferromagnetic term is almost zero, the ferromagnetic term is predominant, which is confirmed by the susceptibility measurements presented above.

The temperature dependence of the molar magnetic susceptibility χ_M of **3**, measured on a powdered sample, is shown in Fig. 5 down to 5 K. At 280 K, χ_M is equal to 1.6×10^{-3} cm^3 mol^{-1} and decreases when cooling down and reaches almost zero at about 40 K. From 40 to 5 K the χ_M increases a little to 0.4×10^{-3} cm^3 mol^{-1}. The susceptibility data were fitted using the formula mentioned earlier with minimisation of the expression $R = \Sigma(\chi_{obs} - \chi_{calc})^2/\Sigma \chi^2_{obs}$ and resulted in the best-fit parameters $J = -305$ cm^{-1}, $g = 2.14$ and $zJ' = 0.07$ and $p = 1 \times 10^{-2}$ with $R = 0.6\%$, which confirms the strong antiferromagnetic type of the interaction. The measurements were repeated several times, but special in the high temperature area the fit is not so good, resulting in a somewhat high R value.

Compound **3** exhibits an elongated octahedral geometry and in this case the Cu(II) orbitals interact with the oxalate σ orbitals, which is consistent with the coordinated *mode a* (Scheme 2) and a strong antiferromagnetic interaction is expected, which is confirmed by the magnetic susceptibility measurements presented above and also with similar cases known in the literature [5,8].

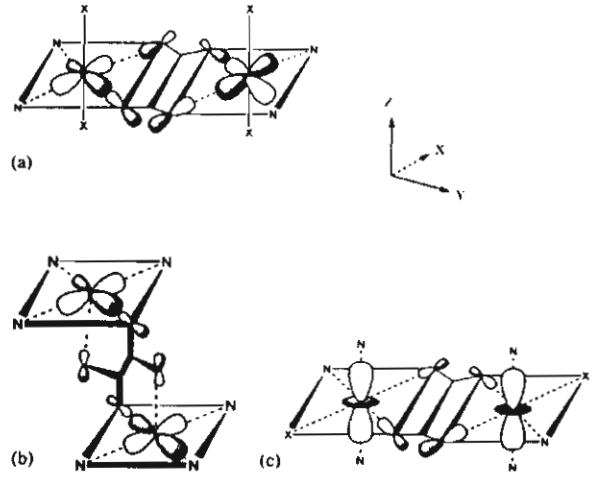

Scheme 2. Three models predicting the magnetic interactions in oxalato-bridged Cu(II) complexes (X–O (**1**) or N (**2**)).

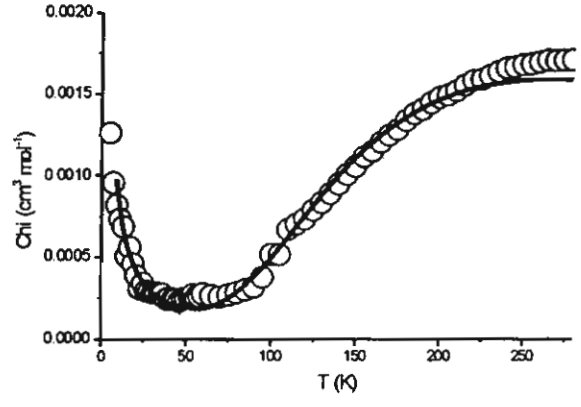

Fig. 5. Temperature dependence of χ_M vs. T for compound **3**. The solid lines represent the calculated curve (see text).

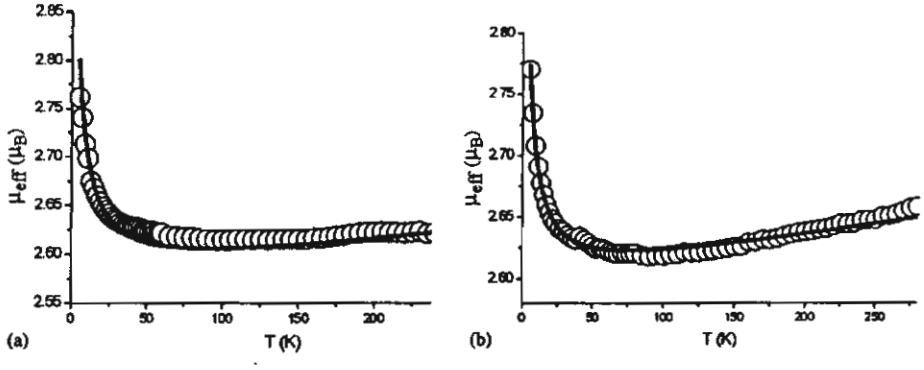

Fig. 4. Temperature dependence of μ_{eff} vs. T for compound **1** (a) and compound **2** (b). The solid lines represent the calculated curve (see text).

4. Conclusions

Three new Cu(II) dinuclear oxalate bridged compounds are presented in this study with the ligand dpyam together with their spectroscopic and magnetic results. Compounds **1** and **2** display a compressed rhombic octahedral geometry, with asymmetrically bound oxalato ligands and have a weak ferromagnetic interaction between the Cu(II) atoms. On the other hand compound **3** has an elongated tetragonal octahedral geometry with a symmetric oxalato bridge and displays a strong antiferromagnetic interaction.

5. Supplementary material

Crystallographic data (excluding structure factors) for the structures in this paper have been deposited with the Cambridge Crystallographic Data Centre, CCDC No. 194972–74 for structures **1**, **2** and **3**, respectively. Copies of the data can be obtained free of charge on application to The Director, CCDC, 12 Union Road, Cambridge CB2 1EZ, UK (fax: (internat.) +44-1223-336-033, e-mail: deposit@ccdc.cam.ac.uk or www: http://www.ccdc.cam.ac.uk).

Acknowledgements

The authors (S.Y, N.C, P.G, P.K) would like to thank the Thailand Research Fund and Khon Kaen University for research grant. Support of the Postgraduate Education and Research Program in Chemistry is also gratefully acknowledged. The work described in the present paper has been supported by the Leiden University Study group WFMO (Werkgroep Fundamenteel Materialen Onderzoek). Part of the work has been supported financially by the Graduate Research School Combination 'Catalysis'.

References

[1] M. Hernández-Molina, P.A. Lorenzo-Luis, C. Ruiz-Pérez, Cryst. Eng. Comm. (2001) article #16.
[2] O. Castillo, A. Luque, S. Iglesias, C. Guzmán-Miralles, P. Román, Inorg. Chem. Comm. 4 (2001) 640.
[3] H.Z. Kou, D.Z. Liao, G.M. Yang, P. Cheng, Z.H. Jiang, S.P Yan, G.L. Wang, X.K. Yao, H.G. Wang, Polyhedron 18 (1998) 3193.
[4] H. Núñez, J.J. Timor, J. Server-Carrió, L. Soto, E. Escrivá, Inorg. Chim. Acta. 318 (2001) 8.
[5] O. Castillo, I. Muga, A. Luque, J.M. Gutierrez-Zorrilla, J. Sertucha, P. Vitoria, P. Román, Polyhedron 18 (1999) 1235.
[6] J. Tang, E. Gao, W. Bu, D. Liao, S. Yan, Z. Jiang, G. Wang, J. Mol. Struct. 525 (2000) 271.
[7] L.S. Tuero, J. Garcia-Lozano, E.E. Monto, M.B. Borja, F. Dahan, J.P. Tuchagues, J.P. Legros, J. Chem. Soc., Dalton Trans. (1991) 2619.
[8] R. Vicente, A. Escuer, J. Ferretjans, H. Stoeckli-Evans, X. Solans, M. Font-Bardía, J. Chem. Soc., Dalton Trans. (1997) 167.
[9] L. Zhang, W.-M. Bu, S.-P. Yan, Z.-H. Jiang, D.-Z. Liao, G.-L. Wang, Polyhedron 19 (2000) 1105.
[10] M.L. Calatayud, I. Castro, J. Sletten, F. Lloret, M. Julve, Inorg. Chim. Acta. 300–302 (2000) 846.
[11] J. Glerup, P.A. Goodson, D.J. Hodgson, K. Michelsen, Inorg. Chem. 34 (1995) 6255.
[12] M. Julve, M. Verdaguer, A. Gleizes, M. Philoche-Levisalles, O. Kahn, Inorg. Chem. 23 (1984) 3808.
[13] G.R. Hall, D.M. Duggan, D.N. Hendrickson, Inorg. Chem. 14 (1975) 1956.
[14] Y. Akhriff, J. Server-Carrió, A. Sancho, J. Garcia-Lozano, E. Escrivá, J.V. Folgado, L. Soto, Inorg. Chem. 38 (1999) 1174.
[15] T.R. Felthouse, E.J. Laskowski, D.N. Hendrickson, Inorg. Chem. 16 (1977) 1077.
[16] J. Cano, P. Alemany, S. Alvarez, M. Verdaguer, E. Ruiz, Chem. Eur. J. 4 (1998) 476.
[17] J. Cabrero, N.B. Amor, C. de Graaf, F. Illas, R. Caballol, J. Phys. Chem., A. 104 (2000) 9983.
[18] O. Castillo, A. Luque, F. Lloret, P. Román, Inorg. Chem. Comman. 4 (2001) 350.
[19] Z. Smékal, Z. Trávnícek, F. Lloret, J. Marek, Polyhedron 18 (1999) 2787.
[20] O. Castillo, A. Luque, P. Román, F. Lloret, M. Julve, Inorg. Chem. 40 (2001) 5526.
[21] O. Castillo, A. Luque, M. Julve, F. Lloret, P. Román, Inorg. Chim. Acta 315 (2001) 9.
[22] H. Oshio, U. Nagashima, Inorg. Chem. 31 (1992) 3295.
[23] Z. Smekal, P. Thornton, Z. Šindelár, R. Klicka, Polyhedron 17 (1998) 1631.
[24] S. Decurtins, H.W. Schmalle, P. Schneuwly, L.M. Zheng, J. Ensling, A. Hauser, Inorg. Chem. 34 (1995) 5501.
[25] G.D. Munno, M. Julve, F. Nicolo, F. Lloret, J. Faus, R. Ruiz, E. Sinn, Angew. Chem., Int. Ed. Engl. 32 (1993) 613.
[26] R. Vicente, A. Escuer, X. Solans, M. Font-Bardia, J. Chem. Soc., Dalton Trans. (1996) 1835.
[27] A. Gleizes, M. Julve, M. Verdaguer, J.A. Real, J. Faus, X. Solans, J. Chem. Soc., Dalton Trans. (1992) 3209.
[28] S.K. Chattopadhyay, T.C.W. Mak, B.S. Luo, L.K. Thompson, A. Rana, S. Ghosh, Polyhedron 14 (1995) 3661.
[29] O. Castillo, A. Luque, J. Sertucha, P. Román, F. Lloret, Inorg. Chem. 39 (2000) 6142.
[30] J. Suárez-Varela, J.M. Domingue-Vera, E. Colacio, J.C. Avila-Rosón, M.A. Hidalgo, D. Martin-Ramos, J. Chem. Soc., Dalton Trans. (1995) 2143.
[31] H.Y. Shen, W.M. Bu, E.Q. Gao, D.Z. Liao, Z.H. Jiang, S.P. Yan, G.L. Wang, Inorg. Chem. 39 (2000) 396.
[32] M. Andruh, R. Melanson, C.V. Stager, F.D. Rochon, Inorg. Chim. Acta 251 (1996) 309.
[33] P. Román, C. Guzmán-Miralles, A. Luque, J.I. Beitia, J. Cano, F. Lloret, M. Julve, S. Alvarez, Inorg. Chem. 35 (1996) 3741.
[34] O. Castillo, A. Luque, M. Julve, F. Lloret, P. Román, Inorg. Chim. Acta 324 (2001) 141.
[35] Z. Smekal, J. Kameníček, P. Klasová, G. Wrzeszcz, Z. Šindelář, P. Kopel, Z. Zák, Polyhedron 21 (2002) 1203.
[36] M. Du, Y.-M. Guo, X.-H. Bu, Inorg. Chim Acta 335 (2002) 136.
[37] J.Y. Lu, M.A. Lawandy, J. Li, T. Yuen, C.L. Lin, Inorg. Chem. 38 (1999) 2695.
[38] I. Castro, J. Faus, M. Julve, M.C. Muñoz, W. Diaz, X. Solans, Inorg. Chim. Acta 179 (1991) 59.
[39] J. Novosad, A.C. Messimeri, C.D. Papadimitriou, P.G. Veltsistas, J.D. Woollins, Trans. Metal Chem. 25 (2000) 664.
[40] G.M. Sheldrick, SHELXS-97, Program for the solution of crystal structures, University of Göttingen, Germany, 1997.

[41] G.M. Sheldrick, SHELXL-97, Program for the refinement of crystal structures, University of Göttingen, Germany, 1997.
[42] SAINT, Data Integration Software, Version 4.0, Bruker AXS, Inc., Madison, WI, 1997.
[43] G.M. Sheldrick, SADABS, Program for empirical absorption correction of area detector data, University of Göttingen, Germany, 1996.
[44] SHELXTL 5.03 (PC-Version), Program library for the solution and molecular graphics, Siemens Analytical Instruments Division, Madison, WI, 1995.
[45] TEXSAN, Single Crystal Structure Analysis Software, Version 1.6, Molecular Structure Corporation, The Woodlands, TX, 77381, USA, 1993.
[46] S. Youngme, C. Pakawatchai, W. Somjitsripunya, S. Chantrapromma, K. Chinnakali, H.K. Fun, Inorg. Chim. Acta. 303 (2000) 181.
[47] S. Youngme, N. Chaichit, P. Kongsaeree, G.A. van Albada, J. Reedijk, Inorg. Chim. Acta 324 (2001) 232.
[48] K. Nakamoto, Infared and Raman Spectra of Inorganic and Coordination Compounds, 5 (Part B), Wiley, New york, (1997) 102.
[49] V.T. Kasumov, F. Köksal, Z. Anorg. Allg. Chem. 627 (2001) 2553.
[50] E. Wasserman, L.C. Snyder, W.A. Yager, J. Chem. Phys. 25 (1964) 1763.
[51] B.J. Hathaway, M. Duggan, A. Murphy, J. Mullane, C. Power, A. Walsh, B. Walsh, Coord. Chem. Rev. 36 (1981) 267.
[52] B.J. Hathaway, Struct. Bonding (Berlin) 57 (1984) 203.
[53] O. Kahn, Molecular Magnetism, VCH Publishers, New York, (1993) 107, 132.
[54] J. Reedijk, B. Nieuwenhuijse, Recl. Trav. Chim. Pays-Bas 91 (1972) 533.
[55] G.J.A.A. Koolhaas, W.L. Driessen, J. Reedijk, J.L. van der Plas, R.A.G. de Graaff, D. Gatteschi, H. Kooijman, A.L. Spek, Inorg. Chem. 35 (1996) 1509.
[56] M. Korabik, M. Materny, W. Surga, T. Glowiak, J. Mrozinski, J. Mol. Struct. 443 (1998) 255.

Transition Metal Chemistry 29: 840–846, 2004.

Dinuclear copper(II) complexes with ferromagnetic and antiferromagnetic interactions mediated by a bridging oxalato group: structures and magnetic properties of $[Cu_2L_4(\mu\text{-}C_2O_4)](PF_6)_2(H_2O)_2$ and $[Cu_2L_2(\mu\text{-}C_2O_4)(NO_3)_2((CH_3)_2NCOH)_2]$ (L = di-2-pyridylamine)

Sujittra Youngme* and Pimprapun Gunnasoot
Department of Chemistry, Faculty of Science, Khon Kaen University, Khon Kaen 40002, Thailand

Narongsak Chaichit
Department of Physics, Faculty of Science and Technology, Thammasat University Rangsit, Pathumthani 12121, Thailand

Chaveng Pakawatchai
Department of Chemistry, Faculty of Science, Prince of Songkla University, Hatyai, Songkla 90112, Thailand

Received 15 April 2004; accepted 04 May 2004

Abstract

Two dinuclear Cu^{II} complexes of formula $[Cu_2(dpyam)_4(\mu\text{-}C_2O_4)](PF_6)_2(H_2O)_2$ *(1)* and $[Cu_2(dpyam)_2(\mu\text{-}C_2O_4)(NO_3)_2(DMF)_2]$ *(2)* (dpyam = di-2-pyridylamine) have been synthesized and their spectroscopic and magnetic properties characterized. Complex *(1)* crystallizes in the non-centrosymmetric monoclinic space group Pc, while *(2)* crystallizes in the non-centrosymmetric triclinic space group P1. Compound *(1)* involves the compressed octahedral Cu^{II} environment, whereas *(2)* exhibits an elongated octahedral Cu^{II} geometry. Both complexes contain six-coordinate metal centers bridged by planar bis-didentate oxalate group. The geometry, spectroscopic properties and the effective magnetic moment of *(1)* are very close to those of the recently published $[Cu_2(dpyam)_4(\mu\text{-}C_2O_4)](ClO_4)_2(H_2O)_3$ and $[Cu_2(dpyam)_4(\mu\text{-}C_2O_4)](BF_4)_2(H_2O)_3$. Thus *(1)* is expected to exhibit a very weak ferromagnetic interaction between the Cu^{II} centers which is confirmed by EPR spectrum. Those of *(2)* are comparable to those of the recently published $[Cu_2(dpyam)_2(\mu\text{-}C_2O_4)(NO_3)_2(DMSO)_2]$. Therefore a strong antiferomagnetic interaction is expected. The effective magnetic moment at room temperature of *(1)* was measured to be 2.55 BM/dimer, which agrees with the spin only value of Cu^{II}, 2.45 BM calculated for two uncoupled spin = 1/2 centers. In *(2)* the room temperature effective magnetic moment of 2.16 BM/dimer indicates the partial spin paring by antiferromagnetic coupling. This is confirmed by the e.p.r. spectrum and is explained as a result of the magnetic interaction between the coplanar $d_{x^2-y^2}$ orbitals on the two copper atoms.

Introduction

It is now well-known that oxalato bridges can propagate magnetic exchange interactions between paramagnetic metal ions. A number of dinuclear copper complexes with an oxalato bridge, generally formulated as $[(NN)_{1\text{ or }2}Cu(\mu\text{-}C_2O_4)Cu(NN)_{1\text{ or }2}]X_n$, where NN is a chelating ligand, and X is a counter anion or a solvent molecule, have been structurally characterized [1–11] in the past decades.

The previous paper describes the crystal structure, spectroscopic properties and magneto-structural correlation of complexes $[Cu_2(dpyam)_4(\mu\text{-}C_2O_4)](ClO_4)_2(H_2O)_3$, $[Cu_2(dpyam)_4(\mu\text{-}C_2O_4)](BF_4)_2(H_2O)_3$ and $[Cu_2(dpyam)_2(\mu\text{-}C_2O_4)(NO_3)_2(DMSO)_2]$ [12]. The exchange interaction between the copper ions *via* the oxalate bridge is known to be strongly dependent on the geometry around the copper ions, which sensitive to nature of counter anions and terminal ligands. In order to extend the investigation by modifying to other counter ions, this paper reports the synthesis, the results of the structure determination and the magnetic properties of two new μ-oxalato copper(II) complexes, $[Cu_2(dpyam)_4(\mu\text{-}C_2O_4)](PF_6)_2(H_2O)_2$ *(1)* and $[Cu_2(dpyam)_2(\mu\text{-}C_2O_4)(NO_3)_2(DMF)_2]$ *(2)*.

Experimental

Materials and physical measurements

All reagents are commercial grade materials and were used without further purification. Elemental analyses (C, H, N) were performed by the microanalytical Service

* Author for correspondence

of Science and Technological Research Equipment Center, Chulalongkorn University on Perkin-Elmer PE2400 CHNS/O Analyzer. The copper content was determined on an atomic absorption spectrophotometer.

I.r. spectra were recorded with a Spectrum One Perkin-Elmer FTIR spectrophotometer as KBr pellets and, or as Nujol mulls in the 4000–450 cm^{-1} spectral range. Solid-state (diffuse reflectance) electronic spectra were recorded as polycrystalline samples on a Perkin-Elmer Lambda2S spectrophotometer over the 8000–18,000 cm^{-1} range. X-band powder e.p.r. spectra were obtained on a JEOL RE2x electron spin resonance spectrometer using DPPH ($g = 2.0036$) as a standard. The room temperature magnetic susceptibility measurements were carried out on a Faraday-type microbalance. The apparatus was calibrated with $Hg[Co(NCS)_4]$. Data were corrected for magnetization of the sample holder and for diamagnetic contributions, which were estimated from the Pascal constants and the temperature independent paramagnetism was estimated to be 60×10^{-6} cm^3 mol^{-1} per copper(II) ion.

Synthesis of complexes (1) and (2)

Complex (1)

Method A. Compound *(1)* was prepared by adding a solution (10 cm^3) of oxalic acid (0.063 g, 0.5 mmol) to a suspension of $CuCo_3$ (0.221 g, 1.0 mmol) in H_2O (10 cm^3). The mixture was added to a solution containing di-2-pyridylamine (0.342 g, 2.0 mmol) in EtOH (20 cm^3) and potassium hexafluorophosphate (0.184 g, 1.0 mmol) in H_2O (10 cm^3). The resulting blue solution was filtered to remove impurities. After two weeks, green crystals of *(1)* were obtained. They were filtered off, washed with mother liquor and were dried in air. Yield approximately 60%. (Found: C, 41.4; H 3.4; Cu, 10.3; N, 13.7. $C_{42}H_{40}P_2Cu_2F_{12}N_{12}O_6$ calcd.: C, 41.15; H, 3.3; Cu, 10.4; N, 13.7%)

Method B. Compound *(1)* was prepared by adding an aqueous solution (25 cm^3) of $CuSO_4 \cdot 5H_2O$ (0.249 g, 1.0 mmol) to a solution of hexafluorophosphate (0.184 g, 1.0 mmol) in H_2O (20 cm^3), followed by a solution of sodium oxalate (0.124 g, 1 mmol) in H_2O (10 cm^3) and a solution of di-2-pyridylamine (0.171 g, 1.0 mmol) in MeOH (20 cm^3). The resulting green solution was allowed to stand at room temperature for two weeks to produce green crystals of *(1)*. The crystals were separated by filtration and washed with the mother liquor. Yield *ca.* 50%. Calcd.: $C_{42}H_{40}P_2Cu_2F_{12}N_{12}O_6$: C, 41.15; H, 3.29; Cu, 10.37; N, 13.71%. Found: C, 41.26; H 3.41; Cu, 10.20; N, 13.65%.

Complex (2)

A solution containing di-2-pyridylamine (0.342 g, 2.0 mmol) in dimethylformamide (10 cm^3) was added to a solution containing $Cu(NO_3)_2 \cdot 3H_2O$ (0.482 g, 2.0 mmol) in DMF (20 cm^3) and sodium oxalate (0.068 g, 0.5 mmol) in H_2O (10 cm^3). Then DMF (30 cm^3) was added to the resulting green solution which was filtered to remove impurities. After 4 months, green crystals of *(2)* were obtained, which were filtered off, washed with the mother liquor and air-dried. Yield *ca.* 70%. Calcd.: $C_{28}H_{32}Cu_2N_{10}O_{12}$: C, 40.6; H, 3.9; Cu, 15.35; N, 16.92. Found: C, 40.5; H, 3.8; Cu, 15.3; N, 16.8.

Found: C, 40.5; H, 3.8; Cu, 15.3; N, 16.8 $C_{28}H_{32}Cu_2N_{10}O_{12}$ calcd.: C, 40.5; H, 3.9; Cu, 15.35; N, 16.9%.

Crystallographic data collection and structure determination of complexes (1) and (2)

Reflection data for *(1)* were collected at 298 K on a 1 K Bruker SMART CCD area-detector diffractometer using graphite monochromated MoK_α radiation ($\lambda = 0.71073$ Å) at a detector distance of 4.5 cm and swing angle of −35°. A hemisphere of the reciprocal space was covered by a combination of three sets of exposures; each set had a different ϕ angle (0°, 88°, 180°) and each exposure of 30 S covered 0.3° in ω. Data reduction and cell refinement were performed using the program SAINT [13]. An empirical absorption correction by using the SADABS [14] program was applied, which resulted in transmission coefficients ranging from 0.5054 to 1.0000. The structure was solved by direct methods and refined by full-matrix least-squares method on F^2_{obs} with anisotropic thermal parameters for all non-hydrogen atoms using the SHELXTL-PC V 6.1 software package [15]. All hydrogen atoms were geometrically fixed and allowed to ride on the attached atoms. One of the hydrogen atoms of each lattice water molecule could not be located and the hexafluorophosphate groups are well ordered.

Reflection data of *(2)* were collected on a 4 K Bruker SMART APEX CCD area-detector diffractometer with graphite monochromated MoK_α radiation ($\lambda = 0.71073$ Å) (at a detector distance of 6.0 cm and swing angle of −28°) using SMART program. Raw data frame integration was performed with SAINT [13], which also applied correction for Lorentz and polarization effects. Absorption corrections were applied using SADABS [14], provided an empirical absorption correction and put the standard deviations of measured intensities onto absolute scale. The structures were solved by direct methods. The software package SHELXTL V 6.12 [15] was used for structure solution and structure refinement. All non-H atoms were refined anisotropically except the nitrate-O atoms and the methyl-C atoms of DMF. The H atoms were introduced in calculated positions and refined with fixed geometry with respect to their carrier atoms. The nitrate groups are disordered with site occupancies of 0.48 and 0.52 for both conformers. Both methyl groups of the DMF ligands are also disordered with site occupancies of 0.44 and 0.56 for both conformers and some of the methyl hydrogen atoms could not be located.

The molecular graphics were created by using SHELXTL-PC [15]. The crystal and refinement details for compounds *(1)* and *(2)* are listed in Table 1. Selected bond lengths and angles are given in Table 2.

Crystallographic data for the structures in this paper have been deposited with the Cambridge Crystallographic Data Centre as supplementary publication CCDC No. 227148 and 227149 for structures 1 and 2, respectively. Copies of the data can be obtained free of charge from The Director, CCDC, 12 Union Road, Cambridge CB2 1EZ, UK (fax: +44-1223-336033; e-mail: deposit@ccdc.cam.ac.uk, www:http://www.ccdc.cam.ac.uk).

Result and discussion

Crystal structure of $[Cu_2(dpyam)_4(C_2O_4)](PF_6)_2(H_2O)_2$ (1)

The structure of *(1)* consists of a noncentrosymmetric dinuclear $[(dpyam)_2Cu(C_2O_4)Cu(dpyam)_2]^{2+}$ cation, two non-coordinated PF_6^- anions and two crystallization water molecules. An ORTEP plot, together with the numbering scheme of the compound is shown in Figure 1, with relevant distances and angles in Table 2.

The chromophore of *(1)* is very similar to the recently published compounds $[Cu_2(dpyam)_4(C_2O_4)](ClO_4)_2(H_2O)_3$ and $[Cu_2(dpyam)_4(C_2O_4)](BF_4)_2(H_2O)_3$ [12]. The two copper(II) ions of the complex cation are linked through an oxalato bridge, leading to a Cu...Cu distance of 5.737(2) Å. The copper atoms are involved in the rather unique $CuN_2O_2N'_2$ (4 + 2) chromophore, and lie in the uncommon compressed rhombic octahedral environment. The equatorial coordination positions are occupied by two oxalate oxygen atoms and two nitrogen atoms of the dpyam ligand (Cu—O and Cu—N distances range from 1.992 to 2.448 Å) and the other two nitrogen atoms from each dpyam ligand in axial positions (Cu—N bond lengths in the 1.979–2.098 Å range). There is a very slight tetrahedral distortion of the equatorial planes [dihedral angles between CuN_2 and CuO_2 planes = 3.2° and 1.2° for Cu(1) and Cu(2) centers, respectively], therefore both four-donor atoms basal planes are planar [r.m.s.d's = 0.0263 and 0.0028 Å] and the copper atoms are displaced by 0.0350 and 0.0168 Å from the basal planes toward N(5) and N(11) atoms for the Cu(1) and Cu(2) centers, respectively. The two basal planes are parallel to each other with dihedral angle of 1.4°. The oxalate divalent anion is planar (r.m.s.d = 0.0132) and it bridges the two copper atoms in the nearly symmetric mode of coordination. The copper atoms deviate by 0.2339, −0.1947 Å for the Cu(1) and Cu(2), respectively, from the oxalate plane. The dimeric entity is slightly folded in a chair form, the basal planes make the angles of 7.2° and 5.7° and with the oxalate mean plane.

The lattice is similarly further stabilized by hydrogen bonding between amine-N and F_{PF6} (N—O distances 3.075–3.391 Å) and O_{water} (N—O distances 2.952–

Table 1. Crystal and refinement data for complexes *(1)* and *(2)*

Complexes	*(1)*	*(2)*
Molecular formula	$[Cu_2(dpyam)_4(\mu\text{-}C_2O_4)](PF_6)_2(H_2O)_2$	$[Cu_2(dpyam)_2(\mu\text{-}C_2O_4)(NO_3)_2(CH_3)_2NCOH)_2]$
Molecular weight	1226.86	829.73
T(K)	293(2)	293(2)
Crystal system	Monoclinic	Triclinic
Space group	Pc	P1
a (Å)	8.5712(2)	8.353(2)
b (Å)	11.3170(2)	9.100(2)
c (Å)	25.8680(5)	12.245(3)
α (°)	90	72.035(4)
β (°)	82.6150(10)	75.228(4)
γ (°)	90	78.552(4)
V (Å^3)	2488.39	848.8(4)
Z	2	1
D_{calc} (g cm^{-3})	1.637	1.623
μ (mm)	1.025	1.330
F(000)	1238	426
Crystal size (mm)	0.25 × 0.30 × 0.43	0.303 × 0.253 × 0.106
Reflection collected	17,865	7532
Unique reflections	10,999 (R_{int} = 0.0407)	6784 (R_{int} = 0.0101)
Observed ref. [$I > 2\sigma(I)$]	7695	6045
Data/restraints/parameter	10,999/2/707	6784/3/534
Goodness-of-fit	1.035	1.063
Final R indices [$I > 2\sigma(I)$]	$R1$ = 0.0657, wR_2 = 0.1686	$R1$ = 0.0377, wR_2 = 0.1011
R indices (all data)	$R1$ = 0.0944, wR_2 = 0.1921	$R1$ = 0.0434, wR_2 = 0.1067
Largest difference peak and hole (e Å^{-3})	1.093 and −0.665	0.365 and −0.389

$R = \sum||F_o|-|F_c||/\sum|F_o||$, $R_w = \{\sum w\{|F_o|-|F_c|\}^2/w|F_o|^2\}^{1/2}$.

Table 2. Selected bond lengths (Å) and angles (°) with e.s.d.s. in parentheses of *(1)* and *(2)*

$[Cu_2(dpyam)_4(\mu\text{-}C_2O_4)](PF_6)_2(H_2O)_2$ *(1)*					
Cu(1)—N(4)	1.992(10)	Cu(1)—N(2)	1.995(9)	Cu(1)—O(1)	2.029(9)
Cu(1)—N(5)	2.049(7)	Cu(1)—N(1)	2.191(6)	Cu(1)—O(2)	2.424(6)
Cu(2)—N(8)	1.979(9)	Cu(2)—O(4)	2.025(8)	Cu(2)—N(7)	2.027(7)
Cu(2)—N(11)	2.098(8)	Cu(2)—N(10)	2.249(8)	Cu(2)—O(3)	2.448(8)
Cu(1)...Cu(2)	5.737(2)				
N(4)—Cu(1)—N(2)	93.0(4)	N(4)—Cu(1)—O(1)	174.7(3)		
N(2)—Cu(1)—O(1)	86.6(4)	N(4)—Cu(1)—N(5)	87.13)		
N(2)—Cu(1)—N(5)	170.4(3)	O(1)—Cu(1)—N(5)	92.5(3)		
N(4)—Cu(1)—N(1)	96.8(3)	N(2)—Cu(1)—N(1)	87.4(3)		
O(1)—Cu(1)—N(1)	88.4(3)	N(5)—Cu(1)—N(1)	102.1(3)		
N(4)—Cu(1)—O(2)	99.7(3)	N(2)—Cu(1)—O(2)	88.6(3)		
O(1)—Cu(1)—O(2)	75.0(3)	N(5)—Cu(1)—O(2)	82.0(3)		
N(1)—Cu(1)—O(2)	163.1(3)	N(8)—Cu(2)—O(4)	90.9(3)		
N(8)—Cu(2)—N(7)	88.7(4)	O(4)—Cu(2)—N(7)	173.8(3)		
N(8)—Cu(2)—N(1)1	171.5(4)	O(4)—Cu(2)—N(11)	89.4(3)		
N(7)—Cu(2)—N(11)	90.1(3)	N(8)—Cu(2)—N(10)	101.5(3)		
O(4)—Cu(2)—N(10)	87.2(3)	N(7)—Cu92)—N(10)	98.9(4)		
N(11)—Cu(2)—N(10)	87.0(3)	N(8)—Cu(2)—O(3)	79.9(4)		
O(4)—Cu(2)—O(3)	75.0(2)	N(7)—Cu(2)—O(3)	98.8(3)		
N(11)—Cu(2)—O(3)	91.9(3)	N(10)—Cu(2)—O(3)	162.2(3)		
$[Cu_2(dpyam)_2(\mu\text{-}C_2O_4)(NO_3)_2((CH_3)_2NCOH)_2]$ *(2)*					
Cu(1)—N(2)	1.979(7)	Cu(1)—N(1)	1.990(6)	Cu(1)—O(2)	2.005(6)
Cu(1)—O(1)	2.012(6)	Cu(1)—O(5)	2.254(7)	Cu(2)—N(4)	1.956(7)
Cu(1)—O(10B)	2.786(2)	Cu(1)—O(8B)	2.679(2)	Cu(2)—N(5)	1.973(7)
Cu(2)—O(4)	1.978(5)	Cu(2)—O(3)	2.002(6)	Cu(2)—O(6)	2.295(7)
Cu(1)...Cu(2)	5.212(2)				
N(2)—Cu(1)—N(1)	90.8(3)	N(2)—Cu(1)—O(2)	173.1(3)		
N(1)—Cu(1)—O(2)	92.1(2)	N(2)—Cu(1)—O(1)	93.2(2)		
N(1)—Cu(1)—O(1)	170.4(3)	O(2)—Cu(1)—O(1)	82.9(2)		
N(2)—Cu(1)—O(5)	89.2(3)	N(1)—Cu(1)—O(5)	92.7(3)		
O(2)—Cu(1)—O(5)	96.8(2)	O(1)—Cu(1)—O(5)	96.1(3)		
N(4)—Cu(2)—N(5)	92.1(3)	N(4)—Cu(2)—O(4)	170.6(3)		
N(5)—Cu(2)—O(4)	92.8(2)	N(4)—Cu(2)—O(3)	91.0(3)		
N(5)—Cu(2)—O(3)	169.2(3)	O(4)—Cu(2)—O(3)	82.8(2)		
N(4)—Cu(2)—O(6)	90.0(3)	N(5)—Cu(2)—O(6)	93.0(3)		
O(4)—Cu(2)—O(6)	97.8(2)	O(3)—Cu(2)—O(6)	97.4(3)		

Symmetry code: *B*; *x*, *y*, *z*−1.

2.965 Å) and between the O_{water} and F_{PF6} (O—F distance 3.088 Å) and $O_{oxalate}$ (O—O distances 2.956–3.348 Å).

Crystal structure of $[Cu_2(dpyam)_2(\mu\text{-}C_2O_4)(NO_3)_2(C_3H_7NO)_2]$ *(2)*

The asymmetric unit consists of a non-centrosymmetric dinuclear $[Cu_2(dpyam)_2(C_2O_4)(NO_3)_2(C_3H_7NO)_2]$ molecules. A drawing of the dimeric structure showing the labeling scheme is given in Figure 2. Selected bond lengths and angles are reported in Table 2.

Compound *(2)* has two copper centers bridged by a planar bis(didentate) oxalate ligand. The geometry around each copper(II) ion is considered as an elongated octahedral environment with two nitrogen atoms of dpyam and two oxygen atoms of oxalate bridge (Cu—N/O distances 1.956(7)–2.012(6) Å) in the equatorial plane CuN_2O_2, with the axial sites occupied by an oxygen atom of the DMF group [Cu—O 2.295(7) and 2.254(7) Å] and the oxygen atom of the nitrato group [Cu—O 2.786 and 2.679 Å], giving an approximately $CuN_2O_2O'O''$ chromophore (Figure 2). The four basal atoms are not coplanar, showing a slight but significant tetrahedral distortion with dihedral angles of 10.2° and 12.4° formed between the O—Cu—O and N—Cu—N planes for Cu(1) and Cu(2) centers, respectively. The copper atoms are displaced by 0.1259 and 0.1530 Å from the basal planes toward O(5) and O(6) atoms for Cu(1) and Cu(2) centers, respectively in the opposite side. The dimeric entity is slightly folded: the equatorial planes make the angles of 12.5° and 15.4° with the mean plane of the oxalate ligand. As a result, the dinuclear complex displays a chairlike structure. However, because of the copper atoms, the central Cu—OX—Cu core is planar (see Figure 2). The copper–copper separation across the oxalate bridge is 5.212 Å. The axial C_3H_7NO—Cu—O-NO_2 angles are 165.9° and 168.6°. The copper atoms deviate by −0.2651 and 0.2570 Å for the Cu(1) and Cu(2), respectively from the oxalate planes.

The lattice structure is stabilized by hydrogen bonding between the amine-N and the nitrate-O of a neighboring

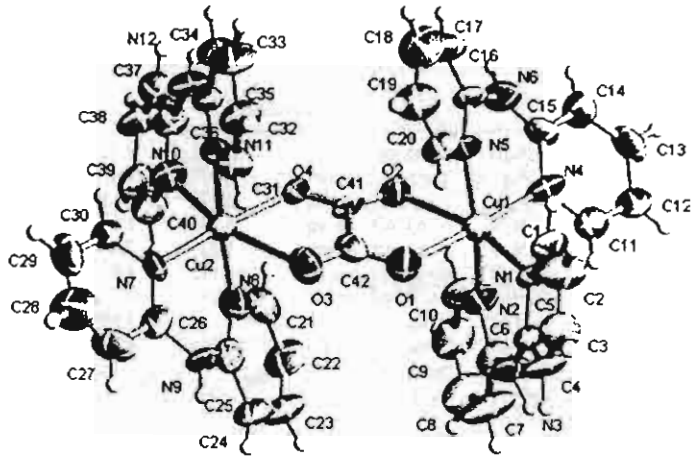

Fig. 1. ORTEP 50% probability plot of the cation in $[Cu_2(dpyam)_4(\mu\text{-}C_2O_4)](PF_6)_2(H_2O)_2$ *(1)*.

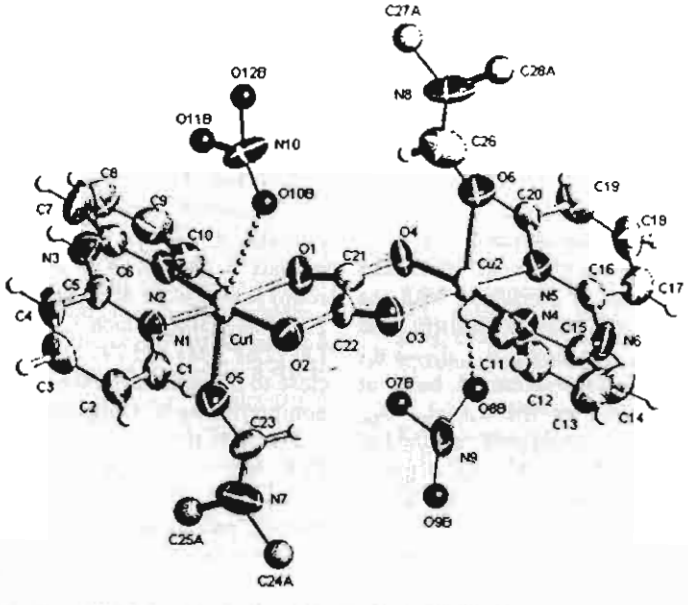

Fig. 2. ORTEP 50% probability plot of $[Cu_2(dpyam)_2(\mu\text{-}C_2O_4)(NO_3)_2((CH_3)_2NCOH)_2]$ *(2)*.

unit with distances of 2.803–3.164 Å, resulting in a polymeric chain.

Structure comparisons

The chromophore of *(1)* is very similar to the recently published compounds $[Cu_2(dpyam)_4(C_2O_4)](ClO_4)_2(H_2O)_3$ *(3)* and $[Cu_2(dpyam)_4(C_2O_4)](BF_4)_2(H_2O)_3$ *(4)* [12], Table 3 which exhibit the compressed octahedral $CuN_2O_2N_2$ chromophore. The axially compressed octahedral (2 + 4) geometry was rarely found in dinuclear-μ-oxalatodicopper(II) complexes. This geometry has only been previously observed in the dinuclear oxalato-bridged copper (II) complexes with a tetradentate-terminal ligand [7] and differs from compounds *(2)*, and *(5–10)* (Table 3) which exhibit axially-elongated (4 + 2) structure. The compounds *(1)*, *(3)* and *(4)* are three rare examples of 2 + 4 compressed rhombic coordination with a didentate-terminal ligand resulting from a pseudo Jahn–Teller effect. As in almost all the cases of observed Jahn–Teller compression examined in detail to date, the apparent compression is due to dynamic interconvertion between two of the possible axial elongation [16, 17]. There is some similarity to other dinuclear-μ-oxalatodicopper(II) complexes which exhibit a square-pyramidal structure with two oxygen atoms

Table 3. Structural data and magnetic properties for *12* selected oxalato-bridged Cu(II) complexes

Compounds[a]	Donor set	Geometry[b]	Oxalato-bridged Coordination	d_{Cu-Cu} (Å)	Dihedral angle[c]	Mode of magnetic interaction	J (cm^{-1})	Ref.
$[Cu_2(dpyam)_4(\mu\text{-}C_2O_4)](PF_6)_2 \cdot 2H_2O$ *(1)*	$O_2N_2N'_2$	comp. oct	eq–eq	5.737	7.16/5.73	c	–	This work
$[Cu_2(dpyam)_2(\mu\text{-}C_2O_4)(NO_3)_2(DMF)_2]$ *(2)*	$O_2N_2O'O$	elong. oct	eq–eq	5.213	9.9/12.8	a	–	This work
$[Cu_2(dpyam)_4(\mu\text{-}C_2O_4)](ClO_4)_2 \cdot 3H_2O$ *(3)*	$O_2N_2N'_2$	comp. oct	eq–eq	5.752	11.3/11.3	c	2.42	[12]
$[Cu_2(dpyam)_4(\mu\text{-}C_2O_4)](BF_4)_2 \cdot 3H_2O$ *(4)*	$O_2N_2N'_2$	comp. oct	eq–eq	5.745	11.4/11.0	c	3.38	[12]
$[Cu_2(dpyam)_2(\mu\text{-}C_2O_4)(NO_3)_2(DMSO)_2]$ *(5)*	$O_2N_2O'O$	elong. oct	eq–eq	5.22	7.0	a	−305	[12]
$[Cu_2(bpy)_2(\mu\text{-}C_2O_4)(NO_3)_2(H_2O)_2]$ *(6)*	$O_2N_2O'O''$	elong. oct	eq–eq	5.143	4.6	a	−382	[1]
$[Cu_2(mpym)_2(\mu\text{-}C_2O_4)(NO_3)_2(H_2O)_2]$ *(7)*	$O_2N_2O'O''$	elong. oct	eq–eq	5.217	d	a	−142	[3]
$[Cu_2(deen)_2(\mu\text{-}C_2O_4)(ClO_4)_2(H_2O)_2]$ *(8)*	$O_2N_2O'O''$	elong. oct	eq–eq	d	3.88	a	−300	[4]
$[Cu_2(tacn)_2(\mu\text{-}C_2O_4)(ClO_4)_2]$ *(9)*	O_2N_3O'	elong. oct	eq–eq	5.176	d	a	−41	[5]
$[Cu_2(bpca)_2(\mu\text{-}C_2O_4)(H_2O)_2](H_2O)_2$ *(10)*	O_2N_3O'	elong. oct	ax–eq	5.631	d	b	1.1	[6]
$[Cu_2(bispicen)_2(\mu\text{-}C_2O_4)](ClO_4)_2$ *(11)*	$O_2N_2N'_2$	comp. oct	eq–eq	5.608	d	c	2.3	[7]
$[Cu_2(bispicMe_2en)_2(\mu\text{-}C_2O_4)](ClO_4)_2$ *(12)*	$O_2N_2N'_2$	comp. oct	eq–eq	5.494	d	c	2.14	[7]

[a] dpyam – di-2-pyridylamine; bpy – 2,2′-dipyridine; mpym – meripirizole; deen – *N,N*-diamine; tacn – 1,4,7-triazacyclonone; bpca – bis(2-pyridylmethyl)1-3,3-propanediamine; bispicen – *N,N′*-bis(2-pyridylmethyl)-1,2-ethanediamine; bispicMe$_2$en – *N,N′*-bis(2-pyridylmethyl)-*N-N*-dimethyl-1,2-ethanediamine.

[b] comp.oct – compressed octahedral; elong. oct – elongated octahedral.

[c] Dihedral angle between the basal and oxalate planes.

[d] Not reported.

of oxalate bridge and two nitrogen atoms of the diamine occupying the base of the pyramid and the counter anion or a solvent molecule occupying the axial position-[1–10].

Spectroscopic properties

The electronic diffuse reflectance spectrum of *(1)* consists of two clearly resolved peaks at 14.49 and 8.90×10^3 cm^{-1}. This spectrum is consistent with the compressed rhombic octahedral stereochemistry and assigned to be the $d_{x^2-y^2} \rightarrow d_{z^2}$ and the $d_{xz},d_{xy}, d_{yz} \rightarrow d_{z^2}$ transitions. Compound *(2)* shows a broad band at 14.22×10^3 cm^{-1}, corresponding to the d_{z^2}, d_{xz}, d_{xy}, $d_{yz} \rightarrow d_{x^2-y^2}$ transition of the elongated octahedral stereochemistry. The i.r. spectrum of *(1)* displays characteristic bands of the oxalate bridging ligand [2, 4–6]: ν_{asym}(C—O) at 1655s and ν_{sym}(C—O) at 1356 m. A weak signal of the δ(O—C—O) bending at 850 m cm^{-1} is superimposed by the strong band at *ca.* 849 cm^{-1} of the F–P–F stretching mode of the PF_6^- groups. That of *(2)* shows the characteristic bands of the oxalate bridging ligand: ν_{asym}(C—O) at 1653s, ν_{sym}(C—O) at 1356 m and δ(O—C—O) at 823 m cm^{-1} and the absorption frequencies at 1384, 1332 and 1034 cm^{-1} suggesting monodentate coordination of the nitrate ion.

The polycrystalline powder e.p.r. spectrum at room temperature of compound *(1)* displays a broad absorption centered around g of 2.09. No half-field signal was observed at room temperature. Complex *(1)* was also measured as solids at 77 K, in which the signal appears as more resolved at $g_\perp = 2.05$, $g_{//} = 2.21$, corresponding to the pattern of Cu(II) in an elongated geometry, $g_{//} > g_\perp > 2.0$ with the $d_{x^2-y^2}$ ground state. This suggests that the apparent compressed geometry at room temperature could be caused by a dynamic Jahn–Teller effect [16, 17]. This is because compound *(1)* adopts the time averaged structure found crystallographically which arises due to the short time scale of the X-ray technique, but the e.p.r. spectra at 77 K are related to the underlying static axial elongated chromophore [16, 17]. Also the half-field signal at approximately 1600 G, corresponding to $\Delta M = \pm 2$ transition was observed, which indicates that indeed a weak interaction between two Cu(II) ions within these compounds is present. The effective magnetic moment at room temperature of compound *(1)* was measured to be 2.55 BM/dimer, which is comparable to the values of *(3)* (2.62 BM) and *(4)* (2.64 BM) [12]. These values are close to the spin only value of 2.45 BM expected for two noninteracting d^9 Copper(II) ions.

The structure, structural distortions, electronic and EPR spectra and the effective magnetic moment of compound *(1)* are very comparable to those of the recently published compounds *(3)* and *(4)*. The magnetic orbitals (d_{z^2}) are perpendicular to the oxalate plane, so the overlap of the oxalate σ orbitals. This situation is corresponding to the coordination mode C, Scheme 1 and consequently a very weak ferromagnetic interaction is expected for *(1)*, based on the previously reported singlet-triplet energy gap (J) of 2.42 cm^{-1} for *(3)* and +3.38 cm^{-1} for *(4)* [12].

The room temperature e.p.r. spectrum of *(2)* appears to be an asymmetric broad resonance with a center at $g = 2.10$. The observed triplet signal is not resolved, apparently due to exchange narrowing, resulting from nearby triplet molecules in the lattice. That of *(2)* recorded at 77 K is better resolved than the room-temperature and shows resolved hyperfine resonances on the low field side of the $\Delta M = \pm 1$ signal due to the coupling of the unpaired electrons with two equivalent copper nuclei and is indicative for a small zero-field splitting. So the observed signal is typical for triplet copper (II) dinuclear in an isolated state [18, 19] with a

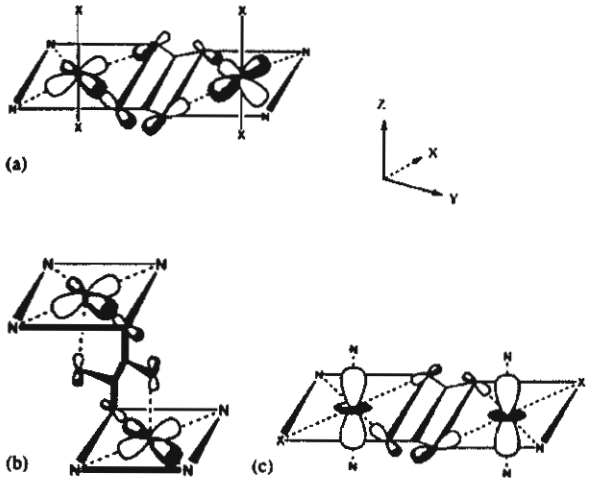

Scheme 1. Three models predicting the magnetic interaction in oxalato-bridged Cu(II) complexes [X = O *(1)* or N *(2)*].

small amount of triplet signal thermally accessible at 77 K. The weak signals resolved are observed with $g_{//}$ *ca.* 2.37 and $g_{\perp}$ *ca.* 2.07, are likely to originate from a small paramagnetic impurity. The room temperature magnetic moment of *(2)* is 2.16 BM/dimer, which is smaller than the value of 2.45 BM expected for two noninteracting d^9 Cu(II) ions and is expected to become almost diamagnetic as confirmed by the EPR spectrum at 77 K.

The structure of *(2)* displays an elongated tetragonal octahedral, which is very similar to that of the recently published [12] compound $[Cu_2(dpyam)_2(C_2O_4)(NO_3)_2(DMSO)_2]$ *(5)*. In this case the copper(II) magnetic orbital ($d_{x^2-y^2}$) interacts with the oxalate σ orbital, which consistent with the coordination mode a, Scheme 1. Compound *(5)* was found to display a strong antiferromagnetic interaction with a singlet-triplet gap(J) of -305.1 cm^{-1}. Therefore compound *(2)* is expected to exhibit a strong antiferromagnetic interaction between copper(II) ions of a dimeric unit, which is confirmed by the effective magnetic moment and e.p.r. spectrum.

Conclusions

Dimeric copper (II) complexes of the form $[(dpyam)_{1\text{ or }2}Cu(\mu\text{-}C_2O_4)Cu(dpyam)_{1\text{ or }2})]X_2$, have been characterized by spectroscopic and magnetic results. Compound *(1)* displays the compressed octahedral copper(II) geometry with asymmetrically bound oxalate ligand, which is similar to those the recently published compounds $[Cu_2(dpyam)_4(C_2O_4)](ClO_4)_2(H_2O)_3$ *(3)* and $[Cu_2(dpyam)_4(C_2O_4)](BF_4)_2(H_2O)_3$ *(4)*. Thus *(1)* is expected to exhibit a very weak ferromagnetic interaction. On the other hand compound *(2)* has an elongated tetragonal octahedral geometry with a symmetric oxalate bridge which is very similar to the recently characterized compound $[Cu_2(dpyam)_2(C_2O_4)(NO_3)_2(DMSO)_2]$ *(5)*. Therefore a strong antiferromagnetic interaction is expected for the compound *(2)*. These conclusions have been confirmed structurally and spectroscopically as well as the efficient magnetic moment. This work confirms that the exchange interaction between the copper(II) ions propagated through the oxalate bridge is strongly dependent on the geometry around the copper ions, sensitive to the orientation of the magnetic orbital of each copper(II), relative to the oxalate plane and the bridging mode of the oxalate group.

Acknowledgements

The authors would like to thank The Thailand Research Fund and Khon Kaen University for a research grant. Support of the Postgraduate Education and Research Program in Chemistry is also gratefully acknowledged. The work described in the present paper has been supported by the Leiden University Study group WFMO (Werkgroep Fundamenteel MaterialenOnderzoek).

References

1. O. Castillo, I. Muga, A. Luque, J.M. Gutierrez-Zorrilla, J. Sertucha, P. Vitoria and P. Román, *Polyhedron*, **18**, 1235 (1999).
2. J. Tang, E. Gao, W. Bu, D. Liao, S. Yan, Z. Jiang and G. Wang, *J. Mol. Struct.*, **525**, 271 (2000).
3. L.S. Tuero, J. Garcia-Lozano, E.E. Monto, M.B. Borja, F. Dahan, J.P. Tuchagues and J.P. Legros, *J. Chem. Soc., Dalton Trans.*, 2619 (1991).
4. R. Vicente, A. Escuer, J. Ferretjans, H. Stoeckli-Evans, X. Solans and M. Font-Bardía, *J. Chem. Soc., Dalton Trans.*, 167 (1997).
5. L. Zhang, W.-M. Bu, S.-P. Yan, Z.-H. Jiang, D.-Z. Liao and G.-L. Wang, *Polyhedron*, **19**, 1105 (2000).
6. M.L. Calatayud, I. Castro, J. Sletten, F. Lloret and M. Julve, *Inorg. Chim. Acta.*, **300–302**, 846 (2000).
7. J. Glerup, P.A. Goodson, D.J. Hodgson and K. Michelsen, *Inorg. Chem.*, **34**, 6255 (1995).
8. M. Julve, M. Verdaguer, A. Gleizes, M. Philoche-Levisalles and O. Kahn, *Inorg. Chem.*, **23**, 3808 (1984).
9. G.R. Hall, D.M. Duggan and D.N. Hendrickson, *Inorg. Chem.*, **14**, 1956 (1975).
10. Y. Akhriff, J. Server-Carrió, A. Sancho, J. Garcia-Lozano, E. Escrivá, J.V. Folgado and L. Soto, *Inorg. Chem.*, **38**, 1174 (1999).
11. M. Du, Y.-M. Guo and X.-H. Bu, *Inorg. Chim Acta*, **335**, 136 (2002).
12. S. Youngme, G.A. Albada, N. Chaichit, P. Gunnasoot, P. Kongsaeree, I. Mutikainen, O. Roubeau, J. Reedijk and U. Turpeinen, *Inorg. Chim. Acta.*, **353**, 119 (2003).
13. SAINT, Data Integration Software, Version 6.12, Bruker AXS, Inc., Madison, WI, 1997.
14. G.M. Sheldrick, SADABS, Program for empirical absorption correction of area detector data, University of Göttingen, Germany, 1996.
15. SHELXTL 6.1 (PC-Version), Program library for the solution and molecular graphics, Siemens Analytical Instruments Division, Madison, WI, U.S.A.
16. B.J. Hathaway, M. Duggan, A. Murphy, J. Mullane, C. Power, A. Waslsh and B. Walsh, *Coord. Chem. Rev.*, **36**, 267 (1981).
17. B.J. Hathaway, *Struct. Bonding (Berlin)*, **57**, 203 (1984).
18. V.T. Kasumov, F. Köksal and Z. Anorg *Allg. Chem.*, **627**, 2553 (2001).
19. E. Wasserman, L.C. Snyder and W.A. Yager, *J. Chem. Phys.*, **25**, 1763 (1964).